คุณสมบัติทางกายภาพและการตอบสนองทางชีวภาพของอะปาไทท์มอดิฟายด์กลาสไอโอโนเมอร์ซีเมนต์

นางสาวอรุณี ลายธีระพงศ์

วิทยานิพนธ์นี้เป็นส่วนหนึ่งของการศึกษาตามหลักสูตรปริญญาวิทยาศาสตร์ดุษฎีบัณฑิต
สาขาวิชาทันตชีววัสดุศาสตร์ (สหสาขาวิชา)
บัณฑิตวิทยาลัย จุฬาลงกรณ์มหาวิทยาลัย
ปีการศึกษา 2554

PHYSICAL PROPERTIES AND BIOLOGICAL RESPONSE OF AN APATITE MODIFIED GLASS IONONER CEMENT

Miss Arunee Laiteerapong

A Dissertation Submitted in Partial Fulfillment of the Requirements

for the Degree of Doctor of Philosophy Program in Dental Biomaterials Science

(Interdisciplinary Program)

Graduate School

Chulalongkorn University

Academic Year 2011

Thesis Title	PHYSICAL PROPERTIES AND BIOLOGICAL RESPONSE OF AN APATITE MODIFIED GLASS IONOMER CEMENT
By	Miss Arunee Laiteerapong
Field of Study	Dental Biomaterials Science
Thesis Advisor	Assistant Professor Suchit Poolthong, Ph.D.
Thesis Co-advisor	Professor Shinya Murakami, Ph.D.

Accepted by the Graduate School, Chulalongkorn University in Partial Fulfillment of the Requirements for the Doctoral Degree

..... Dean of the Graduate School
(Associate Professor Pornpote Piumsomboon, Ph.D.)

THESIS COMMITTEE

..... Chairman
(Associate Professor Pasutha Thunyakitpisal, Ph.D.)

..... Thesis Advisor
(Assistant Professor Suchit Poolthong, Ph.D.)

..... Thesis Co-advisor
(Professor Shinya Murakami, Ph.D.)

..... Examiner
(Associate Professor Chaiwat Maneenut, Ph.D.)

..... Examiner
(Assistant Professor Dujreutai Pongkao Kashima, Ph.D.)

..... External Examiner
(Associate Professor Prathip Phantumvanit)

อรุณี ลายธีระพงศ์ : คุณสมบัติทางกายภาพและการตอบสนองทางชีวภาพของอะปาไทท์มอดิฟายด์กลาสไอโอโนเมอร์ซีเมนต์. (PHYSICAL PROPERTIES AND BIOLOGICAL RESPONSE OF AN APATITE MODIFIED GLASS IONONER CEMENT) อ. ที่ปรึกษาวิทยานิพนธ์หลัก: ผศ.ทพ.ดร.สุชิต พูลทอง, อ. ที่ปรึกษาวิทยานิพนธ์ร่วม Prof. Shinya Murakami, Ph.D. 143 หน้า.

วัตถุประสงค์ เพื่อพัฒนาคุณสมบัติทางกายภาพและการตอบสนองทางชีวภาพของวัสดุกลาสไอโอโนเมอร์ (ซีเมนต์) **วิธีการทดลอง** สังเคราะห์ผงแมกนีเซียมคาร์บอเนตอะปาไทท์ (อะปาไทท์) ด้วยวิธีการตกตะกอน พิสูจน์เอกลักษณ์ด้วยกล้องจุลทรรศน์อิเลคตรอนชนิดส่องกราด, ฟูเรียร์ทรานสฟอร์มอินฟราเรดสเปกโทรเมตรีและเอกซเรย์โฟโตอิเลคตรอนสเปกโทรสโกปี เตรียมกลุ่มทดสอบโดยใส่อะปาไทท์ร้อยละ 2.5 โดยน้ำหนักในผงซีเมนต์ (Fuji IX GP®, กลุ่มควบคุม) ผสมผงกับส่วนของเหลว (อัตราส่วน 3.6 ต่อ 1) ด้วยเครื่องปั่นอมัลกัม ทดสอบเวลาแข็งตัว, ความทนแรงอัด, การทนความเค้นการแตก, ความทนแรงยึดเฉือนและระดับการรั่วซึมเล็กตามเกณฑ์มาตรฐานสากล วัดการคายแคลเซียมและแมกนีเซียมไอออนโดยอินดักทีฟคัปเปิลพลาสมาออพติคอลอีมิสชันสเปกโทรสโกปี, ฟลูออไรด์ไอออนด้วยฟลูออไรด์ไอออนซีเล็คทีฟอิเล็กโทรด วัดการตอบสนองทางชีวภาพจากการแบ่งตัวของเซลล์ด้วย WST-1, การทำงานของเอนไซม์อัลคาไลน์ฟอสฟาเตส, การแสดงออกของยีน COL1A1, DMP-1 และ DSPP โดยวิธีเรียลไทม์พีซีอาร์ รวมถึงวัดการสร้างแร่ธาตุด้วยการย้อมสีอะลิซารินเรด **ผลการทดลอง** กลุ่มทดลองมีค่าการทนความเค้นการแตกสูงขึ้น, ระดับการรั่วซึมเล็กบริเวณรอยต่อเนื้อฟันลดลงอย่างมีนัยสำคัญ, มีการแบ่งตัวของเซลล์, การทำงานของเอนไซม์และการแสดงออกของยีน COL1A1, DMP-1และDSPP สูงขึ้นกว่ากลุ่มควบคุม **สรุป** วัสดุกลุ่มทดลองมีคุณสมบัติทางกายภาพและการตอบสนองทางชีวภาพต่อเซลล์เนื้อเยื่อในฟันมนุษย์ที่ดีขึ้นเมื่อเทียบกับกลุ่มควบคุม ควรนำมาพัฒนาเพื่อให้เป็นวัสดุบูรณะฟันที่มีคุณสมบัติที่ดีขึ้นในการใช้งานในทางคลินิกและเพื่อส่งเสริมการสร้างใหม่ของเนื้อฟัน

สาขาวิชา ทันตชีววัสดุศาสตร์ ลายมือชื่อนิสิต .....

ปีการศึกษา 2554 ลายมือชื่อ อ.ที่ปรึกษาวิทยานิพนธ์หลัก.....

ลายมือชื่อ อ.ที่ปรึกษาวิทยานิพนธ์ร่วม .....

5187837920 : MAJOR DENTAL BIOMATERIALS SCIENCE
KEYWORDS : MAGNESIUM CARBONATE APATITE / GLASS IONOMER / TOUGHNESS / MICROLEAKAGE / BIOLOGICAL RESPONSE

ARUNEE LAITEERAPONG : PHYSICAL PROPERTIES AND BIOLOGICAL RESPONSE OF AN APATITE MODIFIED GLASS IONONER CEMENT. THESIS ADVISOR : ASST. PROF. SUCHIT POOLTHONG, Ph.D., CO-ADVISOR : PROF. SHINYA MURAKAMI, Ph.D., 143 pp.

Objectives. To develop a novel glass ionomer cement (GIC) with improved physical properties and *in vitro* biological response to human pulp cells. ***Method***. Magnesium carbonate apatite ($MgCO_3Ap$) was synthesized by precipitation method and characterized by Scanning Electron Microscopy, Fourier Transformed-Infrared Spectroscopy and X-ray Photoelectron Spectroscopy. The test cement was prepared by adding 2.5% by weight of $MgCO_3Ap$ to Fuji IX GP® (control) and encapsulated mixing with the liquid (P/L=3.6:1). Setting time, compressive strength, fracture toughness, shear bond and microleakage tests were performed according to international standards (ISO 9917-1, ASTM E399-90 and ISO/TS 11405). Inductive Couple Plasma Optical Emission Spectroscopy and Fluoride Ion Electrode were used to determine calcium, magnesium and fluoride ion release respectively. WST-1 cell proliferation, Alkaline Phosphatase (ALPase) assay, Real Time-PCR and Alizarin red staining were used to evaluate biological responses. ***Results***. The test cement had significantly improved fracture toughness, less microleakage at dentin interface ($p<.05$) and exhibited higher cell proliferation, improved ALPase activity, early expression of COL1A1, DMP-1 and DSPP compared to the control. ***Conclusion***. 2.5% $MgCO_3ApGIC$ demonstrated improved physical properties and biological response to human pulp cells compared to Fuji IX GP®. This finding indicated a potential of $MgCO_3ApGIC$ to be a restorative material for higher clinical performance and pulp-dentin regeneration.

Field of Study : Dental Biomaterials Science Student's Signature .....
Academic Year : 2011 Advisor's Signature .....
Co-advisor's Signature .....

ACKNOWLEDGEMENTS

First of all, the author would like to thank you Professor Hien Chi Ngo who provided an inspiration to enroll this Dental Biomaterials Course. Assistant Professor Suchit Poolthong, my advisor, for his time in reading my manuscript, thesis and his valuable suggestion during the whole four-year period.

Thank you to Professor Masayuki Okazaki for his kind suggestion and support for my apatite synthesis. Thank you to Dr. Isao Hirata for his time in performing the XPS analysis.

I would like to also thank you very much to Professor Shinya Murakami for his kindness in accepting me to learn, do experiments and stay in his lab in Osaka Graduate School of Dentistry until I finished all biological experiments. Thank you all of his Ph.D. students especially Dr. Tetsuhiro Kagikawa and Dr. Kenta Mori in helping me start my experiments from the first day to the last day I stayed in the lab.

Thank you to Madeline Monaco for her approval for my study and her understanding in my passion to improve oral health for population worldwide. And thank you to Dr. Yossakit Lochaiwatana for his help in analyzing data, statistic consultancy and all administrative works during my absence from Thailand.

Thank you to my dad and my mom in their understanding on not having time spending with them. My husband, who always helps taking good care of our kids.

Finally, Yanakorn and Yanisa, thank you for being a good son and good daughter. Their understanding and their support when I felt discouraged and wanted to give up was really cheer me up. The sentence “Mamee- you are almost graduated! Please keep going, we are OK for your absence”, this really drove me to finish. If one day you have a chance to see this page, I want to say “I love both of you very much!”

CONTENTS

Page

Page

Page

LIST OF TABLES

Page

LIST OF FIGURES

Page

Page

Page

CHAPTER I

INTRODUCTION

Problem Statement

Early Childhood Caries (ECC) is the presence of one or more decayed, missing or filled tooth surfaces in any primary tooth in children aged 71 months or younger[1]. Data from Thailand National Oral Health Survey in 2007 reported an incidence of caries found in 3-year-old children as high as 61.63% and increased to 80.63% at age of 5. Of those incidences, 60.76% and 78.85% are untreated caries in age 3 and 5 accordingly[2].

Consequences of untreated caries to oral health and to general health are well-documented[3]. Untreated caries would result in pain, bacteremia, high treatment costs, reduced growth and development, speech disorders and premature tooth loss. Reasons behind untreated caries in children are mainly related to non-compliant behavior, lacking of dental professionals' skills in managing young children.

Atraumatic Restorative Treatment (ART) is an approach to manage carious lesions introduced by the World Health Organization. ART was first tested in Africa in the mid1980s[4], followed by Thailand and China during 1990s. The procedure involved the removal of carious lesions by hand instruments such as spoon excavators and restoring the cavities with glass ionomer cement (GIC). This allowed restorative treatment in locations with no electricity and required only simple dental equipment. The ART is a non- threatening technique because of no noise of hand-piece, no water-cooling, no suction required and pain can be kept in minimum during treatment without need of anesthesia. Thus, the ART is useful in treating cavities especially in children with management problems. However dentists still have problems in dealing with deep

cavities and they are unconfident in determining how much caries should be removed before restoring. As a consequence, the untreated caries is left such high.

Recently, a new concept in caries removal technique called ultraconservative removal of carious (or partial caries removal) had been introduced. In this technique, practitioners remove most, but not all, of the infected dentin, seal the cavity and proceed with the restoration[5]. In deep lesions, this technique usually involves completed removal of carious tissue at cavity walls but limits removal from the pulpal floor and axial wall. A systematic review revealed four studies comparing complete and ultraconservative caries removal. It was reported that ultraconservative caries removal in symptomless, primary or permanent teeth reduced the risk of pulp exposure. Therefore it was suggested to be preferable to complete caries removal in the deep lesions[6]. However this technique requires materials that can ideally seal the cavity wall. Theoretically, sealing caries and associated bacteria by a good seal restoration can deprive the organisms of sugar substrate from the oral cavity. As a consequence, bacteria will reduce in number and become less in metabolic activity[7]. Moreover it allows time for the pulp-dentin complex to lay down reparative dentin and reduces the risk of pulpal exposure.

Although GIC has been used for the ART for almost 30 years, sealing caries with this material is still questionable because of the limitations associated with its physical properties[8]. For instance, in very deep cavities with very thin remaining dentin thickness (RDT), toxin or bacteria can also reach pulp and stimulate inflammatory process. Hence improving physical properties (toughness, bonding) and biological response to human pulp cells of GIC may enhance the material usage in the future.

In the recent years, the promising advantages of hydroxyapatite (HA) in restorative dentistry had been reported. HA is biocompatible and its hardness is similar to that of natural tooth. Adding HA into GIC demonstrated improvement in compressive strength, working, setting time, fracture toughness and long term bonding to dentin with unimpeded ability of sustained fluoride release[9].

Not only HA but also biological apatite was found to have potential to improve biological response. A study reported that magnesium ions (Mg^{2+}) released from functional grade magnesium carbonate apatite ($FGMgCO_3Ap$) demonstrated the acceleration effect of osteoblast adhesion at the surface of a composite material[10]. Apart from Mg^{2+}, calcium ions (Ca^{2+}) also released from apatite. Recently, a study demonstrated the effect of Ca^{2+}which released from dental materials in stimulating fibronectin synthesis from dental pulp cells. And this might induce the differentiation of dental pulp cells to mineralized tissue forming cells and later form dentin bridge[11].

With the current understanding on interaction between biomaterials and pulp-dentin complex, it may be possible to formulate a restorative biomaterial with good sealing ability, physical properties and potentials in promoting pulp-dentin regeneration. This may lead to the improvement of the clinical performance of restorations and increase the number of deep cavities to be filled. Finally, in long term, might improve oral health and quality of life in the population worldwide.

Research Purposes

1. To develop a novel GIC with improved physical property in term of fracture toughness.

2. To develop a novel GIC with potential pulp-dentin regenerative properties.

Hypothesis

1. Magnesium Carbonate Apatite ($MgCO_3Ap$) GIC has better fracture toughness than conventional GIC (Fuji IX®GP).

2. $MgCO_3$ApGIC has equal microleakage to Fuji IX®GP.

3. $MgCO_3$ApGIC has less *in vitro* cytotoxicity than human pulp cell to Fuji IX®GP.

4. $MgCO_3$ApGIC shows better *in vitro* biological response (cell proliferation and calcification) than Fuji IX®GP.

Expected Outcome

This novel GIC with potentials in promoting pulpal healing together with improved physical properties will improve the quality of treatment and increase the number of deep cavities to be restored in young children.

CHAPTER II

LITERATURE REVIEW

Pulp-dentin Complex

1. Dentin

Dentin is composed of inorganic hydroxyapatite. Collagen is the main organic component of the dentin and the remaining 10% of the organic extracellular matrix (ECM) is non-collagenous proteins (NCPs) and proteoglycans. During primary dentinogenesis, differentiated odontoblasts secrete collagen which provides the framework for apatite crystal deposition. Collagen type I is the predominant collagen in dentin while collagen type V is also detected but in smaller quantities[12]. The crystal deposition is initiated and controlled by the NCPs.

The NCPs were subdivided into molecules predominantly found in mineralized tissues (bone and dentin), and more ubiquitous molecules. Dentin Phosphoprotein (DPP) is the most abundant NCP in dentin (>50%). It interacts specifically with collagen to initiate dentin mineralization[13] and it also controls collagen fibril formation[14]. Dentin Sialoprotein (DSP) was reported to be synthesized by odontoblasts, some pulp cells and by preameloblasts[15, 16]. In a recent finding suggested bone cells also synthesize DSP, and probably DPP, but in a ratio that is estimated to be about 1:400 of that found in dentin[17]. Dentin matrix protein-1 (DMP-1) is expressed by both bone and dentin[18].

Bioactive growth factors are also presented within dentin. These include members of the transforming growth factor-β (TGF-β) superfamily, insulin- like growth factor-1 and 2 (IGF-1 and -2), fibroblast growth factor-2 (FGF-2) and various angiogenic growth factors[19-21]. These bioactive molecules sequestered within the dentin matrix during tooth development and remained in their bioactive state until the matrix is

degraded during carious or other injurious episode. Once released, these molecules may diffuse to the pulp and then participate in the pulp-dentin regeneration. Hence, the ability of any materials to extract these bioactive molecules from the dentin matrix will be essential to enhance the repair process of the pulp-dentin complex.

1.1. Type of Dentin

Primary dentin forms during dentinogenesis and secondary dentin starts to form since the tooth is still embedded. Both primary and secondary dentin formations are controlled by odontoblasts. Tertiary dentin forms in response to external stimuli from secondary odontoblasts (odontoblastic-like cells) which differentiates from pulp cells after primary odontoblast have been destroyed.

1.2. Dentin Permeability[22]

Permeability involves with the passage of fluids, ions, molecules and bacteria. The permeability of dentin is mainly through dentinal tubules. The dentinal tubules are cylindrical in-shape, extending through the entire width of dentin and the density of the tubules is greater near the pulp than the periphery. The dentin permeability is essential to support the physiology and reaction patterns of the pulp-dentin complex.

1.3. Remaining Dentin Thickness (RDT) and Pulp Response[23]

The importance of the remaining dentin thickness (RDT) underlying of any dental materials to pulp responses has been a topic of controversy for more than a century[24]. Over the years, the estimated value of the minimal cavity RDT that will not cause pulp injury has been decreasing. Stanley in 1994 suggested that a RDT of 2 mm would protect the pulp from injury[25] while recent finding suggested 1 mm would be sufficient [26]. The RDT that provides pulp protection can be expected not only from dentinal tubule distance, but also with dentinal tubule permeability. Tubule permeability

is an important factor that allows the progression of caries, bacterial leakage and chemical irritants towards the pulp[27].

2. Dental Pulp

Dental pulp contains a complex mixture of cells, including odontoblasts, odontoblast-like cells, dental pulp stem cells, and fibroblasts. Pulp also contains an ECM which is mainly collagen, including types I, III, V, and VI, fibronectin, and several glycosaminoglycans. The molecular makeup of the pulp and the dentin are different and the absence of certain molecules may provide an explanation, why the pulp tissue does not mineralize. Fibronectin, an ECM glycoprotein, found to be associated with dental basement membrane and played a critical role in terminal differentiation of odontoblast. Recently calcium ions released from calcium hydroxide was reported to stimulate fibronectin gene expression in dental pulp cell[11].

Dental Caries and its Sequel to Pulp-dentin Complex

1. Caries Pathogens and Caries Progression[28]

Dental caries is one of the most prevalent infectious diseases in the world. Cariogenic bacteria is responsible for the disease initiation and progression which results in demineralization of enamel, dentin and subsequent pulpal damage[29]. Degree of pulp damage depends on bacteria antigen and/ or metabolic by-products which diffuse through dentinal tubules and stimulate the immune responses within dental pulp.

The microflora in dental caries is highly complex. Mutans group of streptococci such as *Streptococcus mutans* and *Streptococcus sobrinus* are important in initiating the disease process while lactobacilli relates to the progressing of lesions.

Both streptococci and lactobacilli are capable to invade intra- tubular dentin by binding to collagen type 1. While lesion progresses deeply into the dentin, streptococci will be unlikely to thrive and a transition from bacteria survived in shallow caries to lactobacilli and/or anaerobic bacteria takes place.

2. Pulp Response to Caries and Inflammation[30]

In the healthy adult tooth, odontoblasts and cells of the sub-odontoblastic layer (Höehl cell layer) locate between the inner margin of the dentin and the outer limit of the pulp. These cells are responsible for the production of physiological dentin. In the normal dental pulp, there are heterogeneous cell populations including a majority of fibroblast- like cells, inflammatory and immune cells (dendritic cells, histiocytes/macrophages, T-lymphocytes), and pulp stem cells (progenitors). Although there is a very small proportion of defense cells in dental pulp but bacterial and its component can stimulate those cells to initiate immune response and prolong pulpal inflammation[31-34]. One study clearly demonstrated the negative impact of the inflammatory response on tissue regeneration in an animal model and showed that the presence of inflammation can delay the tissue regeneration[35]. Thus effective control of inflammation will be critical to stimulate tissue regeneration.

In slowly progressing caries lesions, demineralization of enamel from acid will increase mineralization of the underlying dentin. Formation of highly mineralized peritubular dentin will affect the diameter of the dentinal tubules which may reduce the dentin permeability. Furthermore, tertiary dentin will be formed at the pulpal end of the affected tubules (reactionary dentin) which will protect the pulp against exogenous destructive stimuli. However in rapidly progressing lesions, cells located in the Höehl (sub-odontoblastic) layer may differentiate and replace the wounded cells. A lack of formation of tertiary dentin will then result in the reaction of pulp tissue to the

transmission of microbial products through a permeable dentin which can lead to either reversible or irreversible pulpitis.

If the pulp is exposed, odontoblasts and Höehl cells can no longer repair the lesion. However if the cariogenic environment is removed then stem cells will be recruited and then differentiate to a new odontoblast-like cells and form tertiary dentin (reparative dentin)[36]. Reparative dentin can be in form of a thin dentinal bridge which occludes the pulpal exposure site or a bone- like structure (osteo-dentin) which fills the exposure site.

3. Infection and Inflammation within the Dental Pulp[37]

During the caries progression, the molecules involve in the process, including bacteria and its components, and dentin matrix breakdown products will biologically interact with the dental pulp. It has been proposed that in relatively slow progress caries, these molecules are able to induce dentin regeneration[38]. In contrast, under conditions of more rapid caries progression or remained infection, the cellular and molecular interactions are elevated and a more intense immune and inflammatory response occurs which may result in the death of the pulpal tissue[39]. Even the molecular and cellular interactions between the inflammation and regeneration are complex but a fine balance can exist. This can result in either synergy or frustration of the pulpal healing process[37].

Odontoblasts locate at the periphery of the pulp and are the first cells to encounter the invading bacteria and its components. Although odontoblasts provide barrier function to the underlying tissue from the invading bacteria, they are also immune-competent and capable of orchestrating an inflammatory response[40].

Progression of the caries deeper into the underlying dental tissue results in changes in the composition of the bacterial biofilm[41]. A study of pulp-dentin complex and carious lesions explained the molecular events which found heavy collagen type1

synthesis, DPP and DSP expression. The result clearly demonstrated the up-regulation of collagen type1, DPP and DSP during dentinogensis and suggested these proteins have functional roles during reactive and reparative dentin formation[42].

Dental Materials, Biocompatibility and Pulp-dentin Regeneration

1. Dental Materials and Regeneration[43]

With the increasing attention to minimal intervention during carious excavation, there is a greater risk of incomplete removal of all infected tissue. Whilst the survival of entombed bacteria may be compromised[44]. So there are opportunities for antibacterial control during restoration which is an important part of providing a sterile environment within the injured pulp-dentin complex to start for regeneration.

The interaction of dental materials in contact with tooth tissue is influenced by many factors, including the composition of the material, the chemistry and concentration of eluted components or degradation products, and the ability of the tissue to respond to these agents. Previous studies on this interaction were mainly aimed to identify the cellular response and toxic effects of the materials[45, 46]. Now, research focus is shifting to explore how materials contribute to regenerative process in the tooth tissue[43, 47].

Dental materials with their acidity or basicity or chelating ability are capable of extracting bioactive molecules from dentin[47, 48]. Acid such as cavity etchants had been proved to initiate localized demineralization, exposure of collagen fibrils in dentin and release bioactive molecules. It was also reported that actions of etchants go beyond the simple physicochemical effects and impact the potential regenerative responses which mediated by the released bioactive molecules[48]. Releasing of these molecules can be induced by solubilizing effect of dental materials or acid from caries attack. The effect of the released molecules to pulp-dentin regeneration

may be from a combination of the amount released, distance from the pulp cells, and the extent of the injury process[49].

Reactionary dentinogenesis was induced by the presence of bioactive molecules such as growth factors of the TGF-β family. These molecules can be either combined in the capping material or released from the dentin when in contact with the basic calcium hydroxide and acidic resin-modified GIC. Thus, it appears that current GICs, and potentially other acidic dental materials, are capable to extract bioactive molecules from the dentin which contribute to the process of dentin regeneration and pulpal healing.

To identify the ideal properties of dental material to pulp-dentin regeneration, in the recent review[50-52] indicated that the regenerative effects may relate to the abilities of materials to provide a conductive environment for healing which are

a) antibacterial properties which lead to sterilization of the site.
b) biocompatibility of the materials.
c) calcium ion (Ca^{2+}) release to induce the mineralization.
d) ability to liberate bioactive molecules from dentin.

2. Dental Materials and Biocompatibility

Biocompatibility refers to the ability of materials to elicit an appropriate biological response in a specific application[53]. Most dental materials are produced to achieve their physical or mechanical properties and the “appropriate biological response” of materials generally refers to “no adverse reaction” to living system in the presence of the materials[54].

Few materials are truly inert, and their placement within the dynamic tissue environment of the pulp-dentin complex may potentially give rise to a wide spectrum of physicochemical and biological effects. Such effects may differ, depending upon the tissue status either healthy or carious. It must be recognized that the toxic

effects of materials may compromise cell function within the pulp-dentin complex and ultimately cause cell death.

Most studies on the cytotoxicity of dental materials on the pulp are performed on healthy cells and tissues. However, the combination of disease effects such as bacterial infection, inflammation and material cytotoxicity on the tissue may significantly affect the capability of the pulp to regenerate. It is important to recognize that there is a fine balance between regeneration and material toxicity. Although the biocompatibility of dental materials is always a concern but attention should be provided to also understand the potential of current or future materials to participate in the healing and repair process of affected pulp-dentin tissues.

Biomaterials and Roles of Ionic Dissolution Products to Regeneration[55]

1. Hydroxyapatite and Biological Apatite

1.1. Synthetic and Biological Hydroxyapatites[56]

Hydroxyapatite (HA) ($Ca_{10}(PO_4)_6(OH)_2$) is a type of calcium phosphate (CaP), which is the main mineral component of the enamel, comprises about 70% by weight of dentin and comprises the inorganic matrix of human bone.

Biological apatite is also a CaP with multiple substitutions and deficiencies at all ionic sites to HAs. The close relationship between substitutions and bioactivity of synthetic substituted HAs had been demonstrated by *in vitro* and *in vivo* studies. LeGeros in 1967 clarified that the inorganic composition of bone and teeth are composed of carbonate apatite (CO_3Ap) which is a biological apatite[57]. Crystal structural properties of biological and synthetic HAs have been studied extensively because functions, such as solubility and bioactivity of the synthetic material, are controlled by their crystallographic structure.

Biological apatite contains several percent by weight of carbonate (CO_3). Carbonate ions (CO_3^{2-}) can substitute into both phosphate ion (PO_4^{3-}) and hydroxyl ion (OH^-) sites in the HA. However the biological apatite synthesized in an aqueous system demonstrated CO_3^{2-} in the PO_4^{3-} position (Type B substitution). Biological apatite also contains many trace elements and has different crystallographic properties. It is well known that a number of elements can substitute into the apatite crystal structure[58] and both cationic and anionic ions can substitute into $Ca^{2+}$and PO_4^{3-} or OH^- position. Furthermore, some of these substituted ions contribute to metabolism in the human body and cell adhesion.

Considering the differences between biological and synthetic HA, it is known that biological apatite has nano-structure. Materials at the nano-scale have unique chemical, physical and electrical properties. Hence studies regarding to

biological apatite will provide useful insights for designing bio-apatite with optimized performance.

1.2. Magnesium and Carbonate in Biological Apatite[59]

Magnesium (Mg) and CO_3 are two minor but important elements associated with biological apatite. The average concentrations of both Mg and CO_3 are much lower in human enamel (0.26% by weight Mg; 3.8% by weight CO_3) compared to those of either dentin (0.8% by weight Mg; 6% by weight CO_3) or bone (0.8% by weight Mg; 7.5% by weight CO_3)[59].

CO_3^{2-} incorporated into the apatite causes changes in lattice parameter which showed the contraction in the *a*-axis dimension but expansion in the *c*- axis dimension. This causes the reducing in crystal size, changing in crystal shape and increasing in solubility. CO_3 level in bone also plays a role in the biochemistry of hard tissue.

Mg^{2+} incorporated into apatite also causes disturbance in apatite lattice, decreasing in crystal size and consequently increasing the dissolution rate. When Mg^{2+} and CO_3^{2-} present together in the solution, it will cause synergistic effects on the crystallinity and dissolution properties[60, 61].

2. Role of Ionic Dissolution Products to Regeneration[55]

Currently one of the main focuses of biomaterials research is biological adhesion or bioadhesion. Bioadhesion is an important property of biomaterials used for substitution which attach to neighboring tissues. In addition to the biocompatibility, the binding of the cells to biomaterials play an important role in the rapid cure of the defective area.

A study in 2004 reported the expression of αv integrins in human odontoblasts. This study suggested that integrins found in odontoblasts may play a physical role in maintaining the cohesion of the odontoblastic layer which is necessary to maintain the integrity of the peripheral dental pulp. And the integrin may act as a signal transducers for pulp-dentin regeneration[62].

Cationic ions appear to be related to the activity of adhesion molecules such as those of the integrin family[63]. Mg^{2+} was found to play an important role to cell adhesion and to bone metabolism[64]. It is suggested that this ion interacts with integrins of osteoblast cells which are responsible for cell adhesion and stability[10]. Because the apatite was easily dissolved so the Mg^{2+} finally became a source for the remodeling of the bone[10].

Increased evidences indicated that ionic dissolution products from inorganic materials are keys to understand the behavior of the materials in the context of tissue engineering applications. Ca^{2+} and PO_4^{3-} are the main components of biological apatite, these ions also obviously play an essential role in bone regeneration. A study reported that 2-6 mM (80-240 ppm) of Ca^{2+} is suitable of survival and proliferation of osteoblast cells. In the slightly higher concentration of 6-10mM (240-400 ppm) is suitable for osteoblastic differentiation and ECM mineralization, while high concentration (>10 mM, 400 ppm) is toxic[65].

2.1. Magnesium and Pulp-dentin Regeneration

Bone mineral contains $Ca^{2+}$and several ions. Mg^{2+} can easily replace Ca^{2+} in the lattice. Moreover, it has been reported that the presence of such ions will modify the dissolution rate and the biodegradation of the biomaterials.

Following Ca^{2+}, K^{+} and Na^{+}, it was found that Mg^{2+} is the fourth highest concentrated cation in the human body. Mg^{2+} is not directly incorporated into the apatite structure of bone, but rather accumulated in the hydration shell around the hydroxyapatite crystal forming surface-bound ionic complexes.

Mg^{2+} is always associated with the mineralization of calcified tissues, mainly in bones and teeth[66]. It indirectly influences mineral metabolism, for example through activation of alkaline phosphatase (ALPase)[67] while directly influences, or even controls, the crystallization processes (crystal size, lattice parameters) of mineral substances as well as the pattern of mineral formation[68, 69]. Recently an *in vitro* experiment[70], substituted hydroxyapatite crystals were phagocytosed by bone cells. During this process, Mg^{2+} could be released to the culture medium and affected the mineralization of the ECM. It could be expected that Mg^{2+} incorporation would cause apatite crystals to be more soluble. It was also reported an inhibition of the formation and growth of hydroxyapatite crystals by Mg^{2+}. Adsorption of Mg^{2+} at the crystal surface could further inhibit apatite growth.

However, Mg^{2+} was found to be related with the bio-adhesion behavior of integrin[63]. The binding of integrin to specific ligands is dependent on the presence of divalent cations, with most but not all cells prefer Mg^{2+} and Ca^{2+}. Recently it was reported that Mg^{2+} released from functional grade magnesium carbonate apatite ($FGMgCO_3Ap$) demonstrated the acceleration effect of the Mg^{2+} on osteoblast adhesion at the surface of the composite[10].

A study on *in vitro* effects of different divalent ions to odontoblast-like cell reported that high Mg^{2+} concentration in the cell culture had a toxic effect on the odontoblast and inhibited the formation of ECM. Mg^{2+} also affected the cell structure and its ability to adhere. In the lower concentration (1 mM, 24.3 ppm), cells formed smaller size mineralized nodule at day 7 and increased at day 14 while the higher concentration shown no calcification[71].

In conclusion, magnesium seems to be an important factor controlling *in vivo* bone metabolism since it acts on both bone formation and resorption[70].

2.2. Calcium, Fibronectin and Regeneration[11]

It is well known that Ca^{2+} has effects on cells associated with hard tissue formation. Increasing in extracellular Ca^{2+} concentrations enhances ALPase activity of osteoblastic cells. Odontoblasts actively transport Ca^{2+} toward sites of mineral formation. It has also been demonstrated that Ca^{2+} increase the mRNA expressions of osteopontin and bone morphogenetic protein-2 in human pulp cells *in vitro*.

Calcium hydroxide ($Ca(OH)_2$) has been used to induce hard tissue formation for a long time. However the mechanism of the effect is still unclear. It had been suggested that the effects of $Ca(OH)_2$ on differentiation and mineralization of osteoblasts were not dependent on alkalization caused by OH^-, but on dissociated Ca^{2+} under the condition of pH less than 8.5. A study reported that the increased extracellular Ca^{2+} concentrations caused by dissolution of calcium phosphates (CaP) from Poly-CaP contributed to the initiation of the differentiation and mineralization of odontoblasts[72].

Fibronectin (FN) is synthesized by fibroblasts, endothelial cells, chondrocytes, osteoblasts, glia cells and myoblasts. It is present in blood and in tissue as a component of the ECM. This protein has multi-functions, such as to adhesion, migration and differentiation of cells[73]. During tooth development, the differentiation of odontoblasts is regulated by specific basement membrane- mediated epithelial–mesenchymal interactions[74]. FN is present in the dental basement membrane, and mediates the elongation and polarization of odontoblasts by transmembrane–cytokine interaction[75]. It was also assumed that FN had an important role for the terminal differentiation of odontoblasts from undifferentiated cells in dental pulp[76]. Odontoblasts and dentin formation have been found in contact with implants of filters coated with plasma FN[77]. It has been reported that the FN-rich layer formed between necrotic tissue and healthy pulp tissue is associated with hard-tissue forming cells[78, 79]. FN-rich matrix may serve as a reservoir of growth factors, which have participated in the differentiation of odontoblasts[80, 81]. FN is detected immune-histochemically within inter odontoblastic collagen fibres, which means that FN is important for initial dentin bridge

formation[82]. While Mg^{2+} did not influence FN gene expression, this implies that the effect of Ca^{2+} on pulp cells is specific, and is not a common feature of divalent cations.

In conclusion, Ca^{2+} released from dental materials migrates to pulp tissue and elevates extracellular Ca^{2+} concentrations. This elevation induces FN synthesis of pulp cells, follows by accumulating FN in the necrotic tissue adjacent to healthy pulp tissue. High amount of FN might induce differentiation of pulp cells to mineralized tissue forming cells resulting in dentinal bridge formation.

3. Biomaterials and Regeneration

Certain CaP materials have been evaluated the potential to be used as direct pulp capping agents. Octacalcium has shown a similar overall but slower initial healing response when compared to $Ca(OH)_2$. Recently, a CaP cement (CPC) with the additional of polymer microspheres with and without 400 ng TGF-β was used as a pulp capping agent in goat incisors. The result demonstrated that the CPC containing the empty polymer microspheres was capable of enhancing tertiary dentin formation but the effect is greater when adding the protein[83].

Another study also evaluated HA being as a direct pulp capping material. This study found that HA produced little inflammatory reaction. Macrophage, which is the first cell to appear during wound heal participated in phagocytosis of HA. Intracellular solubilization of phagocytosed HA could release a high concentration of free Ca^{2+} and PO_4^{3-}. It has been concluded that the wound healing processes after HA application are more desirable that those after calcium hydroxide placement[84].

HA has an excellent biological behavior. Its composition and crystal structure are similar to the apatite in the human dental structure and skeletal systems. Currently, a number of researchers have attempted to evaluate the effect of addition of HA powders to restorative materials.

Glass Ionomer Cements

GIC was invented by Wilson in 1969[85]. It is a water-based cement from acid base reaction between an alumino-silicate glass and polyacrylic acid.

1. Cement Composition[86, 87]

1.1. Glass Powder

The powder is an acid-soluble calcium fluoroaluminosilicate glass similar to that of silicate but with a higher alumina-silicate ratio that increases its reactivity with liquid. The fluoride portion acts as a "ceramic flux". Lanthanum, strontium, barium or zinc oxide additives provide radiopacity. The raw materials are fused to form a uniform glass by heating them to temperatures of 1100°C to 1500°C. The glass is ground into a powder having particles into a powder in the range of 15 to 50 μm. Normal percentages of the raw materials are:

a) Silica 41.9%
b) Alumina 28.6%
c) Aluminum Fluoride 1.6%
d) Calcium Fluoride 15.7%
e) Sodium Fluoride 9.3%
f) Aluminum Phosphate 3.8%

1.2. Liquid Composition

The original liquid was aqueous poly-acrylic acid in a concentration of about 40-50%. A low molecular weight of acrylic-itaconic acid was required to achieve a high concentration without gelation. However a variety of other unsaturated carboxylic acids and monomers have been used. Recently, the introduction of di-carboxylic or tri-carboxylic acids is not only preventing gelation but also increasing reactivity. This is because of the increased number of carboxyl groups (COO^-) per chain unit and the

higher acidity. Increased chain cross-linking probably also occurs in the final set cement leading to better physical properties.

One problem of the early cements was a slow setting reaction, Wilson *et al*[88] found the addition of tartaric acid increases the rate of setting time and the ultimate compressive and tensile strengths of the material, while leaving the working time unaffected.

2. The Setting Reaction[87]

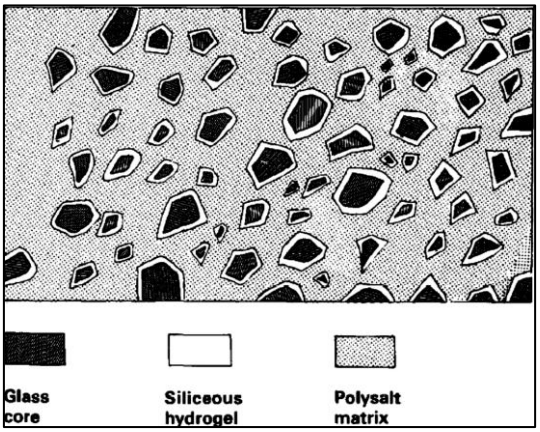

Figure 1 Diagram Demonstrated Structure of Set GIC[87]

The setting reaction of the GIC is complex and may vary with composition. In general, it is an acid base reaction between the ion-leachable glass and a poly-(alkenoic) acid. The setting reaction of GIC had been studied and characterized in two distinct phases, dissolution and gelation.

In the dissolution phase, Ca^{2+} and aluminium ions (Al^{3+}) are released by acid attack on the surface of the glass particles and cross- link with polyacid chains into a network. The Ca^{2+} concentration of the cement sol rises much more rapidly than the Al^{3+}. This is because of the ionic radius of Al^{3+} (5.0 nm) and its larger trivalent charges, result in a lower rate of diffusion of the ionic species through the cement sol when compared with Ca^{2+}. The other reason is both Ca^{2+} and Al^{3+} will readily form complexes

with fluoride (F^-) and because of aluminium-fluoride complexes are more stable than calcium fluoride so it can be formed preferentially. It is of note that there is relatively little free F^- in the sol at this stage.

The pH of the freshly mixed cement is around 2.6 and is rapidly rise during dissolution phase. During initial setting, intermolecular forces cause the polymer chain to be coiled into a tight ball. As the ionization reaction continues, the molecule becomes more polars in nature, and the polar forces developed during this phase result in the molecule adopting a more linear format. This allows for much greater access to the carboxylic acid (-COOH) groups by the metallic ions, thus allowing gelation to occur and hence enhancing the rate of setting.

The gelation phase is now regarded as due to chain entanglement as well as weak ionic cross-linking. This corresponds with the viscoelastic behavior of the freshly set cement. Studies confirmed that there is no sequential release of Ca^{2+} and Al^{3+}. Instead, these and other species are liberated together with differential rates of reaction in matrix formation[89, 90]. As the cement matures over the first 24 hours and beyond, progressive cross- linking occurs possibly with hydrated Al^{3+} since the sensitivity to moisture of the set cement decreases and the percentage of bound water and glass transition temperature increase[91, 92]. The final set structure (Figure 1) has been presented as a complex composition of original glass particles sheathed by siliceous hydrogel and bonded together by a matrix phase consisting of hydrated fluoridated calcium and aluminum polyacrylates[92].

2.1. The rate of acid-base reaction depends on four variables

2.1.1. Temperature

Working time can be increased due to the cold temperature for instance the cold mixing slab while mixing. However the cold temperature does not affect the physical properties of material[93].

2.1.2. Physical Presentation of the Powder

The rate of reaction will be influenced by powder: liquid ratio and the surface area of the powder[94].

2.1.3. Availability of Fluoride Ions

The large F^- inclusions in low fusion temperature glass are attacked by the poly-acid, giving rapid release of F^-[95]. This results in binding of metal cations to the polyanion chain, release of hydrogen ions with the maintenance of low pH and release of fluoride to form complexes with Al^{3+}.

2.1.4. The Presence of Tartaric Acid

Tartaric acid is an acid chelating agent which aids in extraction of cations from the glass, suppressing the ionization and unwinding of polyacid chain. It also ensures a buildup of metallic ions from cross link. Thus will retard the onset of the setting reaction and prolong the working time[88].

In summary, the setting reaction of GIC results in ionic cross linking between the polyacid chains, giving a rigidly bound polyacid/salt matrix. The initial cross linking is performed by the more readily available Ca^{2+}. This markedly increases the viscosity of the freshly mixed cement, and is responsible for much of the early 'clinical setting' of the material. However the divalent linkages are not as stable as they should be and the setting reaction continues with further cross linking by the less mobile trivalent Al^{3+}. This latter phase produces a rise in the physical properties and results in a stable hard brittle material with a highly cross linked polyacid salt matrix.

3. Properties of Glass Ionomer Cements

GICs have desirable properties, such as adhesion to moist tooth structure and an anticariogenic action (due to fluoride release). In addition, the coefficient of thermal expansion for GICs is close to that of tooth structure and they are

biocompatible. Because of these unique properties, GICs are very useful and important as dental restorative materials. In addition to their advantages, GICs suffer from the disadvantage of being brittle. Significant improvements have been made. Although stronger and more aesthetic materials with improved handling characteristics are now available, lack of strength and toughness are still major problems.

3.1. Mechanical Strength[96]

Three mechanical strength tests (compressive strength, flexural strength, and diametral tensile strength) are usually used for GICs. Since GIC would only fracture at the atomic level by tensile or shear fracture so it is considered measuring of compressive strength had no fundamental meaning. Many brittle dental materials have tensile strength markedly lower compare to compressive strength. These materials fail by crack propagation that is favored by tensile rather than compressive loading. Prosser *et al*[97] suggested that the most appropriate measure of the strength of the GICs is obtained with a flexural test. While direct measurements of tensile strength are difficult to brittle materials, it has been suggested that the measurement of flexural strength offers the best practical and reliable estimate of tensile strength.

3.2. Adhesion to Enamel and Dentin[98]

Determination for adhesion or sealing ability of dental materials requires two tests, a bonding test and a microleakage test. The rationale behind bond strength testing is that the higher the actual bonding capacity of an adhesive, the better it will withstand such stresses and the longer the restoration will survive *in vivo*.

Bond strength test is relatively easy and fast. However bond strength is a material property and the data obtained from the tests largely depends on the actual test set-ups which make the results unable to be compared between studies[99]. Most commonly, bond strength is measured by subjecting materials bonded-to enamel/dentin to tensile or shear stress. However, at bond strength values higher than 20 MPa in a shear test, cohesive failures of the substrate will more likely occur[100].

Marginal leakage has been defined as the clinically detectable passage of bacteria, fluids, molecules or ions between a cavity wall and the restorative materials[101]. Today's adhesives are incapable of completely sealing restorative margins and preventing long term microleakage[102].

A review in 2003[103] stated that theoretical mechanisms of adhesion include adsorption, involving chemical bonding (primary bond: ionic, covalent; secondary bonds: hydrogen, Van der Waals') and diffusion (bonding between mobile molecules across the interface)[104].

A fundamental requirement of effective adhesion in any adhesive technology is a clean substrate surface. In addition, the surface energy of the substrate (enamel and dentin) should exceed the surface tension of GIC. In the context of GIC, the tooth surface must free from biofilm, blood, saliva and other contamination. All cavities should be conditioned with an appropriate conditioned and polyacrylic acid 10% is the most appropriate. Polyacrylic acid conditioned will remove surface smear layer, leaving the smear plugs in the dentin tubule intact and increase the energy of the tooth surface which will enhance the wettability by the freshly mixed GIC.

Placement if the freshly mixed GIC onto the conditioned calcified tissue results in an initial polar attraction, with weak hydrogen bonds predominating. The free acid in the cement dissolves any residual smear layer but will be minimal demineralization because of the buffering action of the PO_4^{3-} from HA and because of polyacrylic acid is quite weak. As PO_4^{3-} is displaced from HA, Ca^{2+} is also displaced in order to maintain electrolyte balance and both $Ca^{2+}$and PO_4^{3-} are adsorbed into the cement. This results in an "ion-exchange" layer[105] which is strongly bound to the hard tissue and to the cements. The nature of this layer had been investigated by several authors[105-108].

In 1999, Sennou[109] investigated this layer using x-ray photoelectron spectrometry (XPS), and the name "interphase" was given. The interphase was found to

consist of “reciprocal diffusion” of ions from GIC and dentin. The dentin yielded $Ca^{2+}$and PO_4^{3-} and the GIC yielded Al^{3+}, silica and fluoride ions, together with $Ca^{2+}$and/ Sr^{2+} depending on the glass composition. A further XPS study[110] clearly demonstrated a chemical bond between the COO^- of polyalkenoic acid and the Ca^{2+} component of HA. The COO^- was found to replace PO_4^{3-} of the HA in creating these ionic bonds and about 68% of the COO^- became bonded. Geiger[111], using Fourier-transformed infrared spectroscopy, identified this layer as “fluoridated carbonatoapatite”.

Chemical bonding occurs through the forming of ionic bonds between the carboxyl group (COO^-) of the polyalkenoic acid and $Ca^{2+}$of HA remain around the exposed surface collagen. The COO^- group played an important role in bonding because it entered the structure of HA by displacing the PO_4^{3-}. Hence the adhesion is permanent because of the development of a multiplicity of adhesive groups that are connected by covalent bonds. Once the material has matured, any failure will be cohesive within the GIC matrix (the weaker material), leaving behind the ion-enriched layer bonded to the dentin and enamel at the restoration/tooth interface.

Currently, GIC remains as the only material that is self- adhesive to tooth structure. The actual auto-adhesion to tooth structure may be from micromechanical interlocking by shallow hybridization of the micro-porous, hydroxyapatite coated collagen fibril network and the true primary chemical bonding. Ion exchange adhesion between tooth structure and GIC occurs because of the presence of the polyalkenoic acid in the freshly mixed cement. The ions are released from both the glass particles (Ca^{2+} and Al^{3+}) and the tooth structure ($Ca^{2+}$and PO_4^{3-}). These released ions serve to buffer the acid, effect the initiation of setting, and produce an ion-enriched interfacial layer firmly attached to both the restoration and the tooth.

3.3. Fluoride release and ion-exchange

Ion migration within or through any material can only occur in the presence of water. Since GIC is water-based, numerous studies have reported

continuing release of fluoride from set GIC over prolonged periods and higher levels of fluoride release from GIC as compared to other fluoride-containing restorative materials. Initial fluoride release levels also likely reflect dissolution of small amounts of the material mass from the surface during the minimally mature stage when solubility of the material is highest.

A review in 2011[112] stated that fluoride in the surrounding environment has been shown to provide a situation conductive remineralization and a subsequent cariostatic effect. Laboratory findings indicate that a fluoride concentration of 2 mg/L (2 ppm) inhibits the formation of carious lesions by inhibiting bacterial plaque formation and encouraging the formation of fluorhydroxyapatite which is resistant to the acid dissolution[113].

Additionally, uptake of fluoride by enamel and dentin walls adjacent to GIC restorations has been demonstrated in both *in vitro* and *in vivo* studies. The high level of fluoride release observed in the day immediately following restoration placement reflects release of fluoride from the exposed glass particles at the outer surface of the restoration.

These properties of GICs give rise to a variety of clinical indications but no materials can be regarded as a prevention or cure for caries. However, GIC is most valuable in assisting the healing of remaining tooth structure that has been demineralized and damaged.

4. The Biocompatibility of Glass Ionomer Cements[114]

GICs have been in use since the 1970s. It is critical to assess the biocompatibility of any restorative material as there is contact with living tissues (pulp, dentin, gingival/oral mucosa) for a prolong period of time. For the intracoronally-placed dental materials, the presence of dentin is critical to the biological response seen the

pulp when a material is placed on the dentin[115]. Many materials contain components which can move into the biophase before, and in some cases after, setting and such material may be cytotoxic when placed in close contact with cells. The rate of permeation of substances through dentin depends on the molecular size of the products and its component, the surface area available for diffusion, the patency of dentinal tubules and the remaining dentin thickness[116]. Moderate thickness of dentin (1mm or more) can protect pulp cells in vivo from the chemical components of such materials and in experimental settings dentin thickness of 500 μm prevented major diffusion. Permeability characteristics increased exponentially with increasing dentin thickness[117]. Toxicity may be regarded as only one reason for non-biocompatibility of a dental material[54] and dental materials in contact vital tissue ought to be tested for their biocompatibility prior to general use.

The most important standard for dental products in terms of biocompatibility regulation is ISO 10993. Tests developed for dental materials are described in ISO 7405. *In vitro* tests are conducted mainly to evaluate the cytotoxicity (cell damage) and often preferred to measure biocompatibility aspects in the early stages of assessment of a new material, in the interests of time, cost and ethics.

Important issues with GICs which ought to be assessed and resolved when considering biocompatibility are degradation products, pH, cytotoxicity and host response and tissue reaction over time such as the biological effects of movements of ions and other compounds on the immediate environment (dentin, pulp and gingival response).

4.1. Degradation Products and pH

Various ions leached out from GICs at the different times and in different condition. The species that may be released from the GICs are F^-, sodium silicon, Ca^{2+}, Sr^{2+} and Al^{3+} [118-120]. The release of fluoride from GICs is well documented[121-123]. The first and greatest interaction between the material and tooth tissue is likely to be the time of

initial contact at the unset condition. A study reported the leaching ions at the high concentration and at low pH in the unset cement decreases as the set condition is approached[119]. However the cytotoxic of eluate from GICs has been studied and there is some evidence that dentin prevents the diffusion of strong acids.

Because of the acid component has pH at 1.9 and the initial set of the earlier GICs was slow, as Ca^{2+} and then Al^{3+} were leached from the glass, the pH will be at 2.0 at 5 minute and 3.0 at 10 minute[124]. The newer generation of GICs is much faster setting so perhaps the pH problem may be resolved. The pH within the first 24 hours is around 4.0-5.5, however, studies of direct pulp capping with GIC show it to be less well tolerated and less clinically successful than $Ca(OH)_2$[125, 126]. A study of using GIC in the ART involving in minimal tooth preparation followed by sealing with GIC, dentin sampled from primary molar cavities before and after treatment was shown to contain fewer bacteria and higher calcium content[127] . Finally, it appears that GICs are capable of causing the release of bioactive molecules from the dentin to contribute to the process of dentin regeneration and pulpal healing.

4.2. Cytotoxicity of GICs

In general, GICs are cytotoxic in culture when placed in direct contact with cells however when applied *in vivo* in the absence of bacteria, after an initial inflammatory response tertiary dentin formation is evident and the pulp remains healthy[128].

The earlier versions of GICs were toxic when freshly prepared but this decreased with time after setting until they were non-toxic at 24 hours[124]. Another *in vitro* study found freshly mixed GICs were toxic to fibroblasts[129]. However until to date, the great range of responses to different products make it rather difficult to arrive at a conclusion as regards to the biocompatibility of GICs and should be implied that biocompatibility testing should be conducted on every product and repeated on materials with new formulations.

5. Apatite Modified Glass Ionomer Cements

GIC is known for its relative ease to use, chemical bonding to tooth substrate, fluoride ion release and recharge, low coefficient of thermal expansion and acceptable esthetic quality[130]. GIC was also found to be biocompatible with pulp tissue[128]. However, the use of GIC is limited due to its relatively inferior mechanical properties and sensitivity to initial desiccation and moisture[131].

In the recent years, HA has shown promising advantages in restorative dentistry. Since its excellent biocompatible properties, and a composition and crystal structure similar to apatite in the human dental structure and skeletal system, a number of studies have tried to evaluate the effect of the addition of HA powders to restorative dental materials such as GICs[9, 132, 133]. GICs have been found to interact with HA via the carboxylate groups in the polyacid. Therefore, the incorporation of HA into GICs may not only improve the biocompatibility of GICs, but also have the potential of enhancing the mechanical properties. In addition, it has the ability to increase the bond strength to tooth structure due to its similar composition and structure to enamel and dentin.

A study[9] reported that HA whiskers can be used as strengthening material for GIC. Addition of sufficient amount of HA whiskers and granules may increase the flexural strength and improve microstructure of GIC[132]. This study found that addition of HA into GIC enhanced and hastened the rate of development of fracture toughness of the cement. Moreover, it also maintained long-term bond strength to dentin and did not impede sustained fluoride release. Another study also reported that the addition of HA did not hamper continued fluoride release and maintained long-term bond strength to dentin[133]. Gu *et al*. found GICs containing 4% by weight HA particles exhibited improved mechanical properties in comparison with commercial GICs[134]. The recent report showed the addition of HA in GIC resulted in a constant level of compressive strength, working and setting time. Recently the development of HA-ionomer bioactive cement, where HA was incorporated into GIC, demonstrate the increased hardness[135].

From the above literature review, several points needed to be stated and used for the rationale for this research.

a) Many NCPs and growth factors are sequestered within the dentin structure during development.

b) Many of the bioactive molecules have been shown to have a role in dentin mineralization as well as dentin remineralization.

c) The ability to extract these potentially bioactive molecules from the dentin structure to facilitate their interaction with pulpal cells has the potential to naturally enhance the process of repair of the pulp-dentin complex.

d) It appears that current GICs, and potentially other acidic dental materials, are capable of causing the release of bioactive molecules from the dentin to contribute to the process of dentin regeneration and pulpal healing.

e) Currently, GIC remains as the only material that is self- adhesive to tooth structure. Chemical bonding occurs through the forming of ionic bonds between the COO^- of the poly-alkenoic acid and Ca^{2+} of HA that remain around the exposed surface collagen.

f) GICs have desirable properties, such as adhesion to moist tooth structure and an anticariogenic action (due to fluoride release). However major disadvantage is brittleness and lack of toughness.

g) GICs have been found to interact with HA in dentin via the COO^- in the polyacid. Incorporation of HA particles into GICs demonstrated the improved fracture toughness and may have the ability to increase the bond strength to tooth structure due to its similar composition and structure to enamel and dentin.

h) CO_3^{2-} in bone plays a role in the biochemistry of hard tissue.

i) $Mg^{2+}$was founded to relate with the bioadhesion behavior of integrin and seems to be an important factor controlling *in vivo* bone metabolism.

j) Mg^{2+} and CO_3^{2-} in solution cause synergistic effects in disturbing apatite lattice, decreasing its crystallinity and consequently increasing the dissolution rate.

k) FN had an important role for the terminal differentiation of odontoblasts from undifferentiated cells present in dental pulp.

l) Ca^{2+} released from dental materials especially from apatite can migrate to pulp tissue and elevate extracellular calcium ion concentrations. This elevation induces FN synthesis of pulp cells.

CHAPTER III

MATERIALS AND METHODS

Instruments and Materials

1) Amalgamator (Ultramat 2, SDI, Melbourne, Victoria, Australia)
2) Apatite apparatus (Hiroshima University, Hiroshima, Japan)
3) Capsulefuge (PMC-060, TOMY, Tokyo, Japan)
4) Centrifuge (MX-300, TOMY, Tokyo, Japan)
5) CO_2 incubator 37ºC (MCO-18AIC(UV), SANYO, Tokyo, Japan)
6) Digital Balance (40SM-200A, Precisa, Dietikon, Switzerland)
7) Digital Balance (CP 225D, Sartorius, Goettingen, Germany)
8) Digital Caliper (Micrometer, Mitutoyo, Japan)
9) Peltier thermal cycler (DNA engine® PTC-200, Bio-Rad Laboratories, UK)
10) Fine coater (JFC-1200, JEOL, Tokyo, Japan)
11) Fluoride Selective Electrode (SL518, Select Bioscience, Essex, UK)
12) Fourier Transform Infrared Spectrometer (FT-IR) (FT-IR 8400S, Shimadzu Co. Ltd., Kyoto, Japan)
13) Indenter, 400±5 g flat end (needle size 1.0±0.1 mm) (King Mongkut's Institute of Technology Latkrabang, Bangkok, Thailand)
14) Incubator 8-100ºC (Contherm160M, Contherm Scientific Ltd., Petone, Wellington, New Zealand)
15) Inductively Couple Plasma-Optical Emission Spectrophotometer (ICP-OES) (OPTIMA 7300, PerkinElmer, Shelton, CN, USA)
16) Lamina flow (clean bench type ccv form 811B, SANYO, Tokyo, Japan)
17) Low Speed Cutting Machine (ISOMET 1000, Buehler, Lake Bluff, IL, USA)
18) Microplate Reader (Bio-Rad Model 680, Bio-Rad Laboratories, UK)
19) Microscope used for cell count (YS100, Nikon, Tokyo, Japan)
20) Microscope used for seeing cells (T1AHX2, Nikon, Tokyo, Japan)

21) Mobile Unit (Super Mobile 85, T.D.P., Bangkok, Thailand)
22) Spectrophotometer (NanoDrop™ 1000, Thermo Fisher Scientific, DE, USA)
23) Orbital shaker (LABO SHAKER BC-740, Bio craft, Tokyo, Japan)
24) Plate spinner (PlateSpin, Kubota Corp., Tokyo, Japan)
25) Polishing Machine (DPS 3200, PACE TECHNOLOGIES, Tuscon, AZ, USA)
26) Quantitative Real-time PCR machine (Step One Plus™ 7500 Fast, Applied Biosystems, Tokyo, Japan)
27) Scanning Electron Microscope (SEM) (JSM-5410LV, JEOL, Tokyo, Japan)
28) Stereomicroscope (SZH10, OLYMPUS OPTICAL Co. Ltd., Tokyo, Japan)
29) Thermo-cycling machine (TC301+CWB332R+HWB332R, King Mongkut's Institute of Technology Latkrabang, Bangkok, Thailand)
30) Ultrasonic Disrupters (UR-20P, TOMY, Tokyo, Japan)
31) Universal Testing Machine (EZ-S, SHIMADZU, Kyoto, Japan)
32) Universal Testing Machine (LR 10K, LLOYD Instruments, Fareham, Hants, UK)
33) Versatile refrigerated centrifuge (AX-310, TOMY, Tokyo, Japan)
34) Vortex Genie2 (Scientific Industries Inc., NY, USA)
35) Water bath (Incubator personal, TAIYO, Osaka, Japan)
36) X-ray photoelectron spectroscope (XPS) (AXIS-HS, Kratos, Manchester, UK)
37) 0.5 mL nuclease-free thin wall tube (Sigma Aldrich, St. Louis, MO, USA)
38) 10 cm culture dish, Costar® (Corning Inc., MA, USA)
39) 2.0 mL microcentrifuge tube (eppendorf) (Sigma Aldrich, St. Louis, MO, USA)
40) 96-well plate, Costar® (Corning Inc., NY, USA)
41) 96-well plate, SUMILON MS-8596F (Sumitomo Bakelite, Tokyo, Japan)
42) Diamond bur, S835010 (Edenta AG, AU/SG, Switzerland)
43) Fast SYBR® Green Master Mix (Applied Biosystems, Tokyo, Japan)
44) Filter paper (Whatman® No.1, Sigma Aldrich, St. Louis, MO, USA)
45) Filter paper (ADVANTEC® No. 5A, Advantec MFS Inc., Dublin, CA, USA)
46) High Capacity RNA-to-cDNA Kit (Applied Biosystems, Tokyo, Japan)
47) Human collagen type I ELISA kit (COSMO BIO CO., LTD., Tokyo, Japan)

48) Metal block 8.0×7.5×10 mm (King Mongkut's Institute of Technology Latkrabang, Bangkok, Thailand)

49) MicroAmp™ 96-Well Support Base (Applied Biosystems, Tokyo, Japan)

50) MicroAmp™ Fast Optical 96-Well Reaction Plate (Applied Biosystems, Tokyo, Japan)

51) MicroAmp™ Optical Adhesive Film (Applied Biosystems, Tokyo, Japan)

52) Minisart® syringe filter 0.2 μm (Sartorius Stedim Biotech, Goettingen, Germany)

53) Silicon carbide abrasive paper P 600 (Buehler GmbH, Düsseldorf Germany)

54) Silicone mold size (3.0±0.1) mm height and (4.0±0.1) mm diameter (King Mongkut's Institute of Technology Latkrabang, Bangkok, Thailand)

55) Silicone mold size (6.0±0.1) mm height and (4.0±0.1) mm diameter (King Mongkut's Institute of Technology Latkrabang, Bangkok, Thailand)

56) Stainless spilt mold and plates, mold size (6.0±0.1) mm height and (4.0±0.1) mm diameter (King Mongkut's Institute of Technology Latkrabang, Bangkok, Thailand)

57) Stainless split mold size 2.5×5.0×20 mm (Dankook University, Korea)

58) Transwell® Permeable Support, 8.0 μm Polycarbonate Membrane, 24 mm Insert, 6-well plate, Costar® (Corning Inc., NY, USA)

59) Transwell® Permeable Support, 8.0 μm Polycarbonate Membrane, 6.5 mm Insert, 24-well plate, Costar® (Corning Inc., NY, USA)

60) 0.01 M Tris HCl (pH 8.8)

61) 0.04% Triton-X (Wako Pure Chemical Industries, Osaka, Japan)

62) 0.5 L 0.06 M $(NH_4)_2CO_3$

63) 0.5 L solution 0.12 M $NH_4H_2PO_4$

64) 0.5 L solution of 0.01 M $Mg(CH_3COO)_2 \cdot 4H_2O$

65) 0.5 L solution of 0.2 M $Ca(CH_3COO)_2 \cdot H_2O$

66) 0.5 mM p-nitrophenyl phosphate (pNPP)

67) 0.5% Chloramine-T trihydrate bacteriostatic/bacteriocidal solution)

68) 1 L of 1.3 M CH_3COONH_4

69) 1% alizarin red S in 0.1% NH_4OH (pH 6.4)

70) 1.0 M Tris HCl (pH 9.0)

71) 1.8% NaCl

72) 10 mmol/L β-glycerophosphate (β-GP) (Sigma Aldrich, St Louis, MO, USA)

73) 10% Fetal Calf Serum (FCS) (JRH Bioscience, Lenexa, KS, USA)

74) 100% ethanol (-20°C)

75) 150 mM acetic acid solution

76) 150 mM NaCl

77) 200 mM Tris HCl

78) 5 mM $MgCl_2$

79) 50 μg/mL ascorbic acid

80) 50 mM acetic acid solution

81) 60 mg/mL kanamycin (henceforth denoted standard medium)

82) ALP standard

83) Amalgam capsule

84) Chloroform

85) Dehydrate ethanol

86) DEPC-treated 75% ethanol

87) Diethylpyrocarbonate (DEPC) treated water

88) Distilled water

89) Double distilled water (ddH_2O)

90) GC dentin conditioner (GC, Tokyo, Japan)

91) GC varnish (GC, Tokyo, Japan)

92) Glass ionomer cement liquid, Fuji IX® GP Gold Label, Lot 1106211 (GC, Tokyo, Japan)

93) Glass ionomer cement powder, Fuji IX® GP Gold Label, Lot 1106211 (GC, Tokyo, Japan)

94) Isopropanol

95) Methylene blue

96) Nail varnish

97) Pepsin powder

98) Phosphate Buffer Saline (PBS)

99) Potassium Bromide (KBr)

100) Primers for COL1A1, DMP-1, DSPP

101) RNAbee (TEL-TEST, Friedswood, TX, USA)

102) TISAB III (Orion Research Inc., Beverly, MA, USA)

103) Trypsin (0.05%)-ethylenediaminetetraacetic acid (0.53 mmol/L) solution (Trypsin EDTA)

104) Ultrapure PCR water

105) WST-1 reagent (Roche Applied Science, Mannheim, Germany)

106) α-Modified Eagle's Medium (α-MEM) (Nikken Biomedical Laboratory, Kyoto, Japan)

107) Human premolar teeth

108) Human dental pulp cells (Osaka University Graduate School of Dentistry, Osaka, Japan)

Methods

1. Synthesis of Magnesium Carbonate Apatite ($MgCO_3Ap$)

1.1. $MgCO_3Ap$ was synthesized at 60±1°C and pH 7.4±0.2 using a gradient magnesium supply system with apatite apparatus (Figure 4) as described by Yamazaki[10].

1.2. Solution A was a mixture of a 0.5 L solution of 0.2 M calcium acetate monohydrate ($Ca(CH_3COO)_2 \cdot H_2O$) and a 0.5 L solution of 0.01 M magnesium acetate tetrahydrate ($Mg(CH_3COO)_2 \cdot 4H_2O$).

1.3. Solution B was a mixture of a 0.5 L 0.12 M ammonium dihydrogen phosphate ($NH_4H_2PO_4$) and a 0.5 L 0.06 M ammonium carbonate ($(NH_4)_2CO_3$).

1.4. Both solutions were stirred in a 1 L of 1.3 M ammonium acetate (CH_3COONH_4) for 3 hours and then kept at room temperature for a day.

1.5. $MgCO_3Ap$ powder was separated by filter paper (ADVANTEC® No. 5A, Advantec MFS Inc., Dublin, CA, USA), washed with distilled water, and dried at 60°C for another 24 hours.

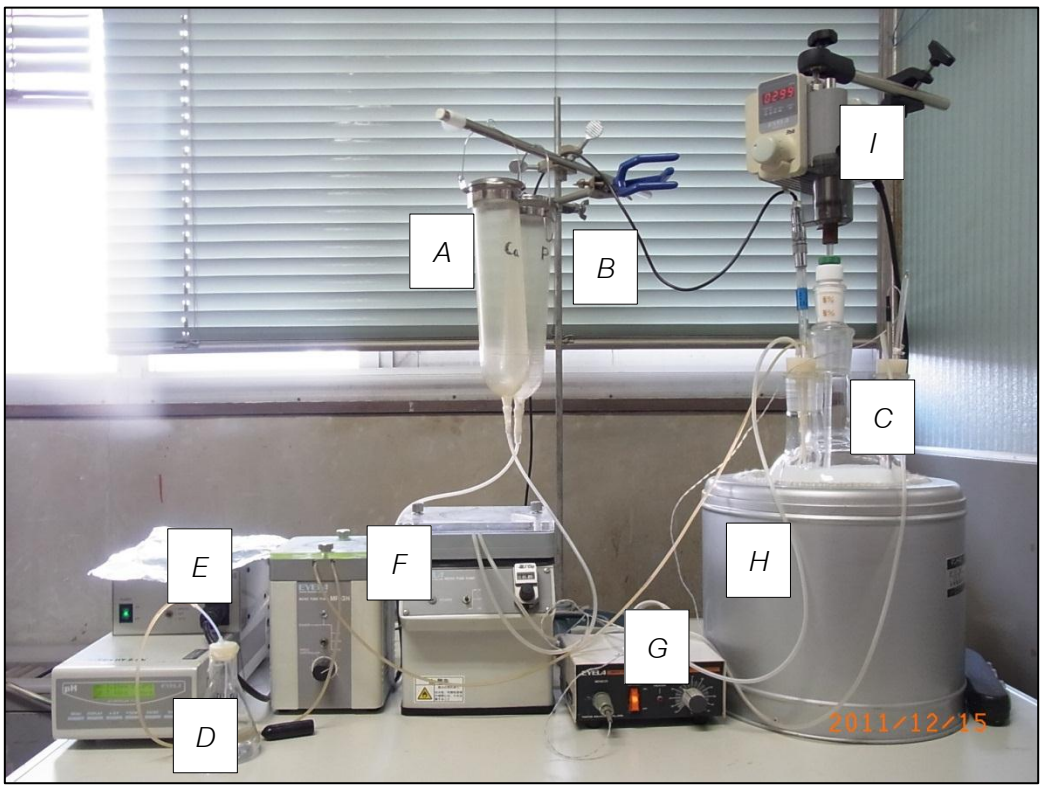

Figure 2 *Apatite Apparatus*

A=Solution A, B=Solution B, C=CH_3COONH_4, D=NH_4OH, E=pH controller at 7.4, F=Microtube pump, G=Temperature controller at 60°C, H=Heater, I=Motor.

2. Cement Preparation

2.1. Test powder was prepared by encapsulated mixing of 2.5% by weight of $MgCO_3$Ap powder with glass ionomer cement (GIC) powder (Fuji IX GP® Gold label, GC, Japan) using an amalgamator (Ultramat2, SDI, Melbourne, Victoria, Australia) at a speed of ± 4000 rpm for 5 seconds.

2.2. All control and test cements were prepared by encapsulated mixing of control powder or test powder with Fuji IX GP® Gold label liquid respectively at powder liquid ratio of 3.6:1 using the amalgamator for 10 seconds at 23±1°C, 50±10%RH.

Table 1 Formulation

Formulation	GIC powder (%wt)	$MgCO_3Ap$ (%wt)
Control powder	100	0
Test powder	97.5	2.5

3. Characterization and Chemical Analysis

3.1. Particle size and morphology of $MgCO_3Ap$ powder and GIC powder were observed under scanning electron microscope (SEM) (JSM-5410LV, JEOL, Tokyo, Japan) (Figure 3) after dried and gold coated with Fine coater (JFC-1200, JEOL, Tokyo, Japan).

3.2. The absorption band of $MgCO_3Ap$ powder was carried out by Fourier transformed infrared spectroscopy (FTIR) (FT-IR 8400S, Shimadzu Co. Ltd., Kyoto, Japan) (Figure 4) by diffuse reflectance method at concentration: 1 mg/100 mg KBr with number of scan at 100 and recorded in a range of 4000- 400 cm^{-1}.

3.3. $MgCO_3Ap$ powder and test cement specimen (1 mm thickness) (Figure 5) were analyzed quantitatively for the chemical composition using an X-ray photoelectron spectroscope (XPS) (AXIS-HS, Kratos, Manchester, UK) (Figure 6) under 10^{-7} Pa.

Figure 3 Scanning Electron Microscope (JSM-5410LV)

Figure 4 Fourier Transform Infrared Spectrometer (FT-IR 8400S)

a)  b) 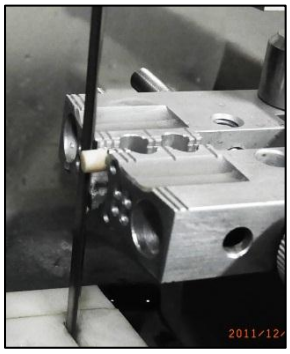 c) 

Figure 5 Specimen Preparation for XPS Analysis

a) $MgCO_3Ap$ powder in a stub, b) Prepare test cement specimen (1 mm thickness), c) Test cements in a stub.

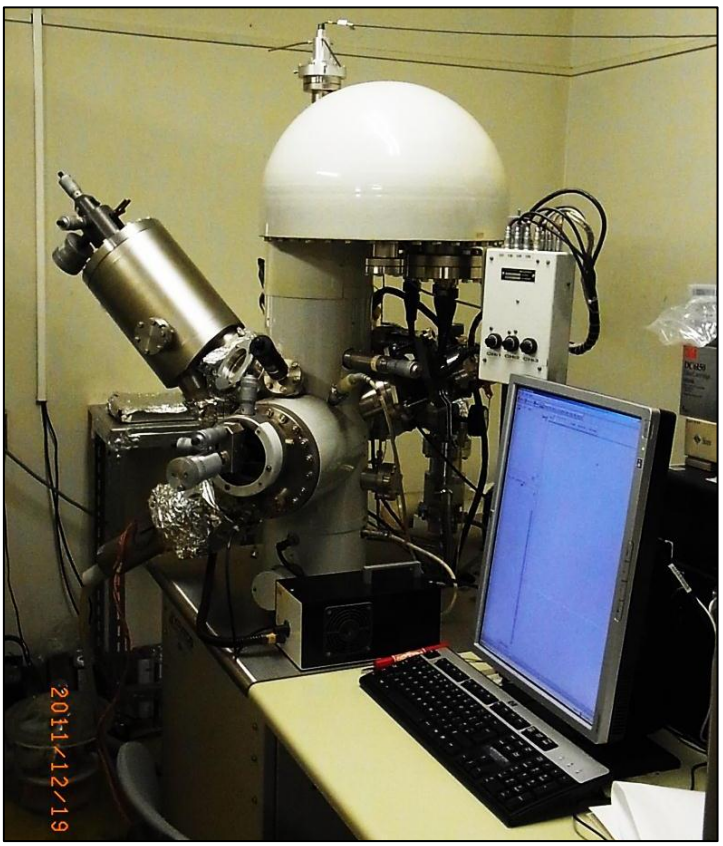

Figure 6 X-ray Photoelectron Spectroscope (AXIS-HS)

4. Setting Time

4.1. The test protocol was conducted according to ISO 9917.

4.2. Control cements (n=5) and test cements (n=5) were mixed and loaded into a metal block of 8.0×7.5×10 mm on a glass slab and flattened the surface with a glass slide.

4.3. Sixty seconds after the end of the mixing, the specimens were transferred to an incubator at 37±1°C and 95±5% RH.

4.4. At ninety seconds after the end of the mixing, each specimen was loaded by indenter with load of 400±5 g positioned with flat end needle (1.0±0.1 mm) (Figure 7) perpendicular to the long axis of the needle for 5 seconds. The same procedure was repeated at 10 second-intervals on different position.

4.5. The net setting time was the time elapsed between the end of mixing and the time when the needle failed to make a complete circular indentation on the cement surface.

4.6. Treatment of the result, all specimens should have net setting time between 1.5-6 minutes.

Figure 7 Indenter, 400±5 g Flat End (Needle Size 1.0±0.1 mm)

5. Compressive Strength Test

5.1. The test protocol was conducted following the method described in ISO 9917 with five specimens per group.

5.2. Sixty seconds after mixing, cements were loaded in a split stainless steel mold (6±0.1 mm height and 4±0.1 mm diameter) (Figure 8a) which was conditioned with 100% pure petroleum jelly.

5.3. Within 120 seconds after the end of mixing, cements were packed in the molds, covered with the plates (Figure 8b), clamped (Figure 9) and transferred to cabinet at 37±1°C and 100% relative humidity (RH).

5.4. One hour after the end of mixing, the plates were removed. Surfaces of the cements were ground with wet 400 grade silicon carbide paper. Then specimens were removed and stored in water at 37±1°C for another 23 hours.

5.5. The compressive strength was measured using a universal testing machine (LR 10K, LLOYD Instruments, Fareham, Hants, UK) (Figure 10) at a crosshead speed of 1 mm/minute.

5.6. The maximum load at fracture was used to calculate the compressive strength (N/mm^2, MPa) using the equation $CS = 4F/\pi pd^2$ while F is the failure load and d is the diameter of the specimen.

5.7. Treatment of the result, at least four of five results are above 100 MPa.

a) 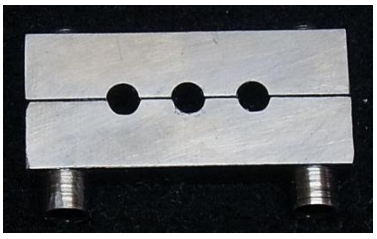 b) 

Figure 8 Stainless Steel Split Mold for Compressive Strength Test
a) Stainless split mold, b) Plates

Figure 9 Clamp for Compressive Strength Test

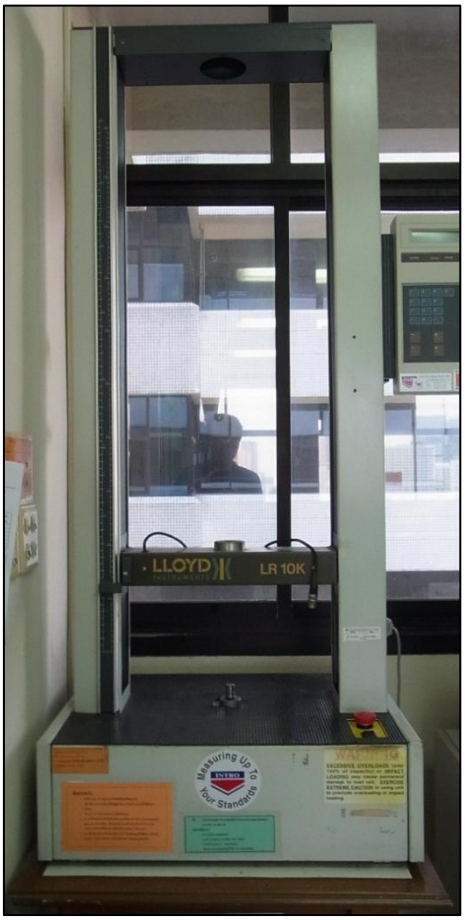

Figure 10 Universal Testing Machine (LR 10K)

6. Fracture Toughness

6.1. The test was conducted according to the method outlined in ASTM specification E-399-90 for single-edge notch specimens loaded in transverse bending.

6.2. Twenty eight single edge notch specimens (n=14/group) with dimension of 25×2.5×5.0 mm, 0.5 mm notch width and 2.5 mm depth were prepared in a stainless steel split mold (Figure 11).

6.3. Cements were prepared by encapsulated mixing and condensed into the mold. Celluloid strips were used to cover the surfaces under the load for 10 minutes.

6.4. Set specimens were removed from the mold and five specimens from each group were immediately tested at 15 minutes after mixing.

6.5. The rest of the specimens were stored at 37°C in 100% RH for another 50 minutes and then kept in distilled water for another 23 hours prior to testing.

6.6. Three-point bending test was carried out using a Universal Testing Machine (EZ-S, SHIMADZU, Kyoto, Japan) (Figure 12) at a crosshead speed of 0.5 mm/minute.

6.7. Fracture toughness, K_Q (MPa·$m^{1/2}$) was calculated from the equation:

$$K_Q = \frac{P_Q S}{BW^{3/2}} F\left(\frac{a}{W}\right)$$

where P_Q is the peak load (kN), S is the span (cm), B is the specimen thickness (cm), W is the specimen width and a is the crack length (cm).

$$F\left(\frac{a}{W}\right) = \frac{3\left(\frac{a}{W}\right)^{1/2} \times \left[1.99 - \left(\frac{a}{W}\right)\left(1 - \frac{a}{W}\right)\left(1 - \frac{a}{W}\right)\right] \times \left[2.25 - 3.93\left(\frac{a}{W}\right) + 2.7\left(\frac{a}{W}\right)^2\right]}{2\left[1 + 2\left(\frac{a}{W}\right)\right]\left[1 - \left(\frac{a}{W}\right)\right]^{3/2}}$$

6.8. The mean and standard deviation were calculated and analyzed with independent t-test.

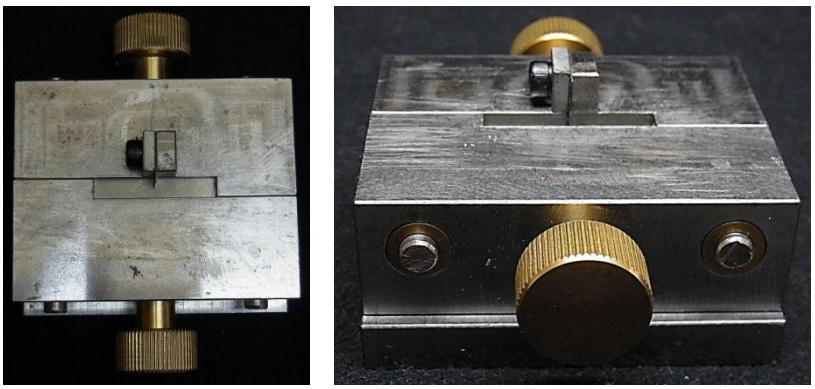

Figure 11 Stainless Steel Split Mold for Single Edge Notch Technique

a)  b) 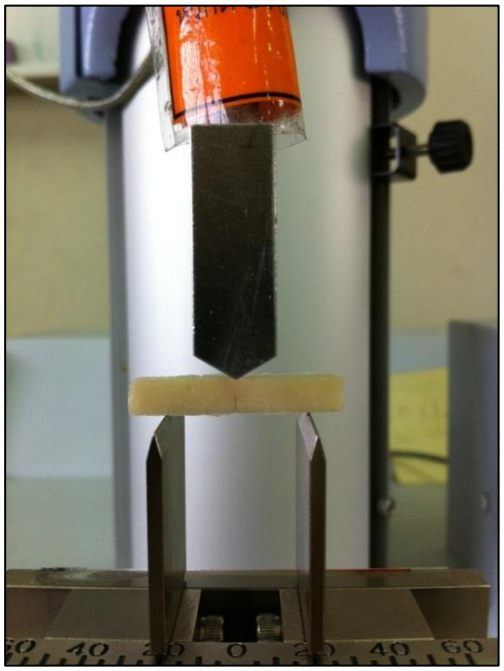

Figure 12 Universal Testing Machine (EZ-S)

a) Universal testing machine, b) Three-point bending test

7. Microleakage Test

7.1. Method was performed according to ISO/TS 11405:2003 (E) and approved by Ethical Committee of Faculty of Dentistry, Chulalongkorn University, Bangkok, Thailand (91/2544).

7.2. Twenty extracted human premolars (10 teeth/group) were collected and stored in a 0.5% chloramine-T-trihydrate bacteriostatic/bacteriocidal solution for one week then stored in distilled water at 4°C.

7.3. The cavity size of 3 mm occluso-gingivally and 3 mm mesio-distally with a 1.5 mm depth was prepared using a 1.0 mm diameter cylindrical diamond bur mounted on a high speed handpiece under copious water spray. The accurate size was examined using a Digital Caliper (Micrometer, Mitutoyo, Japan) at ±0.3 mm accuracy.

7.4. All cavities were located at the CEJ level with the occlusal margin in enamel and the gingival margin in either cementum or dentin.

7.5. The prepared cavities were conditioned with GC dentin conditioner (GC, Tokyo, Japan) for 20 seconds, rinsed with water and slurry dried.

7.6. Cements were mixed and filled into the cavities and surfaces coated with GC varnish (GC, Tokyo, Japan).

7.7. After coated and stored in 37°C water for 24 hours, teeth were submitted to thermo-cycling (TC301+CWB332R+HWB332R, King Mongkut's Institute of Technology Latkrabang, Bangkok, Thailand) (Figure 13) for 500 cycles at 5°C and 55°C at 20 seconds and 5 seconds dwell time.

7.8. After the thermo-cycling process, root apices of all teeth were sealed with wax and entire teeth surface was covered with two layers of nail varnish except the 1 mm area of the cavity margin.

7.9. The coated tooth specimens were soaked in a 2% methylene blue solution for 10 minutes, rinsed in running water, air-dried and then embedded in acrylic resin.

7.10. The experimented teeth were positioned in a Low Speed Cutting Machine (ISOMET 1000, Buehler, Lake Bluff, IL, USA) (Figure 14) and cut with a diamond saw under water coolant into three sections bucco-lingually (mesial, middle and distal sections).

7.11. The cut sections were determined under stereomicroscope (SZH10, OLYMPUS OPTICAL Co. Ltd., Tokyo, Japan) (Figure 15) at 40× magnification and classified the microleakage to 3 groups as follow:

0 = No penetration of the dye solution

1 = Infiltrate of the dye up to the enamel-dentin junction in the occlusal wall or penetration up to ¼ of the length of the gingival wall

2 = Penetration of the dye up to ½ of the length of the cavity wall

3 = Penetration of the dye extending for the total depth of the cavity wall

Figure 13 Thermo-cycling Machine (TC301+CWB332R+HWB332R)

Figure 14 Low Speed Cutting Machine (ISOMET 1000)

Figure 15 Stereomicroscope (SZH10)

8. Shear Bond Strength Measurement

8.1. Ten human extracted premolars (5 teeth per group) were used. Surface treated preparations and method used were conducted followed procedures outline in ISO/TS 11405:2003(E).

8.2. Teeth were cut mesio-distally with low speed cutting machine to generate 20 specimens.

8.3. After mounting in a resin holder, both buccal and lingual specimens were polished with Polishing Machine (DPS 3200, PACE TECHNOLOGIES, Tuscon, AZ, USA) using a median grit silicon carbide paper (Grade P600)

8.4. Prior to the cement application, each dentin surface was conditioned with GC dentin conditioner (GC, Tokyo, Japan) for 20 seconds, rinsed with water and slurry dried.

8.5. Mixed cements were applied into a silicone mold (3.0±0.1 mm height and 4.0±0.1 mm diameter) (Figure 16) attached to the prepared dentin surfaces.

8.6. The specimens were stored in 100% relative humidity at 37°C for 30 minutes and then in distilled water for 23.5 hours prior to the testing with a Universal Testing Machine (EZ-S, SHIMADZU, Kyoto, Japan). The shear bond test was conducted at a crosshead speed of 0.5 mm/minute with a shearing blade.

8.7. Shear bond strength was calculated by load at failure per specimen surface area.

8.8. Mode of failure for all specimens were determined by a SEM (JSM-5410LV, JEOL, Tokyo, Japan) after dried and gold coated with Fine coater (JFC-1200, JEOL, Tokyo, Japan) at 1.5 nm thick.

8.9. The mode of failure was classified as interfacial, cohesive in the cement, cohesive in dentin or mixed mode of failure.

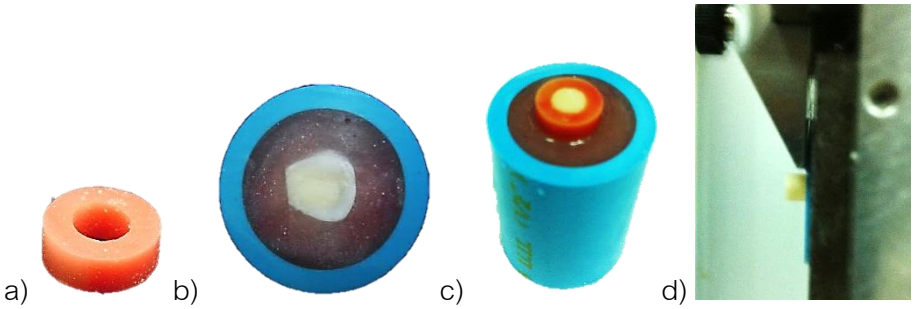

Figure 16 Specimen for Shear Bond Strength Measurement
a) Silicone mold diameter 4 mm height 3 mm, b) Prepared dentin surface, c) Cement in mold on dentin specimen, d) Specimen subjected to shear blade

9. Ion Release: Calcium, Magnesium, Fluoride

9.1. Three specimens per group were prepared by mixing and packing the cements into silicone mold size (6.0±0.1 mm height and 4.0±0.1 mm diameter).

9.2. Mixed cements were loaded to the mold on glass plate, covered with celluloid strip, pressed with another glass plate and put into the cabinet at 37°C 100% humidity for 1 hour before de-mold.

9.3. Suspended specimens in individually capped containers containing 20 mL deionized water and store at 37°C.

9.4. At 1, 2, 6, 12 hours and 1, 7, 14 days, specimens were dried with filter paper and transferred into 20 mL of fresh deionized water.

9.5. The concentration of Ca, Mg was measured from 10 mL eluate using Inductively Couple Plasma-Optical Emission Spectrophotometer (ICP-OES) (OPTIMA 7300, PerkinElmer, Shelton, CN, USA) (Figure 17)

9.6. For fluoride release, a 1 mL of buffer solution (TISAB III) was added to the 10 mL eluate, stirred and recorded with a fluoride selective electrode (SL518, Select Bioscience, Essex, UK).

Figure 17 Inductively Couple Plasma-Optical Emission Spectrophotometer (OPTIMA 7300)

10. Culture Medium Preparation

10.1. Fetal calf serum (FCS) (50 mL) (JRH Bioscience, Lenexa, KS, USA) was activated in 60°C water bath for 30 minutes and was sterilized by filtration using 0.20 μm Sterile Syringe Filter (Corning Inc., NY, USA).

10.2. Standard medium was prepared by adding 550 μL of 60 mg/mL kanamycin (henceforth denoted standard medium) and 50 mL sterilized FCS to 450 mL α-Eagle's minimum essential medium (α-MEM) (ICN Biomedicals Inc., Costa Mesa, CA, USA).

10.3. Mineralized medium was prepared by adding 20 μL of 50 μg/mL ascorbic acid and 200 μL of 10 mmol/L β-glycerophosphate (β-GP) (Sigma, St Louis, MO, USA) to standard culture medium.

10.4. Volume of culture medium used is described in Table 2

Table 2 Culture Medium Volume Used

Corning	Medium volume
10 cm dish	8 mL
6-well plate with Transwell®	4.5 mL
24-well plate with Transwell®	1.4 mL
96-well plate	0.2 mL

11. Cell Preparation

11.1. Cell culture method

11.1.1. Human Dental Pulp cells (HDP) was derived from Department of Periodontology, Osaka Graduate School of Dentistry and were recovered from -80°C.

11.1.2. Cells were cultured in 10 cm culture dish (Corning Inc., NY, USA) with 8 mL standard medium and incubated in 100% humidity at 37°C with 5% CO_2 incubator.

11.1.3. Culture medium was changed every 2 or 3 days until cells reached confluence.

11.2. Cell count

11.2.1. Culture medium was aspirated and cells were washed with phosphate buffer saline (PBS).

11.2.2. PBS was aspirated and cells were added with 3 mL Trypsin (0.05%)-ethylenediaminetetraacetic acid (0.53 mmol/L) solution (Trypsin EDTA). Cells were incubated in the incubator for 1-3 minutes and 3 mL of standard culture medium was added to stop Trypsin EDTA reaction.

11.2.3. Suspension was collected and transferred into new tube and centrifuged (AX-310, TOMY, Tokyo, Japan) with a speed of 1,200 rpm at 4°C for 5 minutes.

11.2.4. Supernatant was aspirated and culture medium (2 mL) was added to the tube and mixed well with pipette.

11.2.5. Suspension (20 μL) was mixed with 60 μL of Tryphan blue. They were pipetted up and down and then 10 μL of the mixture was transferred to the hematocytometer.

11.2.6. Cells were counted from the A, B, C and D part on hematocytometer (Figure 18) under microscope (4×). Total cells were calculated from the equation below.

$$Cells\ per\ mL = \frac{A + B + C + D}{4} \times dilution\ factor \times 10^4$$

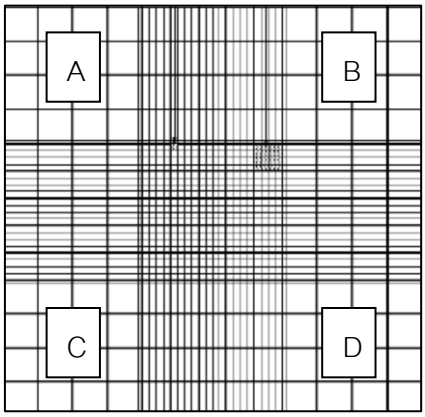

Figure 18 Hematocytometer under Microscope Divided into 9 Square Areas. Total cells were calculated from A+B+C+D.

12. Cytotoxicity Test: Cell Proliferation Reagent WST-1

Proliferation assays were used for analyzing the number of viable cells by cleavage of tetrazolium salts WST-1 to formazan (Figure 19).

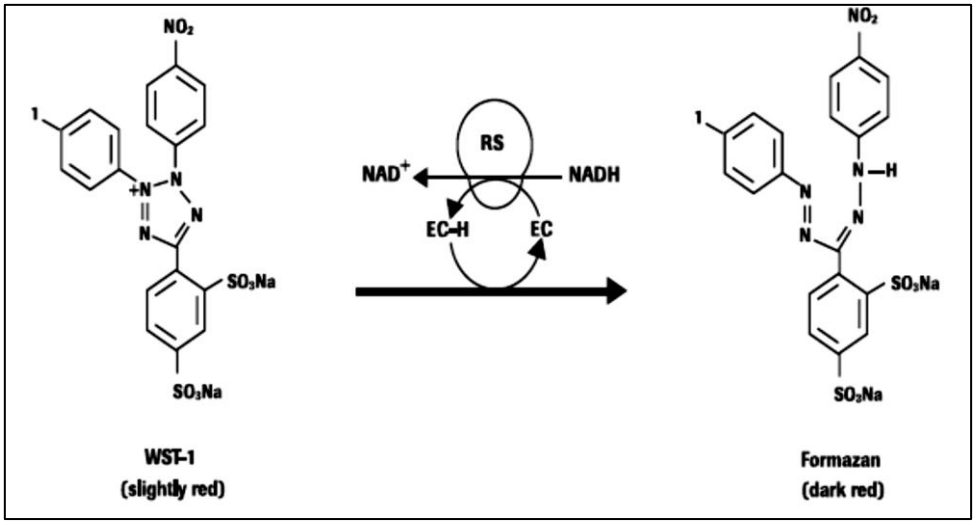

Figure 19 Cleavage of the Tetrazolium Salt WST to Formazan by Mitochondria Dehydrogenase from Viable Cells.
(Picture from Cell Proliferation Reagent WST-1 product information[136])

12.1. Eluate preparation for WST-1 assay

12.1.1. Eluates from control and test cements were collected for the proliferation assay.

12.1.2. Cements (n=3/group) were encapsulated mixed and packed into cylindrical mold (4 mm diameter and 6 mm height), covered with glass slides for 10 minutes and kept in the incubator at 37°C and 100% RH for 1 hour.

12.1.3. The cements were removed and then put into each eppendorf tube and stored in the incubator for another 23 hours. One mL of culture medium was added to each eppendorf with set cements and stored at -4°C.

12.1.4. Eluates were collected at day 1, 7 and 14 and sterilized using 0.2 μm sterile syringe filter before applying onto the wells with cells.

12.2. Assay procedure

12.2.1. Cells (1×10^4 cells/well) were seeded in a 96-well plate with 200 μL culture medium, and cultured in the incubator for 24 hours.

12.2.2. Supernatant was aspirated and replaced with 200 μL prepared eluates and cultured for another 24 hours.

12.2.3. WST-1 reagent was prepared by mixing the electron mediator solution with the entire vial of WST-1 reagent.

12.2.4. The prepared WST mixture was mixed by adding fresh culture medium in 1:10 ratio to WST-1 reagent and then filtered.

12.2.5. A mixture of 200 μL of the WST-1 was transferred to each well with repeating pipette and mixed for 1 minute on orbital shaker.

12.2.6. They were incubated for 2 hours and then shaken for 1 minute on orbital shaker.

12.2.7. The absorbance against blank was measured by microplate reader at 420-480 nm.

13. Alkaline Phosphatase (ALPase) Activity Assay

13.1. Cell preparation

13.1.1. Pulp cells (5×10^4 cells/well) were seeded in 24-well plates with 1.4 mL standard medium and incubated in the incubator for 24 hours.

13.1.2. Cements (n=3/group) were encapsulated mixed and packed into cylindrical mold (4 mm diameter and 6 mm height), covered with glass slides for 10 minutes and kept in the incubator at 37°C and 100% RH for 1 hour.

13.1.3. The set cements were removed, put into each eppendorf tube and stored in the incubator for another 23 hours. Each side of all cements was sterilized with ultraviolet (UV) radiation. Then cements were transferred into Transwell® (Corning Inc., NY, USA) (Figure 20) and put on each well. Culture medium was changed every 2 days.

13.1.4. At day 1, 4, 7, 14 and 21, cells were harvested for ALPase assay.

a)  b) 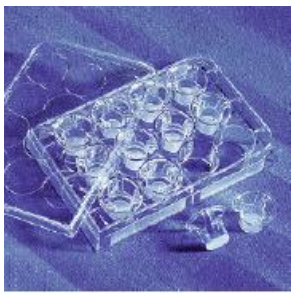

Figure 20 Transwell® Permeable Support 8.0 μm Polycarbonate Membrane, 24 mm Insert. a) 6-well and b) 24-well plate (picture from[137])

13.2. ALPase activity assay procedure

13.2.1. Culture medium was aspirated and cells were washed with 500 μL PBS per well.

13.2.2. PBS was aspirated and 500 μL ddH_2O was added into each well on ice and homogenized by Ultrasonic Disrupters (UR-20P, TOMY, Tokyo, Japan) at power 7 for 15 seconds.

13.2.3. The lysate was transferred to new eppendorf tubes on ice and homogenized by handy sonic at power 7 for another 15 seconds.

13.2.4. ALP standard was prepared by diluting ALP stock (20U/mL) with 0.01 M Tris HCl (Table 3).

13.2.5. The pNPP solution was prepared by mixing 18.56 mg in 10 mL 0.01 M Tris HCl.

Table 3 ALP Standard Preparation

Standard	Start volume (μL)	0.01M Tris (μL)	Dilution	Final concentration
S1	Stock 10	290	1:30	10 mU/15μL
S2	S1 100	100	1:2	5 mU/15μL
S3	S2 100	100	1:2	2.5 mU/15μL
S4	S3 100	100	1:2	1.25 mU/15μL
S5	S4 100	100	1:2	0.625 mU/15μL
S6	S5 100	100	1:2	0.3125 mU/15μL
S7	S6 100	100	1:2	0.15625 mU/15μL

13.2.6. Mixture solution was prepared by adding each well of 96-well plate (SUMILON MS-8596) with 1.0 M Tris HCl (pH 9.0) 50 μL, 0.04% TritonX + 1.8 NaCl 15 μL and 5 mM $MgCl_2$ 10 μL with repeated pipette.

13.2.7. The sample or blank of 15 μL was added into 96-well plate and 10 μL of pNPP was added and incubated at room temperature for 1 hour.

13.2.8. Absorbance was measured at 415-550 nm by a microplate reader.

13.3. Data analysis

Mean and standard deviation of the triplicate assays and subtract the blank values were calculated. Enzyme activity was calculated from Beer-Lambert law following the equation below[138].

$$Enzyme\ activity\ (\mu mol/min/\mu g) = \frac{V\ (\mu L) \times OD_{415nm}\ (cm^{-1})}{\varepsilon \times incubation\ time\ (min) \times enzyme\ (\mu g)}$$

ε = the molar extinction coefficient ($M^{-1} \cdot cm^{-1}$), for pNPP=1.78×10^4($M^{-1} \cdot cm^{-1}$)

OD_{415nm} = the absorbance at 415 nm divided by the light-path length (cm^{-1})

V = final assay volume

14. Real Time Polymerase Chain Reaction (RT-PCR)

14.1. Cell preparation

14.1.1. Pulp cells ($1x10^5$cells/well) were seeded in 6-well plates with 4.5 mL standard medium and incubated for 24 hours.

14.1.2. Cements (n=3/group) were encapsulated mixed and packed into cylindrical mold (4 mm diameter and 6 mm height), covered with glass slides for 10 minutes and kept in the incubator at 37°C and 100% RH for 1 hour.

14.1.3. The cements were removed and put into each eppendorf tube and stored in the incubator for another 23 hours. Each side of all cements was sterilized with ultraviolet (UV) radiation.

14.1.4. The cements were placed into Transwell® (Figure 23) and put on each well. Culture medium was changed every 2 days.

14.1.5. At day 1, 7, 14 and 21, cells were harvested for RT-PCR.

14.2. RNA to cDNA procedure

14.2.1. Homogenization

Culture medium was aspirated and cells were washed with cold PBS twice. PBS was aspirated and 500 μL RNAbee (TEL-TEST, Friedswood, TX, USA) was added into each well. Lysate was passed through pipette several times to ensure complete lysis. Then lysis was transferred to new eppendorf tubes.

14.2.2. Separation

Chloroform (100 μL) was added into each tube. The tubes were capped, shaken by hand for 15-30 seconds and stored on ice for 5 minutes. The tubes were put

into high speed refrigerated micro-centrifuge (Tony MX-300) and centrifuged at 12,000 g (11,500 rpm) at 4°C for 5 minutes.

14.2.3. RNA precipitation

Supernatant (450 μL) was transferred to clean eppendorf tubes. Isopropanol (450 μL) was added into each tube and all tubes were vortexed (Vortex Genie2) and stored at room temperature for 10 minutes. Then all tubes were centrifuged at 12,000 g 4°C for 5 minutes.

14.2.4. RNA wash

Supernatant was aspirated and RNA pellet was washed once with 1,000 μL of 75% DEPC ethanol. Tubes were vortexed and centrifuged at 7,500 g (9,100 rpm) 4°C for 5 minutes. Procedure was repeated and supernatant was aspirated.

14.2.5. RNA solubilisation

RNA pellet was briefly air dried (5-10 minutes). Then RNA pellet was dissolved with 20 μL DEPC water. Two μL of RNA solubilisation was used for RNA detection with a spectrophotometer (NanoDrop™1000, Thermo Fisher Scientific, DE, USA) (Figure 21).

14.2.6. Reverse transcriptase

14.2.6.1. RNA mixture was prepared by adding the components in Table 4 to a 0.5 mL nuclease-free thin well tube.

14.2.6.2. With a High Capacity RNA-to-cDNA kit (Applied Biosystems, Tokyo, Japan), a mixture was prepared on ice (Table 5), briefly centrifuged and then added to 9 μL RNA mixture. All mixtures were mixed well by gently pipette.

Reverse transcriptase was programmed using DNA Engine® PTC-200 Peltier thermal cycler (Bio-Rad Laboratories, UK) (Figure 22) at 37°C for 60 minutes,

95°C for 5 minutes and 4°C forever. cDNA mixture was prepared for RT-PCR by adding 80 μL ultrapure water to 20 μL cDNA.

Figure 21 Spectrophotometer (NanoDrop™ 1000)

Table 4 RNA Mixture Preparation

X=calculate from the RNA concentration from NanoDrop™1000 and Y=9-X

Component	Amount
1 μg total RNA	X μL
DEPC water	Y μL
Total	9 μL

Table 5 RNA-to-cDNA Preparation

Component	Volume/reaction (μL)
2×RT Buffer	10.0
20×RT Enzyme Mix	1.0
Total	11.0

Figure 22 Peltier Thermal Cycler (DNA engine® PTC-200)

14.3. RT-PCR procedure

Primer mixture was prepared by adding 80 µL ultrapure water to each 20 µL primer (Table 6). PCR reaction mixture was prepared by mixing each component in Table 7.

PCR reaction plate was prepared by transferring 20 µL PCR reaction mix to MicroAmp™ Fast Optical 96-Well Reaction Plate (Applied Biosystems, Tokyo, Japan) (Figure 23 b) on MicroAmp™ 96-Well Support Base (Applied Biosystems, Tokyo, Japan) (Figure 23 c) and covered with MicroAmp™ Optical Adhesive Film (Applied Biosystems, Tokyo, Japan) (Figure 23 a).

The reaction plate was centrifuged briefly with a plate spinner (PlateSpin, Kubota Corp., Tokyo, Japan) (Figure 24). All samples were analyzed in triplicate wells with a Quantitative Real-time PCR machine (Step One Plus™, Applied Biosystems, Tokyo, Japan) (Figure 25).

Table 6 Primers Used

Gene		Primer
Hypoxanthine phosphorybosyl transferase (HPRT)	Forward	5´-CGA GAT GTG ATG AAG GAG ATG GG-3´
	Reverse	5´-GCC TGA CCA AGG AAA GCA AAG TC-3´
Collagen type I (COL1A1)	Forward	5´-CTG CTG GAC GTC CTG GTG-3´
	Reverse	5´-ACG CTG TCC AGC AAT ACC TTG-3´
Dentin matrix acidic phosphoprotein (DMP-1)	Forward	5´-AGA TCA GCA TCC TGC TCA TGT TC-3´
	Reverse	5´-TGG TGC CTG AGC CAA ATG AC-3´
Dentin sialophosphoprotein (DSPP)	Forward	5´-TGG AGA CAA GAC CTC CAA GAG TGA-3´
	Reverse	5´-TGC TGG GAC CCT TGA TTT CTA TTC-3´

Table 7 PCR Reaction Mix Preparation

Reagents	Volume per well (μL)
Ultrapure water	7.2
Fast SYBR® Green Master Mix	10
Primer forward	0.4
Primer reverse	0.4
cDNA mixture	2
Total	20

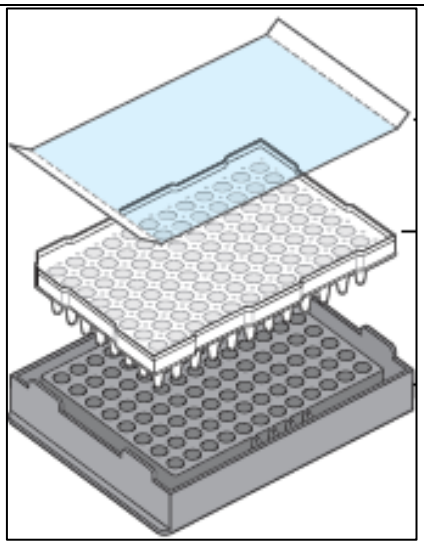

Figure 23 MicroAmp™ Kit for PCR Assay

From top to bottom, MicroAmp™ Optical Adhesive Film, Fast Optical 96-Well Reaction Plate and 96-Well Support Base

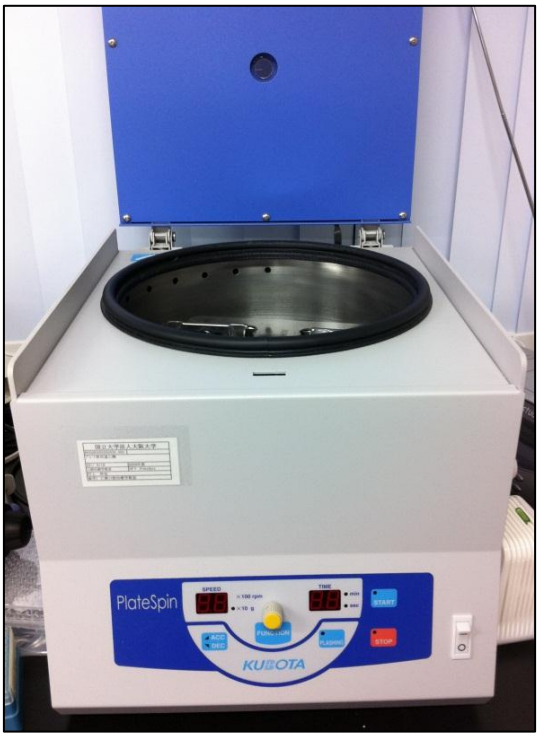

Figure 24 Plate Spinner (PlateSpin)

Figure 25 Quantitative Real-time PCR Machine (Step One Plus™ 7500 Fast)

15. Alizarin Red Staining Assay

15.1. Cell preparation

15.1.1. Pulp cells (5×10^4 cells/well) were seeded in 24-well plates with 1.4 mL mineralized medium, incubated in the incubator for 24 hours.

15.1.2. Cements (n=3/group) were encapsulated mixed and packed into cylindrical mold (4 mm diameter and 6 mm height), covered with glass slides for 10 minutes in the incubator.

15.1.3. For the 24 hour set cement group, after 10 minutes, glass slides were removed, cements were kept in the incubator for 1 hour then demolded and stored in the incubator for another 23 hours.

15.1.4. For the 15 minutes set cement group, after 10 minutes, glass slides and molds were removed from cements. Each side of all cements were sterilized with UV radiation for 40 minutes

15.1.5. Cements were put onto Transwell®. Culture medium was changed every 2 days.

15.1.6. At day 14, calcium deposition of HDPCs was evaluated using 0.1% alizarin red S staining solution (Sigma-Aldrich, St. Louis, MO, USA).

15.2. Assay procedure

15.2.1. Culture medium was aspirated and cells were washed twice with PBS (volume of PBS=volume of culture medium).

15.2.2. Cold 100% ethanol (-20°C) was added into each wells and waited for 10 minutes. The volume of ethanol used was only covered the cell layer. Then ethanol was aspirated and cells were washed with ddH_2O.

15.2.3. Alizarin dyes was added into all wells and waited of 5 minutes. The volume of dye used was only covered the cell layer. Each well was washed twice with ddH_2O and dried up for at least 24 hours. Plates were taken pictures by scanner.

Statistical Analysis

For fracture toughness test, ALP activity assay, analyses were determined by One-Way ANOVA and used Bonferroni's *post hoc* test for multiple comparison.

For microleakage test, analysis was determined by Chi-square test.

For shear bond strength measurement, analysis was determined by Independent t-test.

For proliferation WST-1 assay and RT-PCR were determined by Mann-Whitney U-test.

CHAPTER IV

RESULTS

1. *Synthesis of $MgCO_3Ap$*

a)  b)  c) 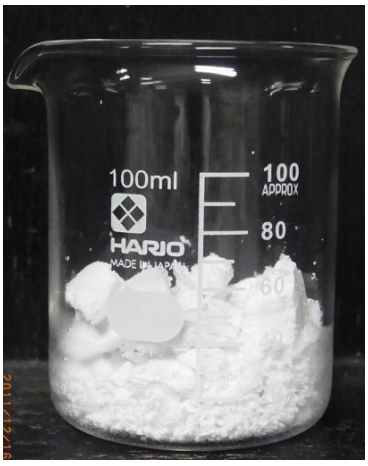

Figure 26 $MgCO_3Ap$ Powder Preparation

a) $MgCO_3Ap$ powder precipitated after 24 hours. b) Filter and suction used for powder filtration. c) $MgCO_3Ap$ powder after filtration ready for put into incubator for dehydration.

2. *Characterization and Chemical Analysis*

2.1. SEM

$MgCO_3Ap$ powder synthesized by wet method showed broccoli-like structure with size in aggregated globules ranged from 20-40 μm (Figure 27a left). While Fuji IX powder had irregular shape with the size from less than 1 to 20 μm (Figure 27b). In Figure 28 the distribution of $MgCO_3Ap$ powder in GIC powder was demonstrated after encapsulated mix.

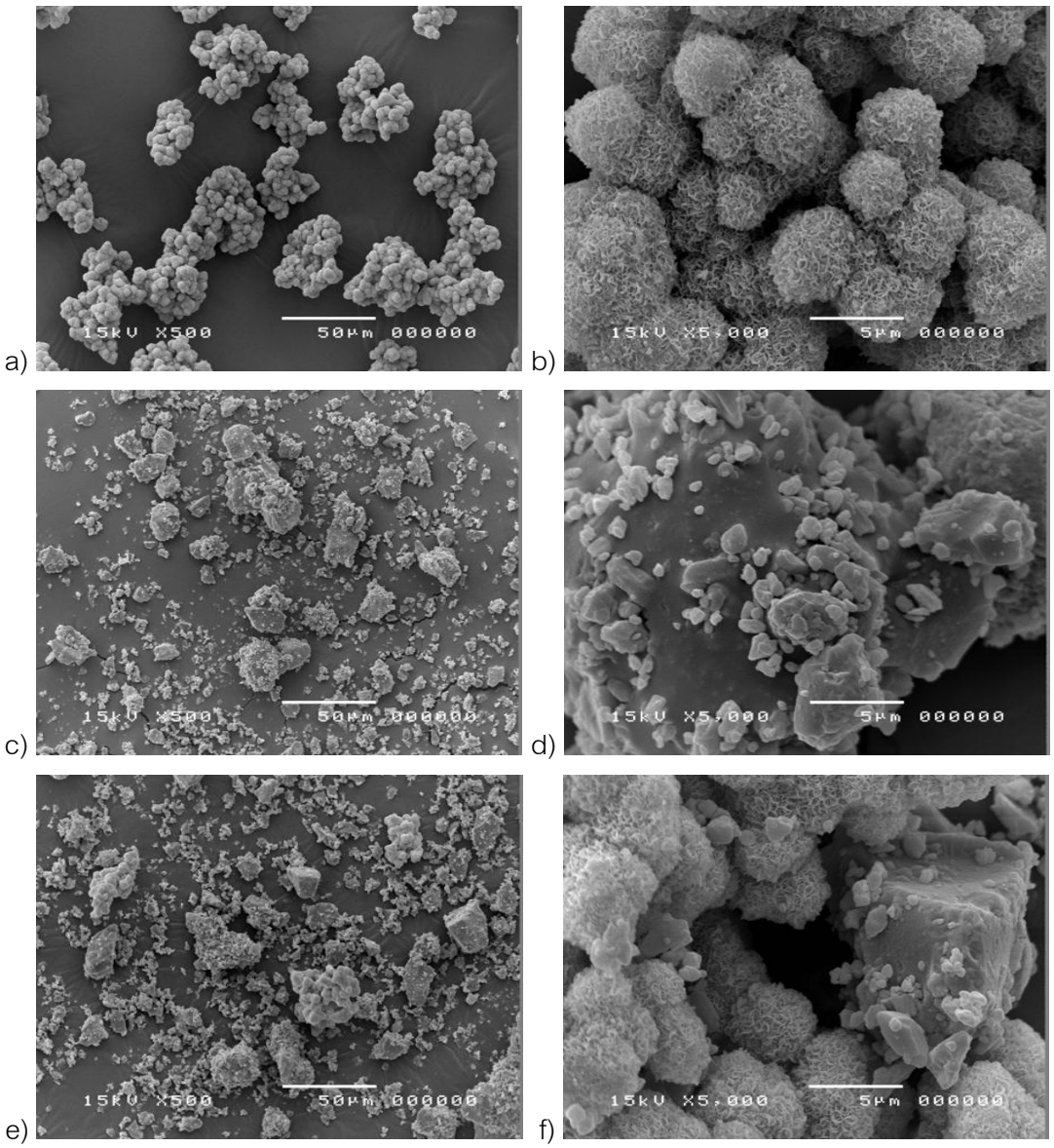

Figure 27 SEM Images of $MgCO_3Ap$ and GIC at Magnification 500× and 5,000× $MgCO_3Ap$ a) At 500× and b) At 5,000×, GIC c) At 500× and d) At 5,000×, 2.5% by weight of $MgCO_3Ap$ in GIC e) At 500× and f) At 5,000×

2.2. FTIR

Data from FTIR analysis of $MgCO_3Ap$ powder showed carbonate incorporation into the synthetic apatite which was evidenced by the carbonate v3 peaks

at 1455, 1413 cm^{-1} and carbonate v2 peak at 873 cm^{-} (Figure 29). The phosphate v3 peak of around 603 cm^{-1} to 567 cm^{-1} was also found in $MgCO_3Ap$ powder.

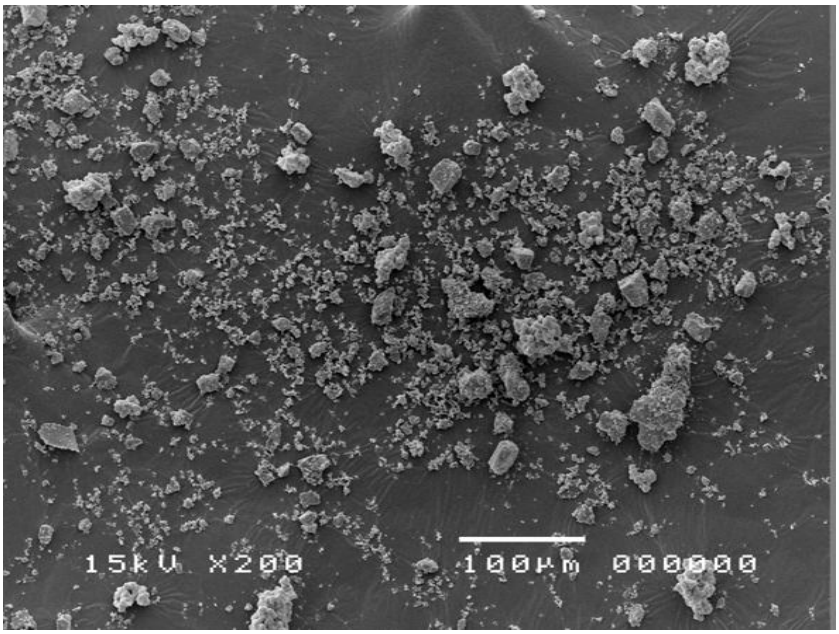

Figure 28 Distribution of 2.5% $MgCO_3Ap$ in GIC Powder at Magnification 200×

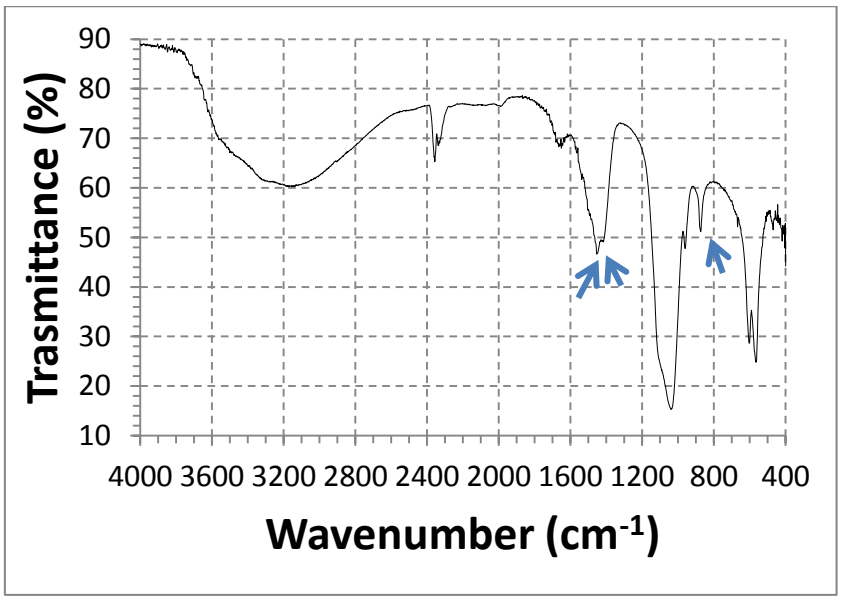

Figure 29 FT-IR Spectra of $MgCO_3Ap$ Powder

Arrows exhibit CO_3 peaks at 1455, 1413, and 873 cm^{-1}, respectively from left to right.

2.3. XPS

Surface chemical analysis by XPS of $MgCO_3Ap$ powder and test cement showed different peaks and concentration as seen in Figure 30a and 30b and Table 8 respectively. Mg was found in the apatite powder but could not be detected in the test cement. In the test cement, addition elements which could not be detected in the $MgCO_3Ap$ powder were found such as F (682 cm^{-1}), Sr (267 cm^{-1}), Si (99.8 cm^{-1}) and Al (71.8 cm^{-1}). Those elements were the composition normally found in GIC.

Table 8 Chemical Analysis of $MgCO_3Ap$ Powder and Test Cement from XPS

Peak	Position BE (eV)	Atomic Concentration (%)		Mass Concentration (%)	
		$MgCO_3Ap$	Test cement	$MgCO_3Ap$	Test cement
Mg 1s	1301.900	0.88	-	0.94	-
F 1s	682.200	-	5.40	-	5.70
O 1s	528.600	63.11	41.44	44.25	36.80
Ca 2p	344.800	20.27	0.37	35.60	0.82
C 1s	287.300	2.59	36.31	1.36	24.21
Sr 3p	267.000	-	2.10	-	10.19
P 2s	188.200	-	1.38	-	2.37
P 2p	130.600	13.14	-	17.84	-
Si 2p	99.800	-	6.93	-	10.81
Al 2p	71.800	-	6.08	-	9.11

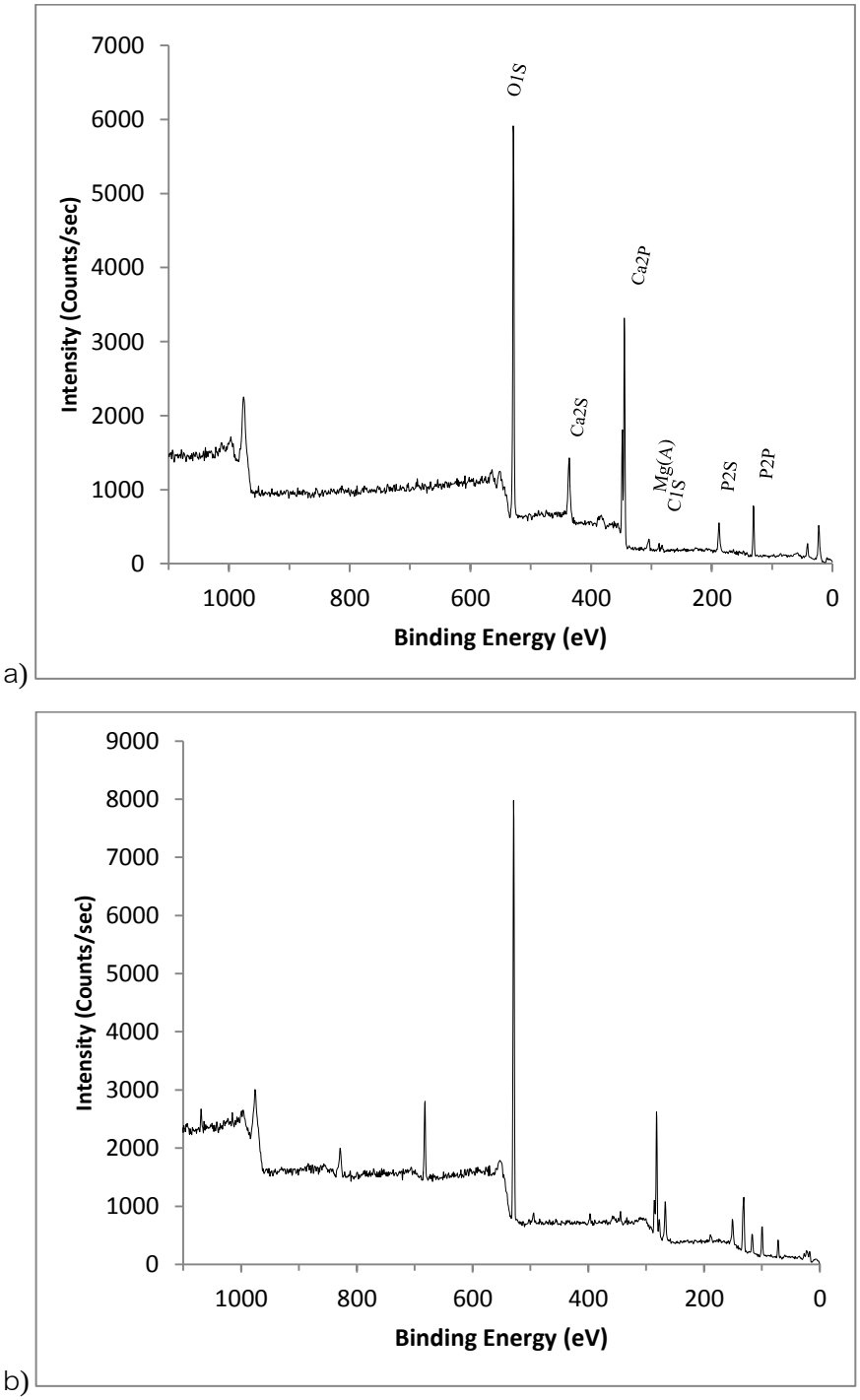

Figure 30 XPS Wide Spectrum (0-1200 eV) of $MgCO_3Ap$ Powder and Test Cement a) $MgCO_3Ap$ powder, b) GIC containing 2.5% $MgCO_3Ap$. Different peaks in b) indicate elements from GIC.

3. Setting Time

Table 9 Setting Time of Control and Test Cements

	n	Setting time, seconds (S.D.)
Control	5	201 (8.22)
Test	5	252 (12.6)

The test cements had longer setting time (~4 minutes) compared to the control cements (~3 minutes). However setting times of both cement groups were within ISO 9917 limit for restorative materials.

4. Compressive Strength

Table 10 Compressive Strength of Control and Test Cements

	n	Compressive strength, MPa (S.D.)
Control	5	132.2 (12.5)
Test	5	132.6 (10.3)

The test and control cements had almost the same compressive strength (~120-140 MPa). The strengths of both cements were above the level required for restorative material by ISO 9917.

5. Fracture Toughness

Table 11 Fracture Toughness of 24-hour and 15-minute Set Cements for Both Control and Test Groups

	24-hour Set Cements		*15-minute Set Cements*	
	n	Fracture Toughness, $MPa{\cdot}m^{1/2}$ (S.D)	*n*	Fracture Toughness, $MPa{\cdot}m^{1/2}$ (S.D)
Control	9	0.429 (0.051)*	5	0.282 (0.054)*, ***
Test	9	0.559 (0.096)*, **	5	0.358 (0.052)**, ***

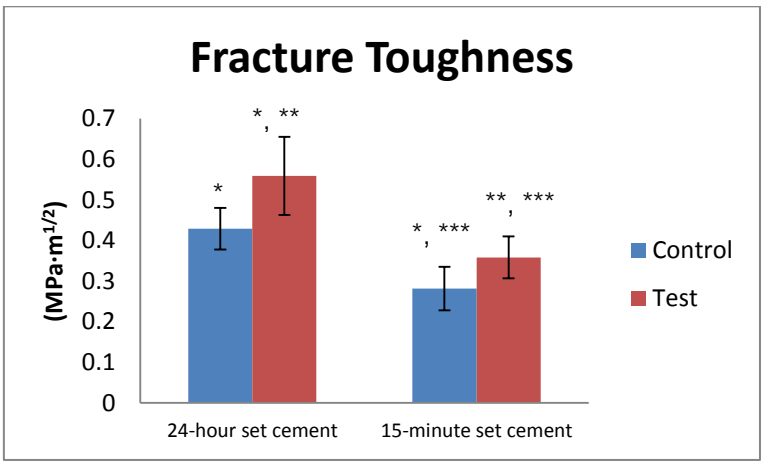

**, **, *** p<0.05*

Figure 31 Fracture Toughness of 24-hour and 15-minute Set Cements for Both Control and Test Groups

Fracture toughness of the 15-minute set cement group was evaluated at 15 minutes after mixing. The data showed that, the test cement had significantly better fracture toughness than the control cement. The toughness for the 24-hour set cement groups demonstrated the same result of significantly higher fracture toughness of test to control cement. Both control and test cements had toughness value significantly increased from 15 minutes to 24 hours.

6. Microleakage Test

Table 12 Enamel Microleakge Test of Control and Test Cements

	Count, surface		
Score	**0**	**1**	**2**
Control	72	8	0
Test	76	4	0

Table 13 Dentin Microleakage Test of Control and Test Cements

	Count,surface		
Score	**0**	**1**	**2**
Control	70	10	0
Test	78	2	0

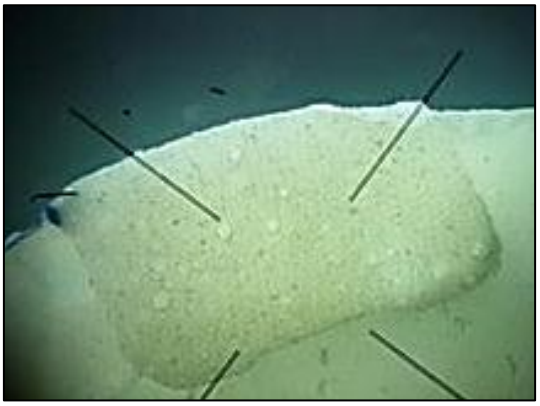

Figure 32 Image for Microleakage Evaluation

Sealing ability of this cement to the tooth surface was evaluated by microleakage test. The result showed that both cements had no dye infiltration above score 1 at the interface (Figure 32). At enamel margin, control cement had more specimens with score 1 (8) than the test cement (4) but was not statistically significant. At the dentin margin, the control cement had 10 specimens on score 1 while test cement had only 2 specimens at the same score. The test cement had significantly less microleakage than control cement at dentin interface.

7. Shear Bond Strength Measurement

Table 14 Shear Bond Strength of Control and Test Cements

	n	Shear bond strength, MPa (S.D.)
Control	5	9.205 (3.036)*
Test	5	6.439 (2.374)*

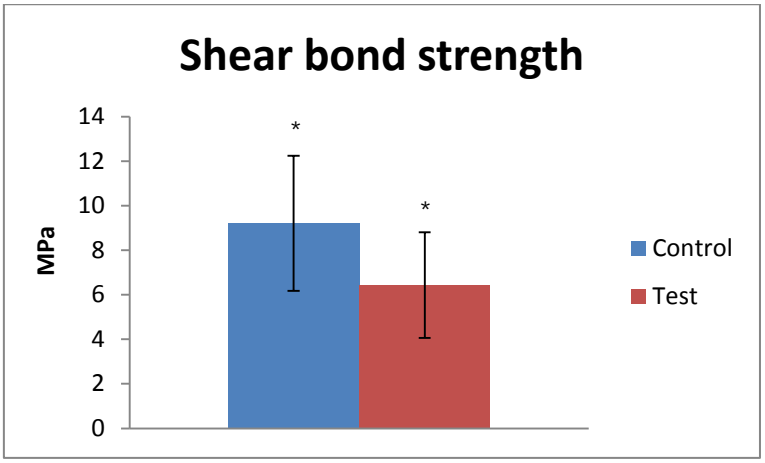

* $p<0.05$

Figure 33 Shear Bond Strength of Control and Test Cements

The result indicated that the control cement had significantly higher shear bond strength than the test cement. However the SEM images demonstrated the cohesive failure of all specimens with some cements penetrated into dental tubules in both control (Figure 34a) and test cements (Figure 34b). Pictures also showed that at the fracture site, found GIC (Figure 35a) and apatite adhered to the dentin (Figure 35b).

a) 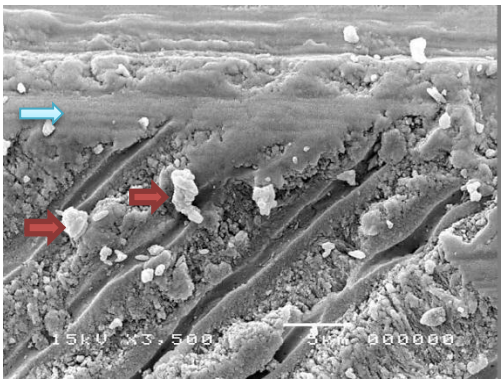 b) 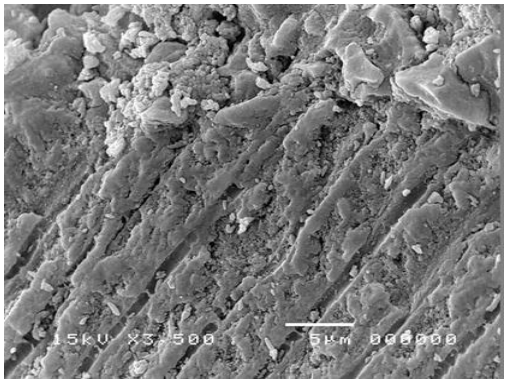

Figure 34 SEM Fracture Site (Cross-section) of Control and Test Cements

a) Control demonstrated cohesive failure with ion exchange layer (blue arrow) and remained glass particle in the matrix (red arrow. b) Test cement also demonstaretd cohesive failure.

a) 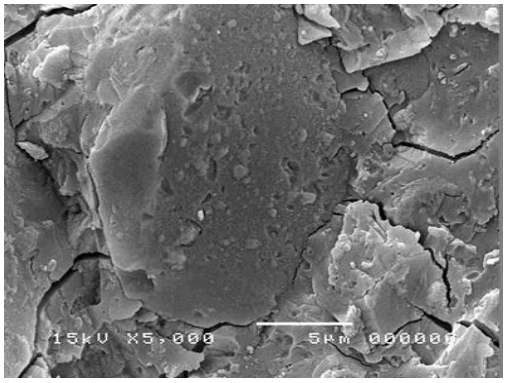 b) 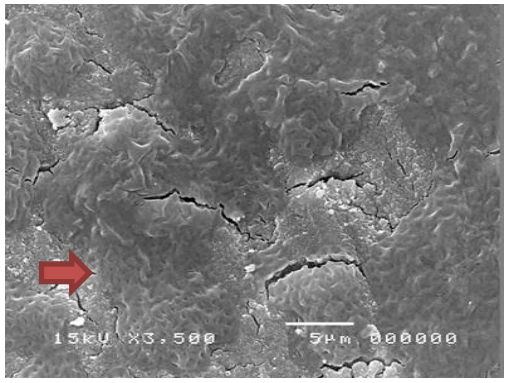

Figure 35 SEM Fracture Site of Control and Test Cements

a) Control demonstrated the cement covered the dentin with some glass particle remained in the matrix. b) Test cement found more homogeneous surface and no glass particle was observed. Red arrow pointed at apatite particle in the matrix bond to matrix smoothly.

8. Ion Release

8.1. Calcium Ion

Table 15 Accumulation Release of Ca^{2+} of Control and Test Cements

	Accumulation release of Ca^{2+} (ppm)							
Hour	1	2	6	12	24	48	168	336
Control	0.031	0.214	0.444	0.601	0.806	0.832	0.842	0.843
Test	0.000	0.979	1.176	1.748	2.135	2.253	2.288	2.288

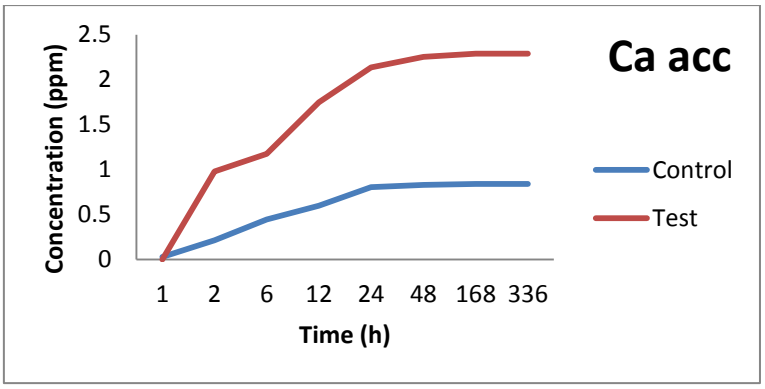

Figure 36 Accumulation Release of Ca^{2+} of Control and Test Cements

For calcium ion release, there is no calcium ion detected in the first hour in the test group. It was found at the second hour (almost 1 ppm) and continued to release to day14. In the control group, calcium ion released from the first hour and continued to release but in a much lower amount (maximum at around 0.200 ppm) compared to the test cement. The test cement demonstrated 2-3 times higher calcium release than the control cement. Data at 48 hours indicated the accumulated calcium release of the test cement at 2.25 ppm and the control cement at 0.83 ppm. The peak accumulation was at 24 hour for both cement groups.

8.2. Magnesium Ion

Table 16 Accumulation Release of Mg^{2+} of Control and Test Cements

	Accumulation release of Mg^{2+} (ppm)							
Hour	1	2	6	12	24	48	168	336
Control	0.008	0.045	0.084	0.099	0.156	0.158	0.158	0.158
Test	0.002	0.095	0.151	0.201	0.294	0.314	0.314	0.314

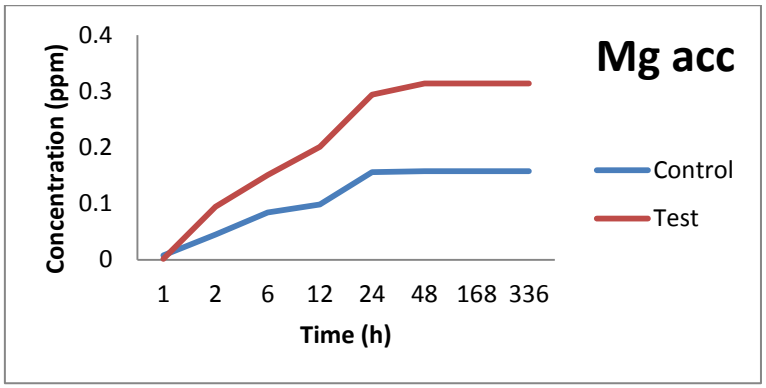

Figure 37 Accumulation Release of Mg^{2+} of Control and Test Cements

Mg^{2+} released from the test cement started from the first hour but in a small amount compared to the control cement. From the first hour to the second hour, the test cement demonstrated the highest difference of Mg^{2+} release (~0.090 ppm). However both cements continued the Mg^{2+} release up to 48 hours only. The test cement showed 2 times higher Mg^{2+} release than control cement. Data at 48 hours indicated the maximum Mg^{2+} release from the test cement was 0.31 ppm and the control cement was 0.16 ppm.

8.3. Fluoride Ion

Table 17 Accumulation Release of F^- of Control and Test Cements

	Accumulation release of F^- (ppm)							
Hour	1	2	6	12	24	48	168	336
Control	0.434	0.612	0.897	1.05	1.24	1.41	1.85	2.15
Test	0.344	0.559	0.899	1.12	1.32	1.5	1.98	2.35

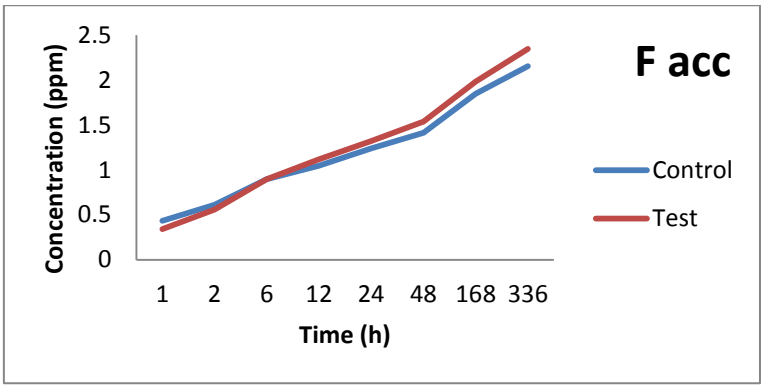

Figure 38 Accumulation Release of F^- of Control and Test Cements

F^- released from the test cement was slightly lower than the control cement only at the first hour (0.34 and 0.38 ppm respectively). However after the first hour, in the test cement had slightly higher F^- release than the control cement at all-time point. Both cements demonstrated continuing F^- release until day 14. The test cement had slightly higher F- release than control cement from the first hour to day 14.

9. WST-1 Assay

Table 18 WST-1 Cell Proliferation of Control and Test Cements

	Cell proliferation, % of control (S.D.)		
Day	1	7	14
Negative control	100.0 (0.00)	100.0 (0.00)	100.0 (0.00)
Control	119.3 (23.11)	131.1 (23.39)	225.6 (10.96)
Test	225.1 (30.71)	189.3 (13.58)	187.9 (14.47)

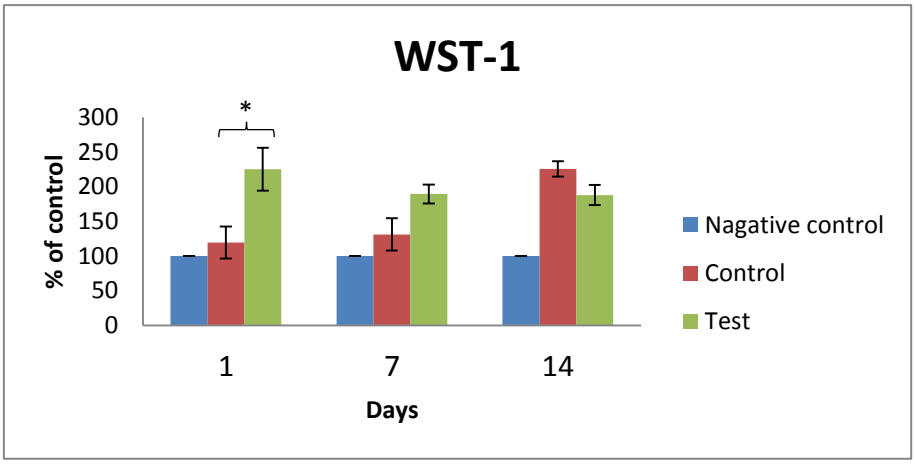

** p<0.05*

Figure 39 WST-1 Cell Proliferation of Control and Test Cements

The result in Figure 39 indicated that at day 1, test cement significantly promoted higher proliferation of pulp cells than control cement ($p<0.05$) and continued the effect until day 7. Even at day 14 control cement showed a little higher effect to test cement but was not statistically significant.

10. ALP Activity Assay

Table 19 ALP Activity of Control and Test Cements

Day	ALP activity, nmol/min/µg of protein (S.D.)				
	1	4	7	14	21
Negative control	3.49(0.815)	4.41(1.40)	37.30(6.89)	690.3(39.54)	146.3(23.15)
Control	2.98(1.49)	6.88(0.974)	20.68(11.64)	565.5(71.34)	126.0(36.87)
Test	1.85(1.46)	3.80(1.29)	33.63(2.26)	715.9(103.9)	234.7(56.88)

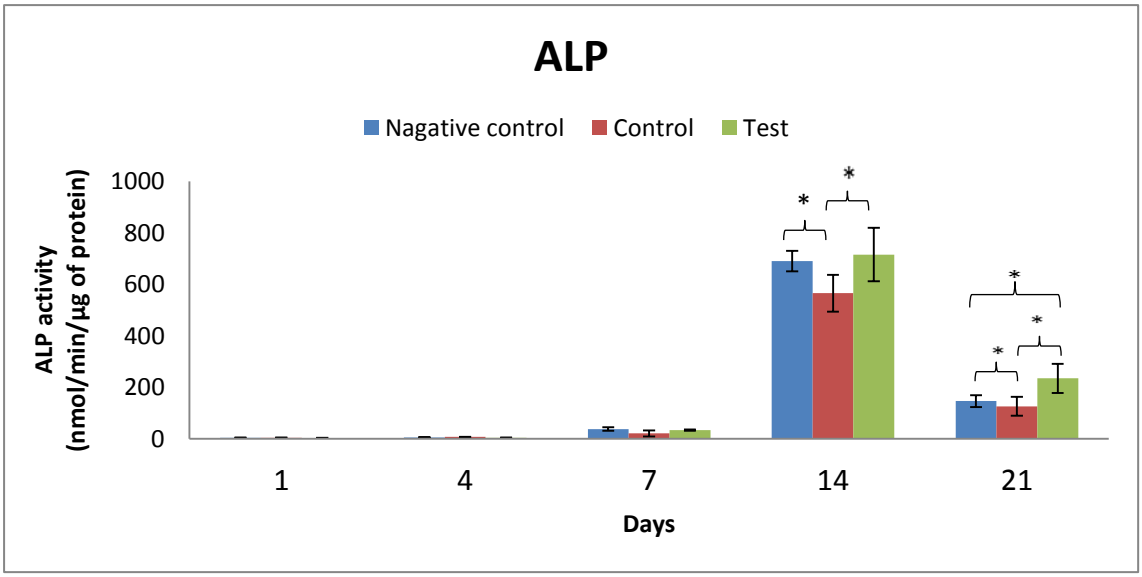

* $p<0.05$

Figure 40 ALP Activity of Control and Test Cements

At day 7, the negative control had the highest APL activity which was significantly different from control but not the test cement. The highest ALPase activity was found at day 14 in every group. However, the test cement showed higher activity than negative control but not statistically significantly different. Both negative control and test cement had significantly higher activity than the control cement. At day 21, the test cement showed the highest ALP activity and it was significantly different from both negative control and the control cement (Fig. 40).

11. RT-PCR

11.1. COL1A1

Table 20 COL1A1 Gene Expression of Control and Test Cements

Day	COL1A1 gene expression, relative ratio to HPRT (S.D.)							
	1		7		14		21	
Negative control	1.87	(1.82)	189.7	(15.0)	476.5	(39.9)	341.5	(39.4)
Control	47.7	(5.85)	217.4	(40.0)	651.8	(87.5)	229.7	(33.9)
Test	225.9	(27.9)	408.9	(104.4)	456.8	(50.0)	229.2	(24.4)

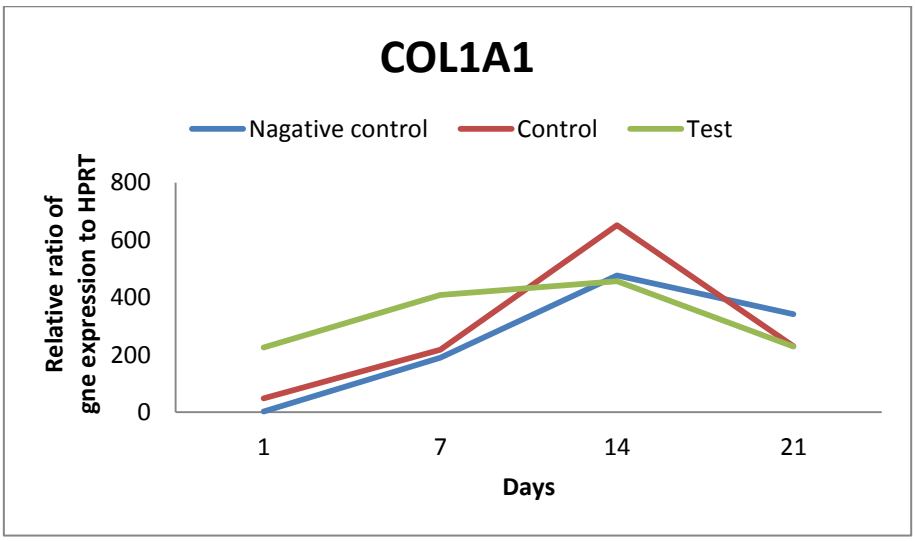

Figure 41 COL1A1 Gene Expression of Control and Test Cements

COL1A1 gene expression demonstrated a very high value in the test cement compared to the control cement and the negative control group at day 1 and day 7. However at day 14, the expression of COL1A1 gene from the test cement was lower than the other two groups. All groups showed the highest expression at day 14.

11.2. DMP-1

Table 21 DMP-1 Gene Expression of Control and Test Cements

Day	DMP-1 gene expression, relative ratio to HPRT (S.D.) ($\times 10^{-4}$)							
	1		7		14		21	
Negative control	1.94	(1.94)	30.96	(25.22)	11.15	(3.62)	3.90	(3.90)
Control	3.89	(0.500)	6.91	(1.33)	21.06	(12.28)	5.07	(1.74)
Test	0.00	(0.00)	34.91	(31.02)	14.56	(5.22)	6.77	(4.83)

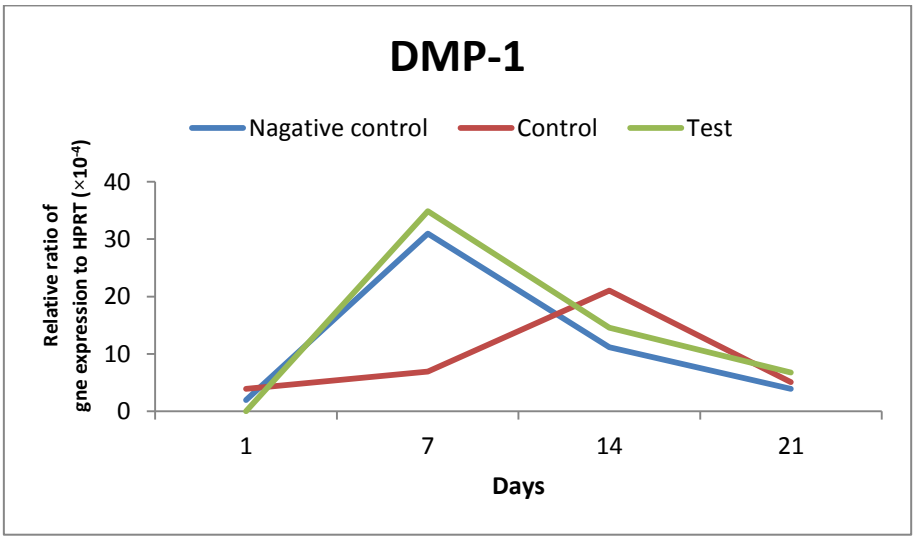

Figure 42 DMP-1 Gene Expression of Control and Test Cements

The DMP-1 in both negative control and test cement groups showed the highest gene expression at day 7. On the other hand, in the control cement group demonstrated the highest expression at day 14. The magnitude of expression was highest in the test cement at day 7. This result indicated that the effect of the test cement in promoting DMP-1 expression was not different from the negative control group and the gene expression was highest at day 7. However in the control cement, the gene expression was very low and lower than the other groups. Moreover the highest expression was delay to day 14.

11.3. DSPP

Table 22 DSPP Gene Expression of Control and Test Cements

Day	DSPP gene expression, relative ratio to HPRT (S.D.) ($\times 10^{-5}$)							
	1		7		14		21	
Negative control	1.86	(3.03)	3.71	(6.43)	11.17	(19.35)	0.00	(0.00)
Control	3.32	(4.06)	0.00	(0.00)	5.98	(9.36)	7.05	(12.21)
Test	0.00	(0.00)	0.00	(0.00)	20.10	(30.33)	5.33	(6.88)

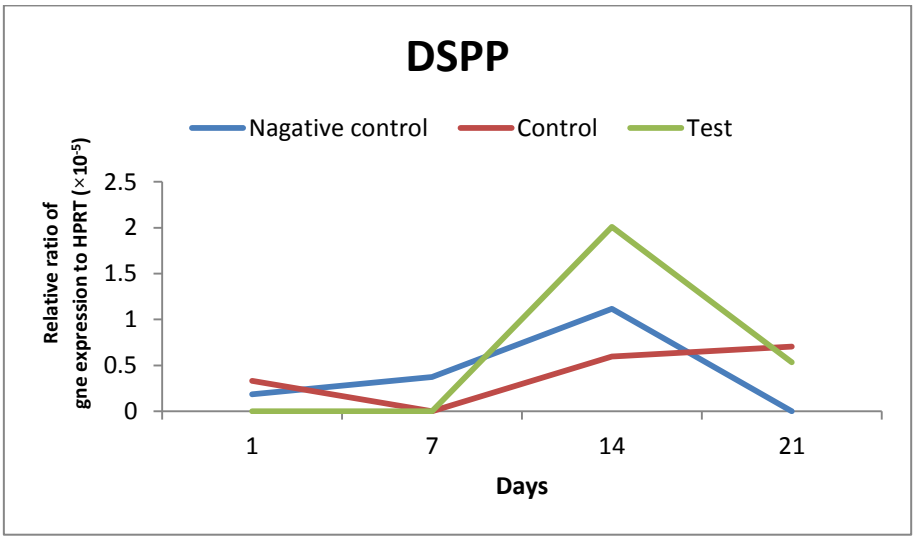

Figure 43 DSPP Gene Expression of Control and Test Cements

DSPP gene expression was highest in the test cement group compared to negative control and control cement groups at day 14 however, it could not detect any expression at day 1 and day 7. The negative control group demonstrated some expression started at day 1 and no expression at day 21. The control cement had lower expression than both negative control and test cement at day 14 but expressed higher level at day 21.

12. Alizarin Red Staining

a) 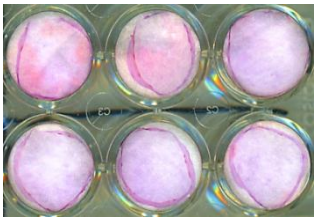 b) 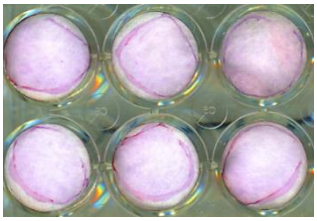 c) 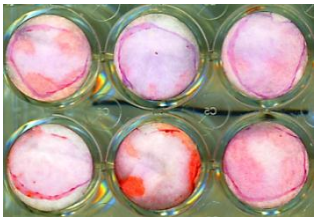

Figure 44 Alizarin Red Staining of Control and Test Cements
a) Negative control, b) Control cements, c) Test cements;
Top: 24-hour set cement, Bottom: 15-minute set cement.

At day 14, pictures demonstrated slightly alizarin staining in test cement wells for both set (Figure 44c top) and 15-minute set cement wells (Figure 44c bottom). For the control cement group there was no staining in all wells (Fig. 44b) while the negative control group had a very soft stain in the 24-hour set cement wells (Figure 44a top).

CHAPTER V

DISCUSSION AND CONCLUSION

Substitution of CO_3^{2-} in the apatite lattice can occur in two ways: Type-A and Type-B substitutions. Type-A substitution, CO_3-for-OH, is obtained by solid-state reactions at 1000°C and Type-B substitution, CO_3-for-PO_4, can be conducted by precipitation[140]. $MgCO_3Ap$ in this study was synthesized by the same method with the same level of carbonate ($0.06CO_3Ap$) synthesized from (0.06 M $(NH_4)_2COO_3$) used in the previous study[141]. The incorporation of CO_3^{2-} by precipitation method in the apatite lattice in this study was confirmed by FT-IR analyses (Figure 51). Carbonate incorporation was evidenced by absorption bands around 1413, 1455(v_3C-O) which assigned to surface CO_3^{2-} while 873cm^{-1} (v_2C-O) is considered to occur competitively between OH^- and CO_3^{2-} . According to the FT-IR results, the synthetic apatite in this study demonstrated the CO_3^{2-} peak between 1410- 1450 cm^{-1} and confirmed the powder was CO_3Ap (Figure 51).

Level of CO_3^{2-} content in the apatite was found to be important for bone formation and the concentration at 4.8 % by weight (4.8%wt.) of CO_3^{2-} appeared to have similar crystallinity and chemical composition to human bone and had the highest bone formation ability[142]. The $MgCO_3Ap$ in this study consisted of CO_3^{2-}at 4.8 %wt. We obtained data from the XPS elements quantification in Table 8 and put into a table to compare the differences between $MgCO_3Ap$ and enamel, dentin and bone. The finding demonstrated $MgCO_3Ap$ with similar chemical composition to human enamel and dentin (Table 27) which may be an advantage to adhesion and biocompatibility to tooth substrate.

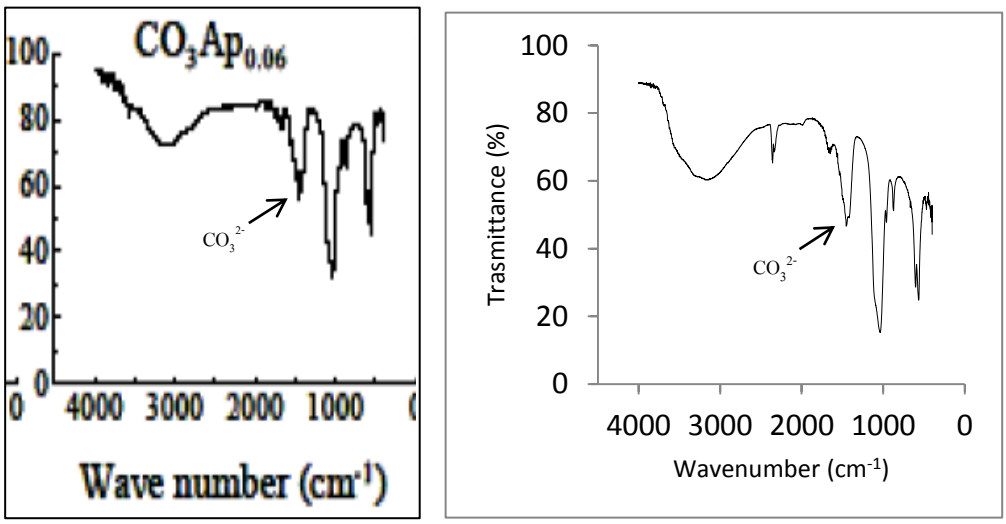

Figure 45 FT-IR Spectra Compare between CO_3Ap[141] and $MgCO_3Ap$.

Table 23 Comparison of Composition and Properties between Inorganic Phases (% Weight) of Enamel, Dentin, Bone and $MgCO_3Ap$.

Composition/Properties	Enamel	Dentin	Bone	$MgCO_3Ap$
Calcium	36.5	35.1	34.8	35.6
Phosphorus	17.7	16.9	15.2	17.8
Stoichiometry (Ca/P)	1.63	1.61	1.71	1.61
Magnesium	0.44	1.23	0.72	0.94
Carbonate	3.5	5.6	7.4	4.8

We first synthesized several different cationic ions substitute to calcium-CO_3Ap using the same method and carried out the SEM images to see the ultrastructure differences between different biological apatites. The SEM images demonstrated the similar flake-like and broccoli-like structure in all $0.06CO_3Ap$. Adding 0.01M $Mg(CH_3COO)_2{\cdot}4H_2O$ to 0.2M $Ca(CH_3COO)_2{\cdot}H_2O$ (Mg/Ca=1/20), the result demonstrated the same structure but the smaller globules and flakes than the $0.06CO_3Ap$. (Fig. 46-49).

From our review, we stated the role of ionic dissolution to regeneration which suggested that several cations, including Sr^{2+}, had a positive effect to regeneration. We also synthesized $SrCO_3Ap$ at concentration Sr/Ca=1/20 and Sr/Ca=1/1000. From SEM images, we found a very interesting data showing that adding

Sr^{2+}at the same concentration to our $MgCO_3Ap$ (Sr/Ca=1/20), the size of agglomerate particles of $SrCO_3Ap$ was larger and the flakes were bigger than $MgCO_3Ap$. However at the very low concentration of Sr^{2+}(Sr/Ca=1/1000), the apatite demonstrated similar structure and size to $0.06CO_3Ap$ (Fig 50, 51). This may suggest that at the same level of CO_3^{2-} ($0.06CO_3Ap$), the apatite will have the similar flake-like and broccoli-like structure. However the size of the agglomerates and appearance of each globule may be different from one to another depending on the type and the concentration of the cationic ions used to substitute the Ca^{2+} in the CO_3Ap. This suggested the importance to characterize and perform chemical analysis to ensure the right apatite and right level of chemicals being used in developing any biomaterials.

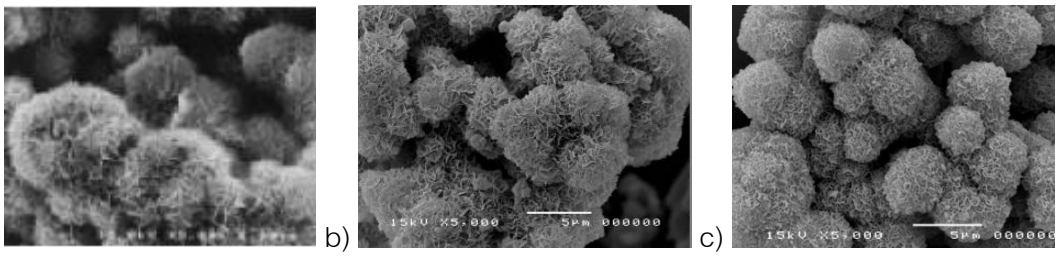

Figure 46 SEM Images Compare the Size between CO_3Ap and $MgCO_3Ap$ at Magnification 5,000×.

a) CO_3Ap from previous study[141], b) CO_3Ap and c) $MgCO_3Ap$ from our study (Mg/Ca=1/20)

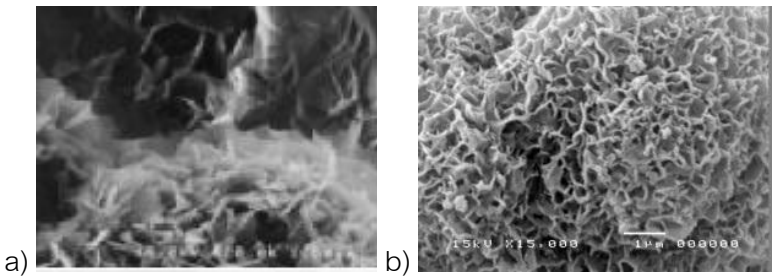

Figure 47 SEM Images Demonstrate the Structure of CO_3Ap and $MgCO_3Ap$ at Magnification 15,000×.

a) CO_3Ap from previous study[141] b) $MgCO_3Ap$

a) 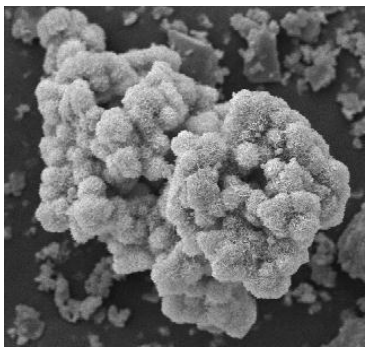 b) 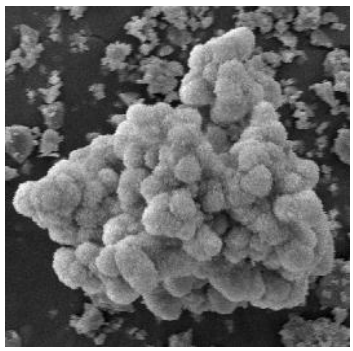

Figure 48 SEM Images Demonstrate the Structure of CO_3Ap and $MgCO_3Ap$ at Magnification 500×.

a) CO_3Ap and b) $MgCO_3Ap$, both demonstrated broccoli-like structure.

a) 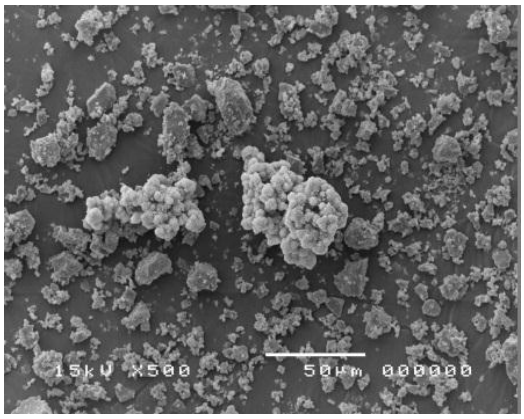

b) 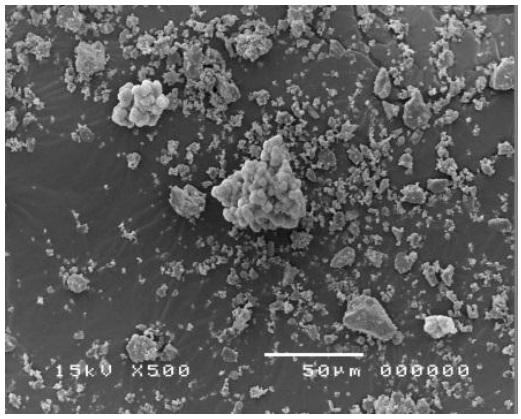

Figure 49 SEM Images Compare the Size between CO_3Ap and $MgCO_3Ap$ at Magnification 500×.

a) CO_3Ap has the bigger agglomerate particle (~50 μm) than b) $MgCO_3Ap$ (~20-40 μm).

a) 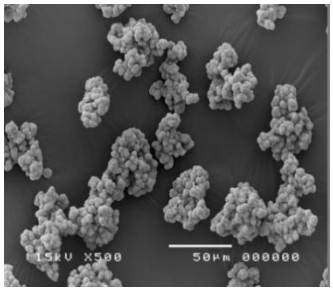 b) 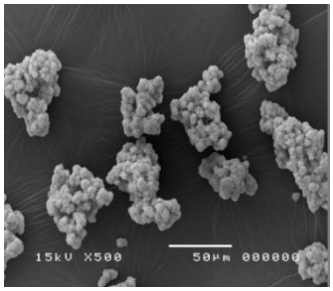 c) 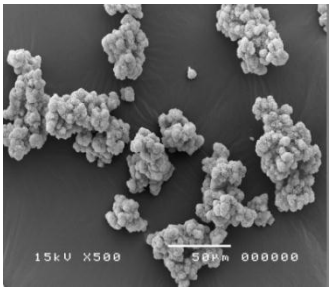

Figure 50 SEM Images Compare the Size of Different Ions Substitution of Ca-CO_3Ap at Magnification 500×.
a) $MgCO_3$Ap (Mg/Ca=1/20), b) $SrCO_3$Ap (Sr/Ca=1/1000), c) $SrCO_3$Ap (Sr/Ca=1/20)

a) 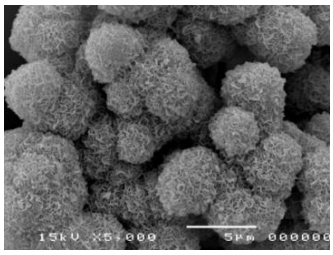 b) 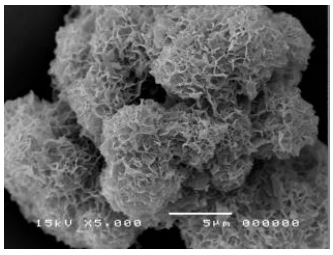 c) 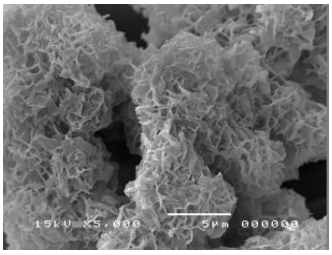

Figure 51 SEM Images Compare between Different Ions Substitution of Ca-CO_3Ap at Magnification 5,000×
a) $MgCO_3$Ap (Mg/Ca=1/20), b) $SrCO_3$Ap (Sr/Ca=1/1000), c) $SrCO_3$Ap (Sr/Ca=1/20).

A review in 1996 clearly explained the role of $Mg^{2+}$and CO_3^{2-} in synthetic apatite[59] which are two minor but important elements associated with biological apatite. The Type B CO_3^{2-} substitution into apatite will cause reduction in crystal size and changes in crystal shape, decrease in apatite content and increase in solubility. The combine of incorporation of $Mg^{2+}$and CO_3^{2-} would increase the extent of dissolution and may enhance the better biological response.

In another review[143], the effect of CO_3^{2-} on bone formation was explained and suggested that CO_3Ap-collagen scaffold with CO_3^{2-} content similar to that of human bone had optimal bone forming ability which confirmed by an *in vivo* study. The study also reported that divalent ions affected cell adhesion in relation to integrin molecule, an

adhesion molecule at the cell surface. Integrins are important receptor protein as they are the main way that cells both bind to and respond to the extracellular matrix. It has been reported that Mg^{2+} promotes cell adhesion[63] and also is an important factor in controlling *in vivo* bone metabolism since it plays a part in both bone formation and resorption[70]. Not only Mg^{2+} but Ca^{2+} had also been reported its ability to regulate cell function in tissue which may play a key role for pulp cells to differentiate to mineralized tissue forming cells[65].

In our study, we found the similar level of CO_3^{2-} compared to enamel, dentin and bone. From the SEM, the pictures demonstrated the smaller size and different shape of $MgCO_3Ap$ to CO_3Ap (Fig 54, 55). We could also detect both divalent ions, Mg^{2+} and Ca^{2+} from our apatite from the XPS data. Because of the synergistic effect of Mg^{2+} in CO_3Ap in apatite solubility, hence we believe this novel synthetic biological apatite will have a higher solubility than CO_3Ap which is a desired property in terms of ions (Mg^{2+} and Ca^{2+}) release to promote the better biological response to human pulp cells.

In our preliminary study, we mixed different % by weight of $MgCO_3Ap$ to GIC powder. We found 1% by weight $MgCO_3Ap$ added GIC had similar setting time to 2.5% by weight of $MgCO_3Ap$ added GIC (around 5 min) but had a higher compressive strength (around 164 MPa). However when we performed biological testing, we found 2.5% $MgCO_3ApGIC$ demonstrated better biological responses than 1% $MgCO_3Ap$ GIC. We also mixed 5% $MgCO_3Ap$ to GIC but we found a delay setting time and longer than the ISO standard (more than 6 minutes). As the result, we decided to formulate the 2.5% by weight $MgCO_3ApGIC$ to compare the physical properties and biological response to the Fuji IX® in our study.

We used encapsulated mixing procedure by an amalgamator in order to prepare GIC and $MgCO_3ApGIC$ in our study. Because of the agglomerate broccoli-like structure of $MgCO_3Ap$, it may affect the distribution of apatite when mixing $MgCO_3Ap$ with GIC powder at 2.5% by weight. The SEM images obtained from hand mixing

(mortar and pestle) and encapsulated mix (Fig. 52) demonstrated the better distribution of apatite and smaller particle size. In the lower magnification image (200×) a well distribution of $MgCO_3Ap$ in the GIC powder after encapsulated mix was observed (Figure 28).

a) 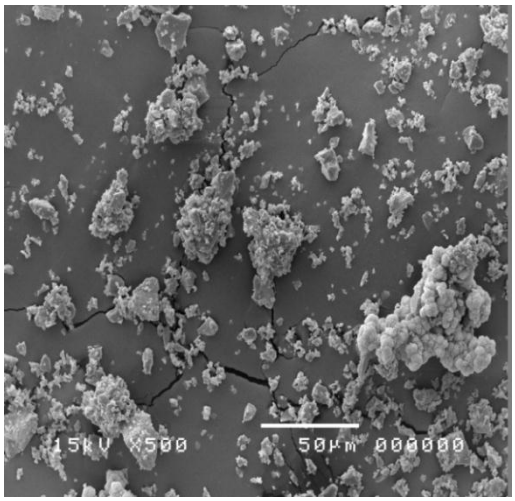

b) 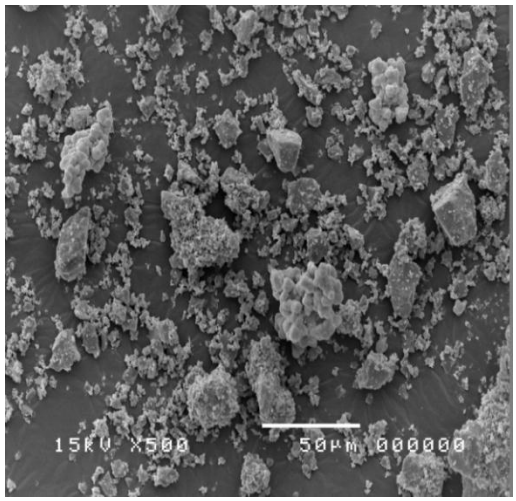

Figure 52 SEM Images Compare the Powder Distribution of $MgCO_3Ap$ at 2.5% by Weight in GIC Powder at Magnification 200×
a) Before encapsulated mix, b) After encapsulate mix. Encapsulated mix provided less agglomerate of the apatite and better distribution of the apatite in the GIC powder.

Developing dental materials require testing according to international standards in order to ensure the quality of the materials. The ISO (the International Organization for Standardization) and the ASTM (American Society for Testing and Materials) are two worldwide international bodies which provide standards for material testing.

In our study, we aimed to develop a dental material for restorative purpose and we tested the material according to the following standards.

a) The ISO 9917-1 Second edition 2007-10-1 Dentistry Water-based cements-Part 1: Powder/liquid acid-base cements

b) The ISO/TS 11405 Second edition 2003-02-01 Dental materials- Testing of adhesion to tooth structure

c) The ASTM E399-90 (Reapproved 1997) Standard Test Method for Plane-Strain Fracture Toughness of Metallic Materials

In Table 24, we summarized the physical properties compared between GIC and $MgCO_3$ApGIC. The setting time of the apatite cement is longer but still within the ISO limit for restorative materials. The ISO 9917-1 has set requirements for dental cements for restoration that the net setting time must be between 1.5- 6 minute and the compressive strength must be above 100 MPa. Our results found the setting time of our $MgCO_3$ApGIC was less than the time indicated (~4 minutes) by this standard.

Table 24 Physical Properties Comparisons of Control and Test Cements

		Control cements		Test cements		Stat. significance
Setting time		201	seconds	252	seconds	N/A
Compressive strength		132.2	MPa	132.6	MPa	N/A
Fracture toughness		0.429	$MPa \cdot m^{1/2}$	0.559	$MPa \cdot m^{1/2}$	$p<0.05$
Microleakage	Enamel	8/80	surfaces	4/80	surfaces	$p>0.05$
	Dentin	10/80	surfaces	2/80	surfaces	$p<0.05$
Shear bond strength		9.205	MPa	6.439	MPa	$p<0.05$

The compressive strength of Fuji IX, in one study [144] was reported at a value of 166.7±31.3 MPa. In our study we obtained a lower value of 132.6 ±10.3 MPa but it is within the ISO standard. Having added 2.5% $MgCO_3$Ap into GIC powder did not deteriorate the compressive strength of its original formulation (GIC = 132.2±12.5 MPa, $MgCO_3$ApGIC = 132.6±10.3 MPa) and this material is suitable to be used as restorative material.

Fracture toughness and adhesion to tooth structure are the key properties that required improvement for the current GICs. We tested the fracture

toughness of our $MgCO_3$ApGIC according to the ASTM E399-90 and the adhesion to tooth structure (microleakage and shear bond test) according to ISO/TS 11405.

Fracture toughness is a measurement of a material's ability to resist catastrophic failure (crack propagation) which is an intrinsic material property and independent of the type of test used. Then fracture toughness is a better indicator of clinical strength of materials than average stress-based tests such as compressive or diametral strength measurement[145]. Unfortunately, specifications for this property are not included in any standards for testing the GICs. The single-etch notch fracture toughness test based on ASTM specification E-399 is actually for the test of metallic materials. We desired to use this standard with our test cement and it was also used by the other researchers for composite and GICs[146, 147].

In a study[9] the fracture toughness of Fuji IX® was reported at 15 minutes to be 0.36±0.06 $MPa{\cdot}m^{1/2}$ which was lower than at 24 hours at 0.45±0.06 $MPa{\cdot}m^{1/2}$. On the other hand, HA- added material was as strong at 15 min to be 0.56±0.10 $MPa{\cdot}m^{1/2}$ as it was at 24h for 0.58±0.09 $MPa{\cdot}m^{1/2}$. The hastened development of cement strength as early as 15 minutes with addition of HA may imply the participation of HA in the initial setting of the cement. HA is soluble in acidic solution so that Ca^{2+} may be extracted from the surface of HA during cement mixing with polyacrylic liquid. The reaction mechanism that took place between HA and GIC may be similar to the mechanism of adhesion of GICs to enamel and dentin. Interaction of apatite found in the tooth structure with the polyacrylic acid produces polyacrylate ions that form strong ionic bonds[92].

In the present study we found the fracture toughness of the GIC increased from 15 minutes (0.28±0.05 $MPa{\cdot}m^{1/2}$) to 24 hours (0.45±0.05 $MPa{\cdot}m^{1/2}$). The $MgCO_3$Ap added GIC had the higher fracture toughness than the GIC and the toughness also increased significantly from 15 minutes (0.36±0.05 $MPa{\cdot}m^{1/2}$) to 24 hours (0.53±0.10 $MPa{\cdot}m^{1/2}$). Interestingly, the result showed that the fracture toughness of apatite added GIC at 15 minutes was not statistically significant from the toughness of

GIC at 24 hour. Our result indicated the improved fracture toughness of this $MgCO_3Ap$ added GIC.

GIC is known for its ability to chemically bond to tooth substrate. We aimed to improve the adhesion to tooth structure by adding $MgCO_3Ap$ to the current GIC. The evaluations of microleakage and shear bond test were conducted in this study.

Microleakage is defined as the clinically undetectable passage of bacteria, fluids, molecules, or ions between a cavity wall and the restorative material applied to it. Many techniques have been used to assess microleakage but the use of organic dyes as tracers is the one of the oldest and most common methods of detecting microleakage *in vitro.* The main disadvantage of microleakage evaluation is that it is a qualitative method. However we can make semi-quantitative by applying the non-parametric scale described in the ISO/TS 11405 which was used in this study.

The results of microleakage at enamel and dentin-GIC interface in this study were shown in Table 24. $MgCO_3ApGIC$ demonstrated a significantly less microleakage at the dentin interface than the GIC. At the enamel interface $MgCO_3ApGIC$ also showed less microleakage but it was not significantly different. The improved toughness and less microleakge may be due to the apatite added in the GIC and the bonding mechanism to tooth structure which will be explained later.

Bond strength tests are the most frequently used to screen adhesives. Currently, shear and microtensile bond tests are the most popular methods. It is important to note that bond strength value cannot be considered as a material property[99]. Hence the absolute value cannot be used to draw conclusion from, or compared with, data gathered from other studies. Only relative study outcomes are a valid basis for the result interpretation.

Mean shear bond strength of GIC to enamel (5.9±1.5 MPa) and dentin (6.0±1.9 MPa) were reported[148] and the 24 hour shear bond strength of GIC had been reported from 3.8-6.28 MPa[149, 150]. Lucas, *et al*. in 2003[9] also reported shear bond

strength of GIC and HA-added cement at 24 hours at 4.1±2.2 and 4.5±1.5 MPa respectively.

In the present study we found the shear bond strength was significantly higher in GIC (9.20±3.04 MPa) compared to the apatite added GIC (6.44±2.37 MPa) however from the SEM images of the fracture sites, all specimens had cohesive and mixed mode of failure. Several studies also reported the same results showing cohesive failure for GICs[135, 149]. This can be implied that the bond between the cement matrix and dental hard tissue was stronger than the bond between the cement matrix and the glass particles[106]. In our study we found lower shear bond strength with less microleakage at dentin interface of the $MgCO_3$ApGIC compared to the GIC. This may be because of the cohesive failure from the shear bond test seen in the SEM images, however, we still suggested that our $MgCO_3$ApGIC had better adhesion to tooth structure than the current GIC.

The exact mechanism for the chemical bonding of GICs to dental structures is not completely known. The mechanism of adhesion explained in an experiment[151] explained that GIC adhered to tooth structure was based on a substitution reaction between the carbonyl anion of polyacrylic acid in the liquid component of GIC, and the OH^-, Ca^{2+} and PO_4^{3-} in the HA which is the main component of tooth. On the basis of adsorption and infrared spectroscopic studies, Wilson *et al*[105] postulated that, during adsorption, polyacrylate penetrated the surface of HA and displaced PO_4^{3-}. Ca^{2+} was displaced by HA along with PO_4^{3-} as a part of a complex series of ionic exchanges. Yoshida *et al*[110] analyzed the chemical interaction of a synthesized polyalkenoic acid with enamel and with synthetic HA (Figure 53) and pointed out that COO^- of the polyalkenoic acid replaced PO_4^{3-} of the substrate and produced ionic bonds with Ca^{2+} of HA. For the HA-GIC, it seemed likely that Ca^{2+} from added HA may participate in this ionic exchange which needed further investigations.

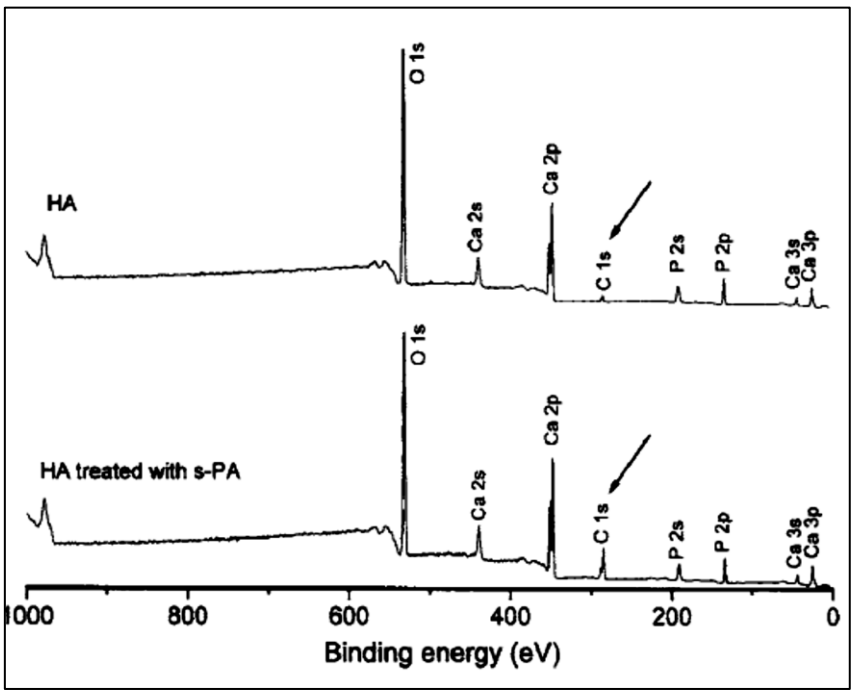

Figure 53 XPS Demonstration of Reaction between COO^- and HA with increasing of C1s peak (picture from Yoshida, et al[152])

The setting chemistry of GIC as described by Walls in 1986[87] occurred when surface layer of glass particles was attacked by the polyacid, resulting in the degradation of the glass with the release of Ca^{2+} and/or Sr^{2+}, Al^{3+} and F^- (dissolution phase). The divalent ions concentration of the cement sol rose rapidly than the trivalent ions because of the larger trivalent charges resulted in a lower rate of diffusion to the cement matrix when compared to the smaller divalent ions. The initial "clinical set" happened because of the cross linking between COO^- from the acid and the more mobile divalent ions. This phase described as gelation phase and over the next 24 hours, a maturation phase occurred because of the less mobile Al^{3+} bound within the cement matrix which lead to more rigid cross linking between the polyacid chains.

The physical properties of our $MgCO_3$ApGIC found in the present study may be due to the setting chemistry and interaction between acid to the added $MgCO_3$Ap. Figure 54 illustrated the distribution of $MgCO_3$Ap powder in the GIC powder. Once the powder mixed with the acid, the complex reaction could be postulated as in the Figure 55.

Immediately after acid attack, dissolution phase occurred, Sr^{2+} released from glass particles and the $MgCO_3Ap$ particles dissolved and released $Ca^{2+}$and Mg^{2+}. The increased of divalent ions may delay the initial clinical setting time. However the Al^{3+} then will start to interact with the COO^- and increase the physical strength.

The COO^- will interact with the Ca^{2+} in the $MgCO_3Ap$ and form an ionic bond which is stronger than the interface between GIC and the matrix. This may be one of the reasons to explain the higher fracture toughness of the $MgCO_3ApGIC$. This is because the force applied during the bending will go direct to the glass core, break the interface and cause the failure. The stronger bond of the $MgCO_3Ap$ to the matrix can resist more catastrophic failure and increase the fracture toughness.

When freshly mixed of the $MgCO_3ApGIC$ is applied on conditioned tooth surface which has available Ca^{2+} and PO_4^{2-}, the COO^- will bond with the Ca^{2+} on the tooth surface. At the same time Ca^{2+} released from the $MgCO_3Ap$ from the matrix will interact with the dentin PO_4^{3-} and some Ca^{2+} from the dentin also bond with the PO_4^{3-} from the $MgCO_3Ap$. This complex reaction may explain the improved bonding efficacy to tooth substrate.

The initial fluoride release from GIC is due to an acid-base reaction, with the amount of fluoride released proportional to the concentration of fluoride in the material[153]. This is responsible for the phenomenon of “burst effect” where in high amount of fluoride is released during the first two days. Fluoride release declines rapidly during the first week. The use of the deionized water to determine fluoride release has been suggested by several investigators. In one study[154] used the deionized water and found fluoride release (μg/dl/mm^2) from Fuji II on day 1 at 11.5±1.70 and 7.7±0.07 on day 2.

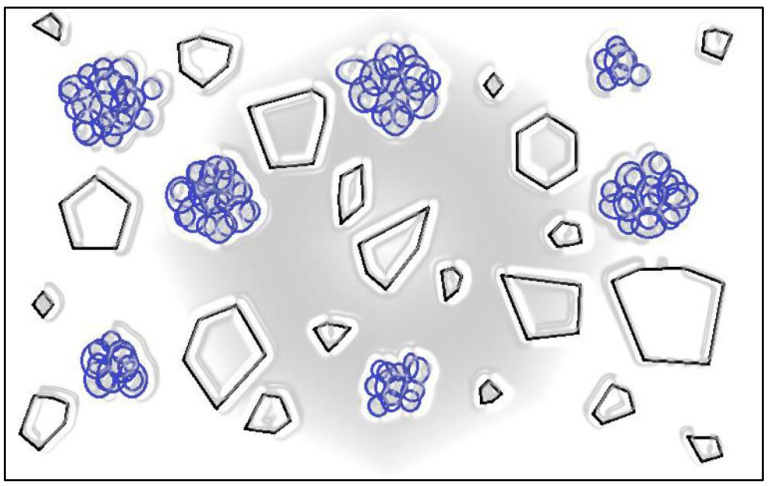

Figure 54 Illustration of $MgCO_3Ap$ Powder in the GIC Powder

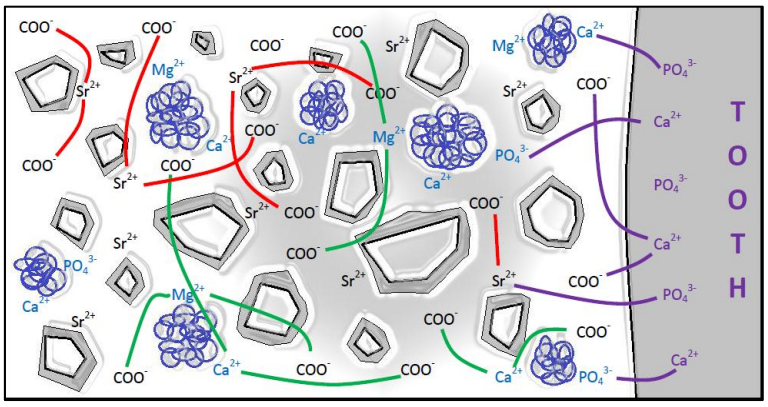

Figure 55 Proposed Complex Reaction within $MgCO_3ApGIC$

In our study we investigated the amount of F^- release from the $MgCO_3ApGIC$ under the expectation that adding $MgCO_3Ap$ into GIC should not deteriorate the F^- releasing behavior which considered as a main advantage of using GIC in preventive restorative dentistry. The result demonstrated non-deteriorate effect of adding $MgCO_3Ap$ which showed slightly higher F^- release throughout the experiment period in the $MgCO_3ApGIC$ group. This is equal to 48 hour accumulate release of 22.14 ppm in 1.4 ml culture medium compared to the release from the GIC group (20 ppm) which is similar to the amount shown in another study[9]. The added $MgCO_3Ap$ did not contain any F^- so the F^- must be originated from the fluoride containing alumino-silicate glass. F^-diffused through the matrix and/ or decomplexation of the F^- in the polysalt matrix can determine the long term F^- release[155].

In our current study, we also found the initial burst from 1-6 hours. From the specimen used in this study (4x6mm) the maximum release of fluoride was found at day 7 for both control and test cements at approximately 0.35 and 0.45 ppm respectively. However, the peak of fluoride release within 24 hours happened within the first 6 hours and drop at 12 hours. This might not affect the cariostatic effect of fluoride because of the ability of GIC to recharge F^- from oral environment in the clinical situation. Although it is not clear how much F^- is really necessary to afford cariostatic effect, evidences from *in vitro* and *in vivo* studies suggested that the present fluoride release from GICs would be able to afford inhibition of demineralization[156, 157] and would have remineralization potential[158]. There was also a report showing that low concentration of fluoride (50 μmol) had an effect on pulp-dentin regeneration[159].

Further investigation on the effect of F^- release and recharge from this $MgCO_3$ApGIC on demineralization, remineralization and on the pulp-dentin regeneration should be performed.

Role of ionic dissolution from biomaterials to regeneration is a topic of interest in this study. We conducted the ICP-OES to evaluate the concentration of Ca^{2+} and Mg^{2+} released from the $MgCO_3$ApGIC specimens at different time interval from the 20 mL of de-ionized water. The results obtained from the ICP-OES at 24 hours and 48 hours were used to estimate the ion release from the cements when put into different amount of culture medium. The culture medium used to conduct the biological evaluation was summarized in Table 25. In this study, the control cement released Mg^{2+} at 0.160 ppm. This ion release was from deionized water (extracted medium) at the volume of 20 mL. The specimen size was 4×6 mm^2 so the total area of the specimen was 100 mm^2. The total release of Mg^{2+} in 20 mL extracted medium was 3.2 μg. In WST-1 assay, we used 1 mL of culture medium to extract the ion so the concentration of Mg^{2+} in 1 mL medium will be 3.2 ppm.

Table 25 Estimated Ion Release in Biological Testing of Control and Test Cements

		Actual release at 24 h from 20 mL extracted medium (ppm)	Calculate release at 24 h from 1 mL extracted medium (ppm)	Actual release at 48 h from 20 mL extracted medium (ppm)	Calculate release at 48 h from 1.4 mL extracted medium (ppm)
Ca^{2+}	control	0.81	16.20	0.83	11.86
	test	2.13	42.60	2.25	32.14
Mg^{2+}	control	0.16	3.20	0.16	2.29
	test	0.29	5.80	0.31	4.43

Studies reported the highest concentration of Ca^{2+} (1.8 mM, 72 ppm) [11, 160] enhance FN gene expression in dental pulp cell. However a study in 2005 found the higher Ca^{2+} concentration (80-240 ppm) promoted the higher cell proliferation and ALPase activity[65]. It had also been identified that Mg^{2+} had a positive effect to cells adhesion at the concentration of 24.3 ppm[71]. Since α-MEM had already contained 1.8 mM $CaCl_2$ (Ca^{2+}, 72 ppm) and 0.813 mM MgSO4 (Mg^{2+}, 19.75 ppm), additional 4.55 ppm of Mg^{2+} and higher than 8 ppm of Ca^{2+} would promote the better biological response of pulp cells.

In our study, we found 5.80 ppm and 10.23 ppm accumulated release of Mg^{2+} from test cement at 24 to 48 hours. At the same time, the test cement also demonstrated 42.60 ppm and 74.74 ppm accumulated release of Ca^{2+}. The ion release from control cement was quite low when compared to the test cement. This may explain the improved effects of Mg^{2+} and Ca^{2+} released from our $MgCO_3$ApGIC to the cell adhesion and proliferation at the early time point due to the highest cell proliferation at day 1 from WST-1 assay, the early expression of COL1A1 gene at day 1 and, the improved ALPase activity of this $MgCO_3$ApGIC to the GIC.

Ascorbic acid (AA) plays a critical role in the production of the collagenous extracellular matrix. AA is an enzyme cofactor and antioxidant that stimulates the transcription, translation and post-translational processing of collagen in

the connective tissue cells[161]. In cultures of bone-derived cells, AA stimulates osteoblastic differentiation, synthesis and deposition of collagen as well as mineralization[162, 163]. Cells cultured in various concentrations of AA demonstrate a dose-dependent synthesis of collagen which increases in the accumulation of the extracellular matrix and results in a higher ALPase activity and ability to form mineralized matrix[164]. β-GP is routinely added to bone cell cultures to induce osteogenesis and promote calcium phosphate deposition. The mechanism by which the β-GP induced mineralization is closely linked to the high ALPase activity. ALPase will hydrolyze β-GP to produce high level of local phosphate ions for chemical reaction in mineral deposition[165, 166].

A study reported that addition of AA to α-MEM, which contains 50 μg/mL of AA, did not result in a significant effect on cell proliferation and ALPase activity. On the other hand, when higher AA presented together with β-GP in the culture medium, it demonstrated the delay in the initiation of the mineralization process[167]. This may be related to the balance accumulation/ maturation of the collagenous matrix because the amount, composition and maturation of the extracellular matrix affect proliferation of bone cells[161, 164].

In the presence of phosphate ions, mineralization can occur when the extracellular matrix is achieved its maturation. On the other hand, in the absence of source of phosphate ions from β-GP hydrolysis, cells can still show a higher proliferation rate. However cells will only present the osteoblastic feature (higher ALPase activity) but not the osteoblastic differentiation feature.

The sequence of differentiation starts with active cell proliferation, expression of osteoblastic markers, synthesis, deposition and maturation of a collagenous extracellular matrix and matrix mineralization[162]. Cell proliferation was reported to decrease after 3 weeks as a result of the accumulation, maturation and mineralization of the extracellular matrix[162, 168]. After the decrease of proliferation, the differentiation of cells will be detected.

In our study, we did not add AA and β-GP for the cultures used for WST-1, ALPase assay and gene expression while we added in the alizarin red staining assay for calcification. As discussed earlier, $MgCO_3Ap$ released Mg^{2+} and Ca^{2+} which may stimulate cell adhesion to promote cell proliferation and ALPase activity. The 50 μg/mL AA in the culture medium stimulated collagen synthesis to produce the ECM. $MgCO_3Ap$ released PO_4^{3-} which was a source for $CaPO_4$ deposition on the ECM. However as review above, when added AA in the presence of β-GP, it may delay the mineralization process because of the imbalance of amount and maturation of collagen matrix. This may explain the delay of mineral nodule formation when added AA and βGP to the alizarin red staining assay since the significantly increase of calcify nodule formation in the test cement at day 14 could not be detected.

The increase in the ALPase levels has been routinely used in the *in vitro* experiments as a relative marker of osteoblastic differentiation. ALPase has been associated with biological calcification. Enhanced expression of this enzyme is needed prior to the onset of matrix mineralization as it will provide source of inorganic phosphate for HA crystal nucleation[165]. Osteoblastic differentiation ability was reported to be decreased after serially passaged human bone marrow cells[169]. The significant increase in the ALPase level suggested the shifting of the cells to a more differentiated stage. The formation of mineral deposits occurred following the maximum ALPase activity. However, the study reported the significant decrease of ALPase and suggested that serial passage resulted in less cell differentiation.

DMP-1 was found to be critical in pulp-dentin regeneration. Mechanism in which DMP-1 induced cytodifferentiation of dental pulp stem cells into odontoblasts had been explained[170]. Dentinogenesis occurs by a two-stage process: formation of the inorganic predentin and its subsequent mineralization which requires odontoblasts. DMP-1 appears to be a macromolecule with inductive properties. Expression of DMP-1 in pluripotent and mesenchyme-derived cells will induce the cells to differentiate into functional odontoblastic like cells. Inflammation induced by trauma of the pulp exposure

will enhance the mobilization of the cells and increase the blood supply. This will recruit more undifferentiated cells to come to the exposure site. DMP-1 then could influence those competent cells at the site of repair and results in the formation of a tissue that is functionally and structurally equivalent to physiologic dentin.

In a recent review[171] it was indicated that there was an association between DMP-1 and DSPP. DMP-1 is primarily expressed in dentin and bone and DSPP may be upregulated by DMP-1 during dentinogenesis. DSPP is dentin-specific and is expressed mostly by odontoblast cells and slightly in bone cells[172]. The expression of the DSPP gene was a significant marker for odontoblast differentiation. The increase of mature odontoblasts was the beginning of dentin mineralization which was considered as a terminal phenotypic marker of mature odontoblasts[173]. DSPP is critical for dentin mineralization although the mechanism is unclear. However, it has been hypothesized that the proteolytic process of DSPP to DPP and DSP is an activation step. This step converts a large precursor into active fragments and directly involves in biomineralization. Functional differentiation of odontoblasts is characterized by amplification of collagen type1 and the synthesis of DPPs. DPP will bind to collagen and calcium and promotes the nucleation and growth of HA crystal.

In the clinical situation, when odontoblasts were destroyed, the surrounding pulp cells started to proliferate. After proliferation, pulp cells differentiated to odontoblastic- like cells and started the dentin regenerative process. In some circumstances with decreased proliferation ability and ALPase activity, it may result in deficient formation of reparative dentin. A study reported the correlation between the proliferation ability and ALPase activity and *in vivo* cellular aging in pulp cells. The result showed the decreasing in proliferation ability and ALPase activity in senior age group (older than 64 year old) compared to younger age group (6-18 year old) with the highest activity in 6 year old donor[174]. However this finding still had a conflict with the other study which found that proliferative activity of human pulp cells in culture did not correlate with donor ages (between 19 year old and around 45 year old)[175].

In our study, the donor was not as young as below 19 years old. Our study proposed to investigate the biological response of the human pulp cells to different materials and also compared to the normal abilities and activities with no materials. Therefore, we didn't compare the impact of different donors to the biological response of the materials. This study supported that the novel material may be a better choice to use as a restorative material for deep cavities. However it is also important to further investigate the biological responses of this novel GIC with different donors in different age groups to confirm the potential of the material for pulp-dentin regeneration in wider population.

In the present study, we found the ability of the $MgCO_3$ApGIC to facilitate earlier and higher pulp cell proliferation than GIC. $MgCO_3$ApGIC also demonstrated improvement of the negative effect of the GIC on the ALPase activity. We also found the highest COL1A1 gene expression since day 1 in the $MgCO_3$ApGIC. The collagen synthesis is critical for healing process and the earlier expression is better. DMP-1 gene in the $MgCO_3$ApGIC expressed as early as day 7 while in the GIC demonstrated the delay effect which started at day 14. For the DSPP gene expression, we also found the earlier expression of this gene in the $MgCO_3$ApGIC at day 14. Even we could not visually detect a significant mineral deposition from the Alizarin red staining at day 14 but we found potential of the $MgCO_3$ApGIC to promote the mineralization.

As a consequent, the data obtained from all biological experiments indicated the improvement in the biological responses of $MgCO_3$ApGIC compared to the GIC. This may suggested a potential of this material in promoting pulp-dentin regeneration.

In conclusion, we aimed to develop a novel GIC with improved physical properties in fracture toughness and microleakage. We also expected this novel GIC to have a potential of pulp-dentin regenerative properties. We successfully developed $MgCO_3$Ap and added this apatite into the GIC used for the ART. We found improved fracture toughness, adhesion to tooth structure (less microleakage) compared to Fuji IX

GP®. Moreover we found a promising data indicated better *in vitro* biological responses. These responses included earlier and higher cell proliferation, early ALPase activity, gene expression related to pulp-dentin regeneration (COL1A1, DMP-1, DSPP) and some calcified nodule formation from our $MgCO_3$ApGIC.

However with the limitation of biological responses obtained from *in vitro* model, it is valuable to further investigate this effect *in vivo*. The results from *in vivo* studies might encourage researchers to conduct clinical studies to confirm the clinical efficacy especially of the treatment of deep cavities. Finally, this novel GIC with improved fracture toughness, sealing ability and potentials in promoting pulpal healing, may ensure managements of deep caries, thus improve the quality of treatment. And in long term, may improve oral health and quality of life of patients.

REFERENCES

(1) American Academy on Pediatric D, American Academy of P. Policy on early childhood caries (ECC): classifications, consequences, and preventive strategies. **Pediatr Dent** 30 (2008):40-3.

(2) The 6th National Oral Health Survey. Bureau of Dental Health, Department of Health Ministry of Public Health, Thailand., 2006-2007.

(3) Kagihara LE, Niederhauser VP, Stark M. Assessment, management, and prevention of early childhood caries. **J Am Acad Nurse Pract** 21 (2009):1-10.

(4) Mjor IA, Gordan VV. A review of atraumatic restorative treatment (ART). **International dental journal** 49 (1999):127-31.

(5) Thompson V, Craig RG, Curro FA, Green WS, Ship JA. Treatment of deep carious lesions by complete excavation or partial removal: a critical review. **J Am Dent Assoc** 139 (2008):705-12.

(6) Ricketts DN, Kidd EA, Innes N, Clarkson J. Complete or ultraconservative removal of decayed tissue in unfilled teeth. **Cochrane Database Syst Rev** 3 (2006):CD003808.

(7) Handelman SL, Washburn F, Wopperer P. Two-year report of sealant effect on bacteria in dental caries. **J Am Dent Assoc** 93 (1976):967-70.

(8) van Amerongen WE. Dental caries under glass ionomer restorations. **J Public Health Dent** 56 (1996):150-4; discussion 61-3.

(9) Lucas ME, Arita K, Nishino M. Toughness, bonding and fluoride-release properties of hydroxyapatite-added glass ionomer cement. **Biomaterials** 24 (2003):3787-94.

(10) Yamasaki Y, Yoshida Y, Okazaki M, Shimazu A, Uchida T, Kubo T, et al. Synthesis of functionally graded MgCO3 apatite accelerating osteoblast adhesion. **J Biomed Mater Res** 62 (2002):99-105.

(11) Mizuno M, Banzai Y. Calcium ion release from calcium hydroxide stimulated fibronectin gene expression in dental pulp cells and the differentiation of

dental pulp cells to mineralized tissue forming cells by fibronectin. **International endodontic journal** 41 (2008):933-8.

(12) About I, Bottero MJ, de Denato P, Camps J, Franquin JC, Mitsiadis TA. Human dentin production in vitro. **Exp Cell Res** 258 (2000):33-41.

(13) Linde A, Lussi A, Crenshaw MA. Mineral induction by immobilized polyanionic proteins. **Calcified tissue international** 44 (1989):286-95.

(14) Clarkson BH, McCurdy SP, Gaz D, Hand AR. Effects of phosphoprotein on collagen fibril formation in vitro. **Archives of oral biology** 38 (1993):737-43.

(15) Bronckers AL, D'Souza RN, Butler WT, Lyaruu DM, van Dijk S, Gay S, et al. Dentin sialoprotein: biosynthesis and developmental appearance in rat tooth germs in comparison with amelogenins, osteocalcin and collagen type-I. **Cell and tissue research** 272 (1993):237-47.

(16) Butler WT, Bhown M, Brunn JC, D'Souza RN, Farach-Carson MC, Happonen RP, et al. Isolation, characterization and immunolocalization of a 53-kDal dentin sialoprotein (DSP). **Matrix** 12 (1992):343-51.

(17) Qin C, Brunn JC, Cadena E, Ridall A, Tsujigiwa H, Nagatsuka H, et al. The expression of dentin sialophosphoprotein gene in bone. **Journal of dental research** 81 (2002):392-4.

(18) George A, Sabsay B, Simonian PA, Veis A. Characterization of a novel dentin matrix acidic phosphoprotein. Implications for induction of biomineralization. **J Biol Chem** 268 (1993):12624-30.

(19) Finkelman RD, Mohan S, Jennings JC, Taylor AK, Jepsen S, Baylink DJ. Quantitation of growth factors IGF-I, SGF/IGF-II, and TGF-beta in human dentin. **J Bone Miner Res** 5 (1990):717-23.

(20) Roberts-Clark DJ, Smith AJ. Angiogenic growth factors in human dentine matrix. **Arch Oral Biol** 45 (2000):1013-6.

(21) Zhao S, Sloan AJ, Murray PE, Lumley PJ, Smith AJ. Ultrastructural localisation of TGF-beta exposure in dentine by chemical treatment. **Histochem J** 32 (2000):489-94.

(22) Mjor IA. Dentin permeability: the basis for understanding pulp reactions and adhesive technology. **Braz Dent J** 20 (2009):3-16.

(23) Murray PE, Smith AJ, Windsor LJ, Mjor IA. Remaining dentine thickness and human pulp responses. **Int Endod J** 36 (2003):33-43.

(24) Stanley HR, Going RE, Chauncey HH. Human pulp response to acid pretreatment of dentin and to composite restoration. **J Am Dent Assoc** 91 (1975):817-25.

(25) Stanley HR. Dental iatrogenesis. **Int Dent J** 44 (1994):3-18.

(26) Pameijer CH, Stanley HR, Ecker G. Biocompatibility of a glass ionomer luting agent. 2. Crown cementation. **Am J Dent** 4 (1991):134-41.

(27) Mjor IA, Ferrari M. Pulp-dentin biology in restorative dentistry. Part 6: Reactions to restorative materials, tooth-restoration interfaces, and adhesive techniques. **Quintessence Int** 33 (2002):35-63.

(28) Hahn CL, Liewehr FR. Relationships between caries bacteria, host responses, and clinical signs and symptoms of pulpitis. **J Endod** 33 (2007):213-9.

(29) Kakehashi S, Stanley HR, Fitzgerald RJ. The Effects of Surgical Exposures of Dental Pulps in Germ-Free and Conventional Laboratory Rats. **Oral Surg Oral Med Oral Pathol** 20 (1965):340-9.

(30) Goldberg M, Farges JC, Lacerda-Pinheiro S, Six N, Jegat N, Decup F, et al. Inflammatory and immunological aspects of dental pulp repair. **Pharmacological research : the official journal of the Italian Pharmacological Society** 58 (2008):137-47.

(31) Bergenholtz G. Effect of bacterial products on inflammatory reactions in the dental pulp. **Scand J Dent Res** 85 (1977):122-9.

(32) Bergenholtz G. Inflammatory response of the dental pulp to bacterial irritation. **J Endod** 7 (1981):100-4.

(33) Warfvinge J, Dahlen G, Bergenholtz G. Dental pulp response to bacterial cell wall material. **J Dent Res** 64 (1985):1046-50.

(34) Murray PE, About I, Lumley PJ, Franquin JC, Remusat M, Smith AJ. Cavity remaining dentin thickness and pulpal activity. **Am J Dent** 15 (2002):41-6.

(35) Rutherford RB, Gu K. Treatment of inflamed ferret dental pulps with recombinant bone morphogenetic protein-7. **Eur J Oral Sci** 108 (2000):202-6.

(36) Bjorndal L, Mjor IA. Pulp-dentin biology in restorative dentistry. Part 4: Dental caries--characteristics of lesions and pulpal reactions. **Quintessence Int** 32 (2001):717-36.

(37) Cooper PR, Takahashi Y, Graham LW, Simon S, Imazato S, Smith AJ. Inflammation-regeneration interplay in the dentine-pulp complex. **Journal of Dentistry** 38 (2010):687-97.

(38) Smith AJ, Cassidy N, Perry H, Begue-Kirn C, Ruch JV, Lesot H. Reactionary dentinogenesis. **Int J Dev Biol** 39 (1995):273-80.

(39) Seltzer S, Bender IB, Ziontz M. The Dynamics of Pulp Inflammation: Correlations between Diagnostic Data and Actual Histologic Findings in the Pulp. **Oral Surg Oral Med Oral Pathol** 16 (1963):969-77.

(40) Veerayutthwilai O, Byers MR, Pham TT, Darveau RP, Dale BA. Differential regulation of immune responses by odontoblasts. **Oral Microbiol Immunol** 22 (2007):5-13.

(41) Takahashi N, Nyvad B. Caries ecology revisited: microbial dynamics and the caries process. **Caries Res** 42 (2008):409-18.

(42) Lee YL, Liu J, Clarkson BH, Lin CP, Godovikova V, Ritchie HH. Dentin-pulp complex responses to carious lesions. **Caries research** 40 (2006):256-64.

(43) Smith AJ, Lumley PJ, Tomson PL, Cooper PR. Dental regeneration and materials: a partnership. **Clinical oral investigations** 12 (2008):103-8.

(44) Kidd EA. How 'clean' must a cavity be before restoration? **Caries Res** 38 (2004):305-13.

(45) Hanks CT, Wataha JC, Sun Z. In vitro models of biocompatibility: a review. **Dental materials : official publication of the Academy of Dental Materials** 12 (1996):186-93.

(46) Bouillaguet S, Wataha JC. Future directions in bonding resins to the dentine-pulp complex. **Journal of oral rehabilitation** 31 (2004):385-92.

(47) Goldberg M, Smith AJ. Cells and Extracellular Matrices of Dentin and Pulp: A Biological Basis for Repair and Tissue Engineering. **Critical reviews in oral biology and medicine : an official publication of the American Association of Oral Biologists** 15 (2004):13-27.

(48) Smith AJ. Vitality of the dentin-pulp complex in health and disease: growth factors as key mediators. **Journal of dental education** 67 (2003):678-89.

(49) Ferracane JL, Cooper PR, Smith AJ. Can interaction of materials with the dentin-pulp complex contribute to dentin regeneration? **Odontology / the Society of the Nippon Dental University** 98 (2010):2-14.

(50) Graham L, Cooper PR, Cassidy N, Nor JE, Sloan AJ, Smith AJ. The effect of calcium hydroxide on solubilisation of bio-active dentine matrix components. **Biomaterials** 27 (2006):2865-73.

(51) Tomson PL, Grover LM, Lumley PJ, Sloan AJ, Smith AJ, Cooper PR. Dissolution of bio-active dentine matrix components by mineral trioxide aggregate. **J Dent** 35 (2007):636-42.

(52) Narita H, Itoh S, Imazato S, Yoshitake F, Ebisu S. An explanation of the mineralization mechanism in osteoblasts induced by calcium hydroxide. **Acta Biomaterialia** 6 (2010):586-90.

(53) Williams DF. Biomaterials and biocompatibility. **Medical progress through technology** 4 (1976):31-42.

(54) Schmalz G. Use of cell cultures for toxicity testing of dental materials--advantages and limitations. **Journal of dentistry** 22 Suppl 2 (1994):S6-11.

(55) Hoppe A, Guldal NS, Boccaccini AR. A review of the biological response to ionic dissolution products from bioactive glasses and glass-ceramics. **Biomaterials**.

(56) Leventouri T. Synthetic and biological hydroxyapatites: crystal structure questions. **Biomaterials** 27 (2006):3339-42.

(57) Legeros RZ, Trautz OR, Legeros JP, Klein E, Shirra WP. Apatite crystallites: effects of carbonate on morphology. **Science** 155 (1967):1409-11.

(58) Van Wazer JR. Phosphorus and its compounds. New York,: Interscience Publishers; 1958.

(59) LeGeros RZ, Sakae T, Bautista C, Retino M, LeGeros JP. Magnesium and carbonate in enamel and synthetic apatites. **Adv Dent Res** 10 (1996):225-31.

(60) LeGeros RZ, Kijkowska R, Bautista C, LeGeros JP. Synergistic effects of magnesium and carbonate on properties of biological and synthetic apatites. **Connective tissue research** 33 (1995):203-9.

(61) Okazaki M, LeGeros RZ. Properties of heterogeneous apatites containing magnesium, fluoride, and carbonate. **Adv Dent Res** 10 (1996):252-9.

(62) Staquet MJ, Couble ML, Romeas A, Connolly M, Magloire H, Hynes RO, et al. Expression and localisation of alphav integrins in human odontoblasts. **Cell and tissue research** 323 (2006):457-63.

(63) Lange TS, Bielinsky AK, Kirchberg K, Bank I, Herrmann K, Krieg T, et al. Mg2+ and Ca2+ differentially regulate beta 1 integrin-mediated adhesion of dermal fibroblasts and keratinocytes to various extracellular matrix proteins. **Exp Cell Res** 214 (1994):381-8.

(64) Zreiqat H, Howlett CR, Zannettino A, Evans P, Schulze-Tanzil G, Knabe C, et al. Mechanisms of magnesium-stimulated adhesion of osteoblastic cells to commonly used orthopaedic implants. **Journal of biomedical materials research** 62 (2002):175-84.

(65) Maeno S, Niki Y, Matsumoto H, Morioka H, Yatabe T, Funayama A, et al. The effect of calcium ion concentration on osteoblast viability, proliferation and differentiation in monolayer and 3D culture. **Biomaterials** 26 (2005):4847-55.

(66) Wiesmann HP, Tkotz T, Joos U, Zierold K, Stratmann U, Szuwart T, et al. Magnesium in newly formed dentin mineral of rat incisor. **J Bone Miner Res** 12 (1997):380-3.

(67) Althoff J, Quint P, Krefting ER, Hohling HJ. Morphological studies on the epiphyseal growth plate combined with biochemical and X-ray microprobe analyses. **Histochemistry** 74 (1982):541-52.

(68) Bigi A, Foresti E, Gregorini R, Ripamonti A, Roveri N, Shah JS. The role of magnesium on the structure of biological apatites. **Calcified tissue international** 50 (1992):439-44.

(69) Tsuboi S, Nakagaki H, Ishiguro K, Kondo K, Mukai M, Robinson C, et al. Magnesium distribution in human bone. **Calcified tissue international** 54 (1994):34-7.

(70) Serre CM, Papillard M, Chavassieux P, Voegel JC, Boivin G. Influence of magnesium substitution on a collagen-apatite biomaterial on the production of a calcifying matrix by human osteoblasts. **Journal of biomedical materials research** 42 (1998):626-33.

(71) Inoue M, LeGeros RZ, Inoue M, Tsujigiwa H, Nagatsuka H, Yamamoto T, et al. In vitro response of osteoblast-like and odontoblast-like cells to unsubstituted and substituted apatites. **Journal of biomedical materials research Part A** 70 (2004):585-93.

(72) Kiba W, Imazato S, Takahashi Y, Yoshioka S, Ebisu S, Nakano T. Efficacy of polyphasic calcium phosphates as a direct pulp capping material. **Journal of Dentistry** 38 (2010):828-37.

(73) Ruoslahti E, Engvall E, Hayman EG. Fibronectin: current concepts of its structure and functions. **Coll Relat Res** 1 (1981):95-128.

(74) Ruch JV. Patterned distribution of differentiating dental cells: facts and hypotheses. **J Biol Buccale** 18 (1990):91-8.

(75) Nakashima M, Akamine A. The application of tissue engineering to regeneration of pulp and dentin in endodontics. **J Endod** 31 (2005):711-8.

(76) Lesot H, Fausser JL, Akiyama SK, Staub A, Black D, Kubler MD, et al. The carboxy-terminal extension of the collagen binding domain of fibronectin mediates interaction with a 165 kDa membrane protein involved in odontoblast differentiation. **Differentiation** 49 (1992):109-18.

(77) Tziafas D, Alvanou A, Kaidoglou K. Dentinogenic activity of allogenic plasma fibronectin on dog dental pulp. **J Dent Res** 71 (1992):1189-95.

(78) Yoshiba N, Yoshiba K, Nakamura H, Iwaku M, Ozawa H. Immunoelectron-microscopic study of the localization of fibronectin in the odontoblast layer of human teeth. **Arch Oral Biol** 40 (1995):83-9.

(79) Piva E, Tarquinio SB, Demarco FF, Silva AF, de Araujo VC. Immunohistochemical expression of fibronectin and tenascin after direct pulp capping with calcium hydroxide. **Oral Surg Oral Med Oral Pathol Oral Radiol Endod** 102 (2006):e66-71.

(80) Tziafas D, Alvanou A, Panagiotakopoulos N, Smith AJ, Lesot H, Komnenou A, et al. Induction of odontoblast-like cell differentiation in dog dental pulps after in vivo implantation of dentine matrix components. **Arch Oral Biol** 40 (1995):883-93.

(81) Murray PE, About I, Franquin JC, Remusat M, Smith AJ. Restorative pulpal and repair responses. **J Am Dent Assoc** 132 (2001):482-91.

(82) Kitasako Y, Murray PE, Tagami J, Smith AJ. Histomorphometric analysis of dentinal bridge formation and pulpal inflammation. **Quintessence Int** 33 (2002):600-8.

(83) Zhang W, Walboomers XF, Jansen JA. The formation of tertiary dentin after pulp capping with a calcium phosphate cement, loaded with PLGA

microparticles containing TGF-beta1. **J Biomed Mater Res A** 85 (2008):439-44.

(84) Hayashi Y, Imai M, Yanagiguchi K, Viloria IL, Ikeda T. Hydroxyapatite applied as direct pulp capping medicine substitutes for osteodentin. **J Endod** 25 (1999):225-9.

(85) Wilson AD, Kent BE. A new translucent cement for dentistry. The glass ionomer cement. **British dental journal** 132 (1972):133-5.

(86) Smith DC. Development of glass-ionomer cement systems. **Biomaterials** 19 (1998):467-78.

(87) Walls AW. Glass polyalkenoate (glass-ionomer) cements: a review. **Journal of dentistry** 14 (1986):231-46.

(88) Wilson AD, Crisp S, Ferner AJ. Reactions in glass-ionomer cements: IV. Effect of chelating comonomers on setting behavior. **Journal of dental research** 55 (1976):489-95.

(89) Cook WD. Degradative analysis of glass ionomer polyelectrolyte cements. **J Biomed Mater Res** 17 (1983):1015-27.

(90) Wasson EA, Nicholson JW. New aspects of the setting of glass-ionomer cements. **J Dent Res** 72 (1993):481-3.

(91) Wilson AD. Glass-ionomer cement--origins, development and future. **Clinical materials** 7 (1991):275-82.

(92) Wilson AD, McLean JW. Glass-ionomer cement. Chicago: Quintessence Pub. Co.; 1988. 274 p. p.

(93) Mount GJ, Makinson OF. Clinical characteristics of a glass-ionomer cement. **Br Dent J** 145 (1978):67-71.

(94) Crisp S, Lewis BG, Wilson AD. Characterization of glass-ionomer cements. 2. Effect of the powder: liquid ratio on the physical properties. **Journal of dentistry** 4 (1976):287-90.

(95) Crisp S, Wilson AD. Reactions in glass ionomer cements: I. Decomposition of the powder. **Journal of dental research** 53 (1974):1408-13.

(96) Xie D, Brantley WA, Culbertson BM, Wang G. Mechanical properties and microstructures of glass-ionomer cements. **Dent Mater** 16 (2000):129-38.

(97) Prosser HJ, Powis DR, Wilson AD. Glass-ionomer Cements of Improved Flexural Strength. **Journal of dental research** 65 (1986):146-8.

(98) Van Meerbeek B, De Munck J, Yoshida Y, Inoue S, Vargas M, Vijay P, et al. Buonocore memorial lecture. Adhesion to enamel and dentin: current status and future challenges. **Oper Dent** 28 (2003):215-35.

(99) Van Noort R, Noroozi S, Howard IC, Cardew G. A critique of bond strength measurements. **Journal of dentistry** 17 (1989):61-7.

(100) Schreiner RF, Chappell RP, Glaros AG, Eick JD. Microtensile testing of dentin adhesives. **Dental materials : official publication of the Academy of Dental Materials** 14 (1998):194-201.

(101) Kidd EA. Microleakage: a review. **J Dent** 4 (1976):199-206.

(102) Bouillaguet S, Duroux B, Ciucchi B, Sano H. Ability of adhesive systems to seal dentin surfaces: an in vitro study. **J Adhes Dent** 2 (2000):201-8.

(103) Tyas MJ. Milestones in adhesion: glass-ionomer cements. **The journal of adhesive dentistry** 5 (2003):259-66.

(104) Davidson CL, Mjor IA. Advances in glass-ionomer cements. Chicago: Quintessence Pub. Co.; 1999. 303 p. p.

(105) Wilson AD, Prosser HJ, Powis DM. Mechanism of adhesion of polyelectrolyte cements to hydroxyapatite. **Journal of dental research** 62 (1983):590-2.

(106) Ngo H, Mount GJ, Peters MC. A study of glass-ionomer cement and its interface with enamel and dentin using a low-temperature, high-resolution scanning electron microscopic technique. **Quintessence Int** 28 (1997):63-9.

(107) Ferrari M, Davidson CL. Interdiffusion of a traditional glass ionomer cement into conditioned dentin. **American journal of dentistry** 10 (1997):295-7.

(108) Hosoya Y, Garcia-Godoy F. Bonding mechanism of Ketac-Molar Aplicap and Fuji IX GP to enamel and dentin. **American journal of dentistry** 11 (1998):235-9.

(109) Sennou HE, Lebugle AA, Gregoire GL. X-ray photoelectron spectroscopy study of the dentin-glass ionomer cement interface. **Dental materials : official publication of the Academy of Dental Materials** 15 (1999):229-37.

(110) Yoshida Y, Van Meerbeek B, Nakayama Y, Snauwaert J, Hellemans L, Lambrechts P, et al. Evidence of chemical bonding at biomaterial-hard tissue interfaces. **Journal of dental research** 79 (2000):709-14.

(111) Geiger SB, Weiner S. Fluoridated carbonatoapatite in the intermediate layer between glass ionomer and dentin. **Dental materials : official publication of the Academy of Dental Materials** 9 (1993):33-6.

(112) Mickenautsch S, Mount G, Yengopal V. Therapeutic effect of glass-ionomers: an overview of evidence. **Australian dental journal** 56 (2011):10-5; quiz 103.

(113) Wahab FK, Shellis RP, Elderton RJ. Effects of low fluoride concentrations on formation of caries-like lesions in human enamel in a sequential-transfer bacterial system. **Archives of oral biology** 38 (1993):985-95.

(114) Sidhu SK, Schmalz G. The biocompatibility of glass-ionomer cement materials. A status report for the American Journal of Dentistry. **American journal of dentistry** 14 (2001):387-96.

(115) Hume WR. Methods of assessment in vitro of restorative material cytotoxicity using an intact human dentine diffusion step. **International endodontic journal** 21 (1988):85-8.

(116) Pashley DH. The influence of dentin permeability and pulpal blood flow on pulpal solute concentrations. **Journal of endodontics** 5 (1979):355-61.

(117) Schmalz G, Hiller KA, Nunez LJ, Stoll J, Weis K. Permeability characteristics of bovine and human dentin under different pretreatment conditions. **Journal of endodontics** 27 (2001):23-30.

(118) Forss H. Release of fluoride and other elements from light-cured glass ionomers in neutral and acidic conditions. **Journal of dental research** 72 (1993):1257-62.

(119) Bapna MS, Mueller HJ. Leaching from glass ionomer cements. **Journal of oral rehabilitation** 21 (1994):577-83.

(120) Geurtsen W. Substances released from dental resin composites and glass ionomer cements. **Eur J Oral Sci** 106 (1998):687-95.

(121) Forsten L. Fluoride release from a glass ionomer cement. **Scandinavian journal of dental research** 85 (1977):503-4.

(122) Forsten L. Short- and long-term fluoride release from glass ionomers and other fluoride-containing filling materials in vitro. **Scand J Dent Res** 98 (1990):179-85.

(123) Swartz ML, Phillips RW, Clark HE. Long-term F Release from Glass Ionomer Cements. **Journal of dental research** 63 (1984):158-60.

(124) Dahl BL, Tronstad L. Biological tests on an experimental glass ionomer (silicopolyacrylate) cement. **Journal of oral rehabilitation** 3 (1976):19-24.

(125) Murray PE, About I, Lumley PJ, Smith G, Franquin JC, Smith AJ. Postoperative pulpal and repair responses. **J Am Dent Assoc** 131 (2000):321-9.

(126) Hilton TJ. Keys to clinical success with pulp capping: a review of the literature. **Oper Dent** 34 (2009):615-25.

(127) Massara ML, Alves JB, Brandao PR. Atraumatic restorative treatment: clinical, ultrastructural and chemical analysis. **Caries Res** 36 (2002):430-6.

(128) Six N, Lasfargues JJ, Goldberg M. In vivo study of the pulp reaction to Fuji IX, a glass ionomer cement. **J Dent** 28 (2000):413-22.

(129) Steinbrunner RL, Setcos JC, Kafrawy AH. Connective tissue reactions to glass ionomer cements and resin composites. **American journal of dentistry** 4 (1991):281-4.

(130) Naasan MA, Watson TF. Conventional glass ionomers as posterior restorations. A status report for the American Journal of Dentistry. **American journal of dentistry** 11 (1998):36-45.

(131) Mount GJ. Glass ionomers: a review of their current status. **Operative dentistry** 24 (1999):115-24.

(132) Arita K, Lucas ME, Nishino M. The effect of adding hydroxyapatite on the flexural strength of glass ionomer cement. **Dent Mater J** 22 (2003):126-36.

(133) Moshaverinia A, Ansari S, Moshaverinia M, Roohpour N, Darr JA, Rehman I. Effects of incorporation of hydroxyapatite and fluoroapatite nanobioceramics into conventional glass ionomer cements (GIC). **Acta biomaterialia** 4 (2008):432-40.

(134) Gu YW, Yap AU, Cheang P, Khor KA. Effects of incorporation of HA/ZrO(2) into glass ionomer cement (GIC). **Biomaterials** 26 (2005):713-20.

(135) Yap AU, Pek YS, Kumar RA, Cheang P, Khor KA. Experimental studies on a new bioactive material: HAIonomer cements. **Biomaterials** 23 (2002):955-62.

(136) Cell Proliferation Reagent WST-1 In: GmbH RD, Science RA, Mannheim, Germany, editors.

(137) Transwell Permeable Supports Selection and User Guide. In: Incorporated C, Sciences L, Tower 2 tF, St. C, Lowell M, editors.

(138) pNPP phosphatase assay protocol. Available from: www.bioassaysys.com.

(139) Human collagen type1 ELISA Ver.03. In: COSMO BIO CO. L, Tokyo, Japan, editor.

(140) LeGeros RZ. Calcium phosphates in oral biology and medicine. **Monogr Oral Sci** 15 (1991):1-201.

(141) Yokota R, Hayashi H, Hirata I, Miake Y, Yanagisawa T, Okazaki M. Detailed consideration of physicochemical properties of CO3apatites as biomaterials in relation to carbonate content using ICP, X-ray diffraction, FT-IR, SEM, and HR-TEM. **Dent Mater J** 25 (2006):597-603.

(142) Matsuura A, Kubo T, Doi K, Hayashi K, Morita K, Yokota R, et al. Bone formation ability of carbonate apatite-collagen scaffolds with different carbonate contents. **Dent Mater J** 28 (2009):234-42.

(143) Okazaki M. Creation of highly functional CO3Ap-collagen scaffold biomaterials. **Dent Mater J** 29 (2010):1-8.

(144) Bonifacio CC, Kleverlaan CJ, Raggio DP, Werner A, de Carvalho RC, van Amerongen WE. Physical-mechanical properties of glass ionomer cements indicated for atraumatic restorative treatment. **Australian dental journal** 54 (2009):233-7.

(145) Mitchell CA, Douglas WH, Cheng YS. Fracture toughness of conventional, resin-modified glass-ionomer and composite luting cements. **Dental materials : official publication of the Academy of Dental Materials** 15 (1999):7-13.

(146) Miyazaki M, Moore BK, Onose H. Effect of surface coatings on flexural properties of glass ionomers. **European journal of oral sciences** 104 (1996):600-4.

(147) Fujishima A, Ferracane JL. Comparison of four modes of fracture toughness testing for dental composites. **Dental materials : official publication of the Academy of Dental Materials** 12 (1996):38-43.

(148) Carvalho TS, van Amerongen WE, de Gee A, Bonecker M, Sampaio FC. Shear bond strengths of three glass ionomer cements to enamel and dentine. **Medicina oral, patologia oral y cirugia bucal** 16 (2011):e406-10.

(149) Fruits TJ, Duncanson MG, Jr., Miller RC. Bond strengths of fluoride-releasing restorative materials. **American journal of dentistry** 9 (1996):219-22.

(150) McCarthy MF, Hondrum SO. Mechanical and bond strength properties of light-cured and chemically cured glass ionomer cements. **American journal of orthodontics and dentofacial orthopedics : official publication of the American Association of Orthodontists, its constituent societies, and the American Board of Orthodontics** 105 (1994):135-41.

(151) Arita K, Yamamoto A, Shinonaga Y, Harada K, Abe Y, Nakagawa K, et al. Hydroxyapatite particle characteristics influence the enhancement of the

mechanical and chemical properties of conventional restorative glass ionomer cement. **Dent Mater J** 30 (2011):672-83.

(152) Yoshida Y, Van Meerbeek B, Nakayama Y, Snauwaert J, Hellemans L, Lambrechts P, et al. Evidence of Chemical Bonding at Biomaterial-Hard Tissue Interfaces. **Journal of dental research** 79 (2000):709-14.

(153) Wiegand A, Buchalla W, Attin T. Review on fluoride-releasing restorative materials--fluoride release and uptake characteristics, antibacterial activity and influence on caries formation. **Dental materials : official publication of the Academy of Dental Materials** 23 (2007):343-62.

(154) Neelakantan P, John S, Anand S, Sureshbabu N, Subbarao C. Fluoride release from a new glass-ionomer cement. **Operative dentistry** 36 (2011):80-5.

(155) Dhondt CL, De Maeyer EA, Verbeeck RM. Fluoride release from glass ionomer activated with fluoride solutions. **Journal of dental research** 80 (2001):1402-6.

(156) Francci C, Deaton TG, Arnold RR, Swift EJ, Jr., Perdigao J, Bawden JW. Fluoride release from restorative materials and its effects on dentin demineralization. **Journal of dental research** 78 (1999):1647-54.

(157) Smales RJ, Gao W. In vitro caries inhibition at the enamel margins of glass ionomer restoratives developed for the ART approach. **Journal of dentistry** 28 (2000):249-56.

(158) ten Cate JM, van Duinen RN. Hypermineralization of dentinal lesions adjacent to glass-ionomer cement restorations. **Journal of dental research** 74 (1995):1266-71.

(159) Nakade O, Koyama H, Arai J, Ariji H, Takada J, Kaku T. Stimulation by low concentrations of fluoride of the proliferation and alkaline phosphatase activity of human dental pulp cells in vitro. **Archives of oral biology** 44 (1999):89-92.

(160) Lopez-Cazaux S, Bluteau G, Magne D, Lieubeau B, Guicheux J, Alliot-Licht B. Culture medium modulates the behaviour of human dental pulp-derived cells: technical note. **Eur Cell Mater** 11 (2006):35-42; discussion

(161) Franceschi RT. The role of ascorbic acid in mesenchymal differentiation. **Nutrition reviews** 50 (1992):65-70.

(162) Stein GS, Lian JB. Molecular mechanisms mediating proliferation/differentiation interrelationships during progressive development of the osteoblast phenotype. **Endocrine reviews** 14 (1993):424-42.

(163) Franceschi RT, Wilson JX, Dixon SJ. Requirement for Na(+)-dependent ascorbic acid transport in osteoblast function. **Am J Physiol** 268 (1995):C1430-9.

(164) Owen TA, Aronow M, Shalhoub V, Barone LM, Wilming L, Tassinari MS, et al. Progressive development of the rat osteoblast phenotype in vitro: reciprocal relationships in expression of genes associated with osteoblast proliferation and differentiation during formation of the bone extracellular matrix. **J Cell Physiol** 143 (1990):420-30.

(165) Bellows CG, Aubin JE, Heersche JN. Initiation and progression of mineralization of bone nodules formed in vitro: the role of alkaline phosphatase and organic phosphate. **Bone and mineral** 14 (1991):27-40.

(166) Bellows CG, Heersche JN, Aubin JE. Inorganic phosphate added exogenously or released from beta-glycerophosphate initiates mineralization of osteoid nodules in vitro. **Bone and mineral** 17 (1992):15-29.

(167) Coelho MJ, Fernandes MH. Human bone cell cultures in biocompatibility testing. Part II: effect of ascorbic acid, beta-glycerophosphate and dexamethasone on osteoblastic differentiation. **Biomaterials** 21 (2000):1095-102.

(168) Lian JB, Stein GS. Development of the osteoblast phenotype: molecular mechanisms mediating osteoblast growth and differentiation. **The Iowa orthopaedic journal** 15 (1995):118-40.

(169) Coelho MJ, Cabral AT, Fernande MH. Human bone cell cultures in biocompatibility testing. Part I: osteoblastic differentiation of serially passaged human bone marrow cells cultured in alpha-MEM and in DMEM. **Biomaterials** 21 (2000):1087-94.

(170) Almushayt A, Narayanan K, Zaki AE, George A. Dentin matrix protein 1 induces cytodifferentiation of dental pulp stem cells into odontoblasts. **Gene therapy** 13 (2006):611-20.

(171) Prasad M, Butler WT, Qin C. Dentin sialophosphoprotein in biomineralization. **Connective tissue research** 51 (2010):404-17.

(172) MacDougall M, Simmons D, Luan X, Nydegger J, Feng J, Gu TT. Dentin phosphoprotein and dentin sialoprotein are cleavage products expressed from a single transcript coded by a gene on human chromosome 4. Dentin phosphoprotein DNA sequence determination. **J Biol Chem** 272 (1997):835-42.

(173) Bleicher F, Couble ML, Farges JC, Couble P, Magloire H. Sequential expression of matrix protein genes in developing rat teeth. **Matrix biology : journal of the International Society for Matrix Biology** 18 (1999):133-43.

(174) Shiba H, Nakanishi K, Rashid F, Mizuno N, Hino T, Ogawa T, et al. Proliferative ability and alkaline phosphatase activity with in vivo cellular aging in human pulp cells. **Journal of endodontics** 29 (2003):9-11.

(175) Moule AJ, Li H, Bartold PM. Donor variability in the proliferation of human dental pulp fibroblasts. **Australian dental journal** 40 (1995):110-4.

APPENDIX

Statistical analysis

Fracture toughness

Normal distribution test

One-Sample Kolmogorov-Smirnov Test

Code			Fracture
Cset	N		5
	Normal Parameters[a,b]	Mean	.46490452040
		Std. Deviation	.053730501964
	Most Extreme Differences	Absolute	.283
		Positive	.229
		Negative	-.283
	Kolmogorov-Smirnov Z		.632
	Asymp. Sig. (2-tailed)		.820
Tset	N		5
	Normal Parameters[a,b]	Mean	.59666120680
		Std. Deviation	.099645391296
	Most Extreme Differences	Absolute	.313
		Positive	.183
		Negative	-.313
	Kolmogorov-Smirnov Z		.700
	Asymp. Sig. (2-tailed)		.711
Cunset	N		5
	Normal Parameters[a,b]	Mean	.31112787400
		Std. Deviation	.052966833304
	Most Extreme Differences	Absolute	.181
		Positive	.181
		Negative	-.138
	Kolmogorov-Smirnov Z		.405
	Asymp. Sig. (2-tailed)		.997
Tunset	N		5
	Normal Parameters[a,b]	Mean	.38297866260
		Std. Deviation	.050664749958
	Most Extreme Differences	Absolute	.431
		Positive	.431
		Negative	-.243
	Kolmogorov-Smirnov Z		.965

Asymp. Sig. (2-tailed)	.310

a. Test distribution is Normal.

b. Calculated from data.

One-Way ANOVA

ANOVA

Fracture

	Sum of Squares	df	Mean Square	F	Sig.
Between Groups	.225	3	.075	16.500	.000
Within Groups	.073	16	.005		
Total	.298	19			

Multiple comparisons

Multiple Comparisons

Fracture

Bonferroni

(I) Code	(J) Code	Mean Difference (I-J)	Std. Error	Sig.	95% Confidence Interval	
					Lower Bound	Upper Bound
Cset	Tset	-.131756686400*	.042648063457	.042	-.26005629934	-.00345707346
	Cunset	.153776646400*	.042648063457	.014	.02547703346	.28207625934
	Tunset	.081925857800	.042648063457	.436	-.04637375514	.21022547074
Tset	Cset	.131756686400*	.042648063457	.042	.00345707346	.26005629934
	Cunset	.285533332800*	.042648063457	.000	.15723371986	.41383294574
	Tunset	.213682544200*	.042648063457	.001	.08538293126	.34198215714
Cunset	Cset	-.153776646400*	.042648063457	.014	-.28207625934	-.02547703346
	Tset	-.285533332800*	.042648063457	.000	-.41383294574	-.15723371986
	Tunset	-.071850788600	.042648063457	.669	-.20015040154	.05644882434
Tunset	Cset	-.081925857800	.042648063457	.436	-.21022547074	.04637375514
	Tset	-.213682544200*	.042648063457	.001	-.34198215714	-.08538293126
	Cunset	.071850788600	.042648063457	.669	-.05644882434	.20015040154

*. The mean difference is significant at the 0.05 level.

Microleakage test

Chi-Square test

Crosstab

Count

		Group		
		C	T2	Total
Dentin	0	70	78	148
	1	10	2	12
Total		80	80	160

Chi-Square Tests

	Value	df	Asymp. Sig. (2-sided)	Exact Sig. (2-sided)	Exact Sig. (1-sided)
Pearson Chi-Square	5.766[a]	1	.016		
Continuity Correction[b]	4.414	1	.036		
Likelihood Ratio	6.255	1	.012		
Fisher's Exact Test				.032	.016
N of Valid Cases	160				

a. 0 cells (.0%) have expected count less than 5. The minimum expected count is 6.00.

b. Computed only for a 2x2 table

Shear bond strength measurement

Normal distribution test

One-Sample Kolmogorov-Smirnov Test

Group			Shear bond strength
GIC	N		10
	Normal Parameters[a,b]	Mean	9.2049
		Std. Deviation	3.03581
	Most Extreme Differences	Absolute	.210
		Positive	.134
		Negative	-.210
	Kolmogorov-Smirnov Z		.664

	Asymp. Sig. (2-tailed)		.770
Test	N		10
	Normal Parameters[a,b]	Mean	6.4390
		Std. Deviation	2.37365
	Most Extreme Differences	Absolute	.258
		Positive	.258
		Negative	-.133
	Kolmogorov-Smirnov Z		.815
	Asymp. Sig. (2-tailed)		.520

a. Test distribution is Normal.

b. Calculated from data.

Independent t-test

Group Statistics

	Group	N	Mean	Std. Deviation	Std. Error Mean
MaxStress	1	10	9.204853	3.0358126	.9600082
	2	10	6.439015	2.3736516	.7506145

Independent Samples Test

		Levene's Test for Equality of Variances		t-test for Equality of Means						
									95% Confidence Interval of the Difference	
		F	Sig.	t	df	Sig. (2-tailed)	Mean Difference	Std. Error Difference	Lower	Upper
MaxStress	Equal variances assumed	.459	.507	2.270	18	.036	2.7658380	1.2186213	.2056096	5.3260664
	Equal variances not assumed			2.270	17.010	.037	2.7658380	1.2186213	.1948911	5.3367849

WST-1

Mann-Whitney U test

Day 1

Ranks

Code	N	Mean Rank	Sum of Ranks
GId1	3	2.00	6.00
Td1	3	5.00	15.00
Total	6		

Test Statistics[b]

	OD
Mann-Whitney U	.000
Wilcoxon W	6.000
Z	-1.964
Asymp. Sig. (2-tailed)	.050
Exact Sig. [2*(1-tailed Sig.)]	.100[a]

a. Not corrected for ties.

b. Grouping Variable: Code

Day 7

Ranks

Code	N	Mean Rank	Sum of Ranks
GId7	3	2.33	7.00
Td7	3	4.67	14.00
Total	6		

Test Statistics[b]

	OD
Mann-Whitney U	1.000
Wilcoxon W	7.000
Z	-1.528
Asymp. Sig. (2-tailed)	.127
Exact Sig. [2*(1-tailed Sig.)]	.200[a]

a. Not corrected for ties.

b. Grouping Variable: Code

Day 14

Ranks

	Code	N	Mean Rank	Sum of Ranks
OD	GId14	3	3.00	9.00
	Td14	3	4.00	12.00
	Total	6		

Test Statistics[b]

	OD
Mann-Whitney U	3.000
Wilcoxon W	9.000
Z	-.655
Asymp. Sig. (2-tailed)	.513
Exact Sig. [2*(1-tailed Sig.)]	.700[a]

a. Not corrected for ties.

b. Grouping Variable: Code

ALP activity assay

Normal distribution test

One-Sample Kolmogorov-Smirnov Test

Day	Group			ALP Enzyme Activity
1	Positive	N		9
		Normal Parameters[a,b]	Mean	3.49326716
			Std. Deviation	.815570448
		Most Extreme Differences	Absolute	.248
			Positive	.248
			Negative	-.196
		Kolmogorov-Smirnov Z		.745
		Asymp. Sig. (2-tailed)		.635
	GI	N		9
		Normal Parameters[a,b]	Mean	2.97950607
			Std. Deviation	1.494329575

		Most Extreme Differences	Absolute	.199
			Positive	.135
			Negative	-.199
		Kolmogorov-Smirnov Z		.596
		Asymp. Sig. (2-tailed)		.870
	Test	N		9
		Normal Parameters[a,b]	Mean	1.84923167
			Std. Deviation	1.462189698
		Most Extreme Differences	Absolute	.250
			Positive	.200
			Negative	-.250
		Kolmogorov-Smirnov Z		.750
		Asymp. Sig. (2-tailed)		.626
4	Positive	N		9
		Normal Parameters[a,b]	Mean	4.41803712
			Std. Deviation	1.395691364
		Most Extreme Differences	Absolute	.199
			Positive	.164
			Negative	-.199
		Kolmogorov-Smirnov Z		.597
		Asymp. Sig. (2-tailed)		.868
	GI	N		9
		Normal Parameters[a,b]	Mean	6.88409036
			Std. Deviation	.974793132
		Most Extreme Differences	Absolute	.347
			Positive	.320
			Negative	-.347
		Kolmogorov-Smirnov Z		1.041
		Asymp. Sig. (2-tailed)		.229
	Test	N		9
		Normal Parameters[a,b]	Mean	3.80152382
			Std. Deviation	1.289530104
		Most Extreme Differences	Absolute	.156
			Positive	.156
			Negative	-.143
		Kolmogorov-Smirnov Z		.468
		Asymp. Sig. (2-tailed)		.981

7	Positive	N		9
		Normal Parameters[a,b]	Mean	37.29905519
			Std. Deviation	10.328898093
		Most Extreme Differences	Absolute	.295
			Positive	.234
			Negative	-.295
		Kolmogorov-Smirnov Z		.886
		Asymp. Sig. (2-tailed)		.412
	GI	N		9
		Normal Parameters[a,b]	Mean	20.68402152
			Std. Deviation	17.455078992
		Most Extreme Differences	Absolute	.278
			Positive	.231
			Negative	-.278
		Kolmogorov-Smirnov Z		.834
		Asymp. Sig. (2-tailed)		.490
	Test	N		9
		Normal Parameters[a,b]	Mean	33.63080101
			Std. Deviation	3.390577983
		Most Extreme Differences	Absolute	.271
			Positive	.271
			Negative	-.230
		Kolmogorov-Smirnov Z		.812
		Asymp. Sig. (2-tailed)		.525
14	Positive	N		9
		Normal Parameters[a,b]	Mean	690.34077770
			Std. Deviation	59.305429980
		Most Extreme Differences	Absolute	.363
			Positive	.240
			Negative	-.363
		Kolmogorov-Smirnov Z		1.088
		Asymp. Sig. (2-tailed)		.187
	GI	N		9
		Normal Parameters[a,b]	Mean	557.61573752
			Std. Deviation	75.205290107
		Most Extreme Differences	Absolute	.356
			Positive	.356
			Negative	-.299

		Kolmogorov-Smirnov Z		1.068
		Asymp. Sig. (2-tailed)		.204
	Test	N		9
		Normal Parameters[a,b]	Mean	715.89525440
			Std. Deviation	155.860018810
		Most Extreme Differences	Absolute	.235
			Positive	.224
			Negative	-.235
		Kolmogorov-Smirnov Z		.704
		Asymp. Sig. (2-tailed)		.705
21	Positive	N		9
		Normal Parameters[a,b]	Mean	146.32943390
			Std. Deviation	34.730283550
		Most Extreme Differences	Absolute	.297
			Positive	.234
			Negative	-.297
		Kolmogorov-Smirnov Z		.890
		Asymp. Sig. (2-tailed)		.407
	GI	N		9
		Normal Parameters[a,b]	Mean	125.98449470
			Std. Deviation	55.307042650
		Most Extreme Differences	Absolute	.250
			Positive	.250
			Negative	-.227
		Kolmogorov-Smirnov Z		.749
		Asymp. Sig. (2-tailed)		.629
	Test	N		9
		Normal Parameters[a,b]	Mean	234.70661673
			Std. Deviation	85.323486109
		Most Extreme Differences	Absolute	.277
			Positive	.231
			Negative	-.277
		Kolmogorov-Smirnov Z		.832
		Asymp. Sig. (2-tailed)		.494

a. Test distribution is Normal.

b. Calculated from data.

One-Way ANOVA

ANOVA

ALPase Activity

Day		Sum of Squares	df	Mean Square	F	Sig.
1	Between Groups	12.733	2	6.366	3.792	.037
	Within Groups	40.289	24	1.679		
	Total	53.022	26			
4	Between Groups	47.891	2	23.946	15.750	.000
	Within Groups	36.489	24	1.520		
	Total	84.380	26			
7	Between Groups	1371.404	2	685.702	4.865	.017
	Within Groups	3382.896	24	140.954		
	Total	4754.299	26			
14	Between Groups	129964.119	2	64982.060	5.825	.009
	Within Groups	267722.521	24	11155.105		
	Total	397686.640	26			
21	Between Groups	60134.828	2	30067.414	7.813	.002
	Within Groups	92361.271	24	3848.386		
	Total	152496.099	26			

Multiple comparisons

Multiple Comparisons

ALPase Activity

Bonferroni

Day	(I) Group	(J) Group	Mean Difference (I-J)	Std. Error	Sig.	95% Confidence Interval	
						Lower Bound	Upper Bound
1	Positive	GI	.513761091	.610778177	1.000	-1.05816268	2.08568486
		T2	1.644035491*	.610778177	.038	.07211172	3.21595926
	GI	Positive	-.513761091	.610778177	1.000	-2.08568486	1.05816268
		T2	1.130274400	.610778177	.230	-.44164937	2.70219817
	Test	Positive	-1.644035491*	.610778177	.038	-3.21595926	-.07211172
		GI	-1.130274400	.610778177	.230	-2.70219817	.44164937
4	Positive	GI	-2.466053236*	.581254322	.001	-3.96199320	-.97011327
		T2	.616513309	.581254322	.898	-.87942666	2.11245327
	GI	Positive	2.466053236*	.581254322	.001	.97011327	3.96199320
		T2	3.082566545*	.581254322	.000	1.58662658	4.57850651
	Test	Positive	-.616513309	.581254322	.898	-2.11245327	.87942666
		GI	-3.082566545*	.581254322	.000	-4.57850651	-1.58662658
7	Positive	GI	16.615033677*	5.596704966	.020	2.21112422	31.01894314
		T2	3.668254187	5.596704966	1.000	-10.73565528	18.07216365

	GI	Positive	-16.615033677*	5.596704966	.020	-31.01894314	-2.21112422
		T2	-12.946779491	5.596704966	.089	-27.35068895	1.45712997
	Test	Positive	-3.668254187	5.596704966	1.000	-18.07216365	10.73565528
		GI	12.946779491	5.596704966	.089	-1.45712997	27.35068895
14	Positive	GI	132.725040178*	49.788675753	.041	4.58686208	260.86321828
		T2	-25.554476700	49.788675753	1.000	-153.69265480	102.58370140
	GI	Positive	-132.725040178*	49.788675753	.041	-260.86321828	-4.58686208
		T2	-158.279516878*	49.788675753	.012	-286.41769498	-30.14133878
	Test	Positive	25.554476700	49.788675753	1.000	-102.58370140	153.69265480
		GI	158.279516878*	49.788675753	.012	30.14133878	286.41769498
21	Positive	GI	20.344939203	29.243750638	1.000	-54.91797693	95.60785534
		T2	-88.377182833*	29.243750638	.018	-163.64009897	-13.11426670
	GI	Positive	-20.344939203	29.243750638	1.000	-95.60785534	54.91797693
		T2	-108.722122037*	29.243750638	.003	-183.98503817	-33.45920590
	Test	Positive	88.377182833*	29.243750638	.018	13.11426670	163.64009897
		GI	108.722122037*	29.243750638	.003	33.45920590	183.98503817

*. The mean difference is significant at the 0.05 level.

RT-PCR

Normal distribution test

One-Sample Kolmogorov-Smirnov Test

Day			COL1A1	DMP-1	DSPP
1	N		6	3	6
	Normal Parameters[a,b]	Mean	2.79378680	.66931305	2.05726960
		Std. Deviation	2.092403506	.149008057	3.026507314
	Most Extreme Differences	Absolute	.287	.219	.252
		Positive	.287	.219	.252
		Negative	-.167	-.189	-.248
	Kolmogorov-Smirnov Z		.704	.379	.616
	Asymp. Sig. (2-tailed)		.705	.999	.842
7	N		11	11	11
	Normal Parameters[a,b]	Mean	1.46912614	1.01884477	1.92332063
		Std. Deviation	.536544656	1.140111530	3.065062623
	Most Extreme Differences	Absolute	.253	.281	.334
		Positive	.253	.281	.334
		Negative	-.127	-.213	-.265
	Kolmogorov-Smirnov Z		.839	.931	1.107
	Asymp. Sig. (2-tailed)		.483	.351	.172
14	N		12	12	6
	Normal Parameters[a,b]	Mean	.90777706	.82923692	.51255949
		Std. Deviation	.212132999	1.214810168	.874764286
	Most Extreme Differences	Absolute	.119	.247	.388
		Positive	.101	.243	.388
		Negative	-.119	-.247	-.279
	Kolmogorov-Smirnov Z		.412	.857	.950
	Asymp. Sig. (2-tailed)		.996	.455	.328
21	N		5	11	5
	Normal Parameters[a,b]	Mean	.67202563	.36130991	.38073795
		Std. Deviation	.136403646	.396966547	.652930217
	Most Extreme Differences	Absolute	.342	.213	.361
		Positive	.342	.213	.361
		Negative	-.226	-.181	-.280
	Kolmogorov-Smirnov Z		.764	.705	.806
	Asymp. Sig. (2-tailed)		.604	.703	.534

a. Test distribution is Normal.

b. Calculated from data.

Independent t-test

Group Statistics

Day		Group	N	Mean	Std. Deviation	Std. Error Mean
1	COL1A1	Control	3	.97448672	.206992254	.119507033
		Test	3	4.61308689	.986395904	.569495941
	DMP-1	Control	3	.66931305	.149008057	.086029842
		Test	0[a]	.	.	.
	DSPP	Control	3	3.61981782	3.852330173	2.224143862
		Test	3	.49472138	.856882563	.494721378
7	COL1A1	Control	6	1.21201898	.324001590	.132273095
		Test	5	1.77765474	.608552072	.272152760
	DMP-1	Control	6	.73824562	.689965683	.281677311
		Test	5	1.35556375	1.547495245	.692060913
	DSPP	Control	6	1.67241427	2.730990978	1.114922398
		Test	5	2.22440826	3.735757535	1.670681559
14	COL1A1	Control	6	.89693037	.243514599	.099414419
		Test	6	.91862374	.198542637	.081054692
	DMP-1	Control	6	.99829402	1.553883529	.634370294
		Test	6	.66017981	.873804030	.356729001
	DSPP	Control	3	.31913194	.552752726	.319131935
		Test	3	.70598705	1.222805443	.705987052
21	COL1A1	Control	3	.67265239	.171931434	.099264660
		Test	2	.67108549	.123693318	.087464384
	DMP-1	Control	6	.31640990	.254004787	.103697020
		Test	5	.41518992	.553764592	.247651054
	DSPP	Control	3	.12438504	.143400263	.082792180
		Test	2	.76526731	1.082251406	.765267308

a. t cannot be computed because at least one of the groups is empty.

Independent Samples Test

Day			Levene's Test for Equality of Variances		t-test for Equality of Means						
										95% Confidence Interval of the Difference	
			F	Sig.	t	df	Sig. (2-tailed)	Mean Difference	Std. Error Difference	Lower	Upper
1	COL1A1	Equal variances assumed	3.451	.137	-6.253	4	.003	-3.638600172	.581899955	-5.254213455	-2.022986890
		Equal variances not assumed			-6.253	2.176	.020	-3.638600172	.581899955	-5.958104406	-1.319095939
	DSPP	Equal variances assumed	3.126	.152	1.372	4	.242	3.125096439	2.278500639	-3.201035507	9.451228385
		Equal variances not assumed			1.372	2.197	.293	3.125096439	2.278500639	-5.880998988	12.131191866
7	COL1A1	Equal variances assumed	.751	.409	-1.978	9	.079	-.565635758	.285893687	-1.212372211	.081100695
		Equal variances not assumed			-1.869	5.852	.112	-.565635758	.302594277	-1.310628398	.179356882
	DSPP	Equal variances assumed	.158	.700	-.283	9	.783	-.551993992	1.947710961	-4.958022293	3.854034309
		Equal variances not assumed			-.275	7.212	.791	-.551993992	2.008538978	-5.273297326	4.169309343
	DMP-1	Equal variances assumed	16.110	.003	-.884	9	.399	-.617318129	.698017093	-2.196342496	.961706239
		Equal variances not assumed			-.826	5.318	.444	-.617318129	.747188339	-2.503962434	1.269326176

Day			Levene's Test for Equality of Variances		t-test for Equality of Means						
										95% Confidence Interval of the Difference	
			F	Sig.	t	df	Sig. (2-tailed)	Mean Difference	Std. Error Difference	Lower	Upper
14	COL1A1	Equal variances assumed	.876	.371	-.169	10	.869	-.021693378	.128269598	-.307495853	.264109097
		Equal variances not assumed			-.169	9.610	.869	-.021693378	.128269598	-.309074772	.265688016
	DSPP	Equal variances assumed	3.989	.116	-.499	4	.644	-.386855116	.774766358	-2.537951378	1.764241146
		Equal variances not assumed			-.499	2.785	.654	-.386855116	.774766358	-2.964004645	2.190294413
	DMP-1	Equal variances assumed	.547	.477	.465	10	.652	.338114213	.727792038	-1.283507503	1.959735929
		Equal variances not assumed			.465	7.875	.655	.338114213	.727792038	-1.344835002	2.021063428
21	COL1A1	Equal variances assumed	1.098	.372	.011	3	.992	.001566893	.143779222	-.456002761	.459136547
		Equal variances not assumed			.012	2.861	.991	.001566893	.132300760	-.431243057	.434376844
	DSPP	Equal variances assumed	188.768	.001	-1.104	3	.350	-.640882267	.580324473	-2.487733740	1.205969207
		Equal variances not assumed			-.833	1.023	.555	-.640882267	.769732809	-9.906741730	8.624977197
	DMP-1	Equal variances assumed	1.288	.286	-.393	9	.703	-.098780024	.251229153	-.667099852	.469539804
		Equal variances not assumed			-.368	5.393	.727	-.098780024	.268484854	-.774087257	.576527209

VITAE

Miss Arunee Laiteerapong was born in Bangkok, Thailand in 1971. She obtained her Doctor of Dental Science (D.D.S.) from Faculty of Dentistry, Chulalongkorn University, Bangkok, Thailand in 1993. She earned her Master of Science (M.S.) in Pediatric Dentistry from the same university in 1998 with the thesis entitled "Inhibitory Effects of a Fluoride Varnish on Initial Caries Progression in Pre-school Children".

Arunee started her career working for Ministry of Public Health (MOH) as a dentist in Dental Department, Saraburee Provincial Health Office in April 1993 and moved to be head of Dental Department of Khang Khoi community hospital in the same year. After her master degree graduation, she came back to work as head Dental Department in Saraburee Provincial Health Office. During that time, she worked closely with MOH, Dental Division to drive Early Childhood Caries Preventive Strategy for Thailand and finally implemented a successful fluoride varnish program in Well Baby Clinic nationwide. In 2001, she moved to work for Thammasat University, Dental School as an assistant to the dean. During her time in the dental school, she worked in curriculum development, managed the comprehensive dentistry course and involved in elective and research courses for final year students. She was also one of the trainers for Atraumatic Restorative Treatment (ART) in Thailand and provided several trainings in glass ionomer sealant for MOH.

In 2005, she has started working with Pfizer Global Company as a Dental Science Liaison for Thailand and transferred to work for Johnson and Johnson Consumer (Thailand) Ltd. in 2007. Currently she holds the position of Manager, Asia-Pacific Scientific& Professional Affairs, Global Research, Development and Engineering. Johnson& Johnson Consumer and Personal Products Worldwide, Division of Johnson& Johnson Consumer Companies Inc.